Regional Frequency Analysis of Peak Flows at Zion National Park and Vicinity Areas, Utah

Gustavo E. Diaz and Jose D. Salas

May 1994

Colorado State University

Computing Hydrology Laboratory
Hydrologic Science and Engineering Program
Engineering Research Center
Fort Collins, Colorado

TECHNICAL REPORT No.2

TABLE OF CONTENTS

APPENDIXES

LIST OF FIGURES

LIST OF TABLES

ABSTRACT

The main purpose of this study was the implementation of a regional flood frequency analysis for Zion National Park and vicinity areas. Two regional models were implemented based on the multivariate lognormal distribution that explicitly accounts for the space correlation among the series of annual peaks in the region. The parameters of the regional models were estimated using the maximum likelihood procedure based on the observed series of peaks from a subset of stations that are known to preserve the assumed structure of the regional models. The models have the capability to estimate flood quantiles (maximum instantaneous peaks) at ungaged river sites based on readily available geographical and meteorological information. Moreover, the models can also be used to increase the reliability of estimated quantiles at sites with very short records. The regional models showed very good fitting capabilities when compared with empirical frequency distributions at three selected stations representative of catchments at low, intermediate and high elevation areas of the Upper Virgin River Basin.

ACKNOWLEDGMENT

The authors of this study would like to acknowledge the financial support received by the National Park Service, Water Resources Division, and the technical support received in the form of data, literature and consultation from the Water Rights Branch personnel involved in this project, particularly Owen Williams, Dan McGlothlin and Bill Hansen.

1.0 INTRODUCTION

1.1 Purpose and Scope of the Study

The general purpose of this study is to undertake a regional peak flows frequency analysis for Zion National Park and its surrounding areas. More specifically, the objectives of the study are two fold: 1) to estimate peak flow quantiles associated to given exceedance probabilities for ungaged river sites, and 2) to increase the reliability of estimated peak flow quantiles for sites with short period of records.

Zion National Park is located in South-western Utah where surface flow records are significantly limited. The limitation is not so much in relation to the number of gaging stations (in operation and discontinued), but regarding the length of the peak records available. The majority of the gaging stations have short (less than 50 years) and very short records (less than 25 years). Only two stations in the Upper Basin of the Virgin River are classified as having long records (more than 50 years).

Moreover, the reliability of estimated quantiles derived from single-site analysis is usually low because of the limited information contained in a single series. Customarily, the problem of insufficient information at a specific site or even the complete lack of data at a site has been tackled by using additional regional information from neighboring stations. Regional flood frequency analysis has been shown to be very effective in improving the reliability of peak flow frequency estimates as demonstrated by a solid body of publications in the field that starts with the pioneering works by Dalrymple (1960) and Benson (1962).

The methodology for flood frequency analysis proposed in this study is based on a multivariate lognormal model that explicitly accounts for the cross correlation among the series of annual peak flows in the region. The model is based on regionalization assumptions derived from the observed series of peak flows. The regional structure allows the model to maintain a relatively low number of parameters and at the same time gain in reliability by using all available hydrological data in the region. It is expected that the limited number of years of data for most streams in the Zion area can be partially compensated by this regional approach.

The terms 'flood' and 'peak flow' are used interchangeable in this report. However, we would like to make a distinction between peak flows with intermediate frequency of occurrence (once every 2, 5, 10, 20 years) versus floods of devastating effects causing severe human and economical losses (those with over 50 or 100 years of recurrence interval). This study focuses primarily on the first group of events. This is in accordance to the general focus of other geomorphological and ecological studies being carried out in the Zion area. Moreover, there is a general agreement among experts on the subject that suggest that the most frequent extreme events are the ones that have the highest significance on the stream ecosystem, see for instance Resh et al (1988).

This report includes the following sections: Section 1: introduces the reader to the purpose and objectives of the study and provides a brief geographical description of the study area. Section 2: presents the basic hydrological information used in the study, they are series of maximum instantaneous peaks and regional precipitation-frequency data. Section 3: provides a detailed characterization of the peaks series in the Zion area. It also explores some criteria for hydrological homogeneity and the statistical relationship between mean annual peaks and hydro-meteorological variables. Section 4: presents the formulation and parameter estimation procedure of two statistical flood frequency models. Section 5: applies the models to the area of interest, including an analysis of their performance. This section also provides an example and recommendations for using the models to estimate flow peak quantiles at ungaged sites. Finally, Section 6: gives a summary of the study and final recommendations. The report ends with literature references and five appendixes.

1.2 Study Area

The general area for this study encompasses a large portion of South-western Utah, between the latitudes N38°07'30" and N37°00'00", and the longitudes W111°15'00" and W114°00'00", covering a total area of 11,400 square miles. It comprises Washington County almost entirely, and parts of Kane, Iron and Garfield counties, see Figure 1. The location of Zion National Park, within the Upper Virgin River Basin, is also shown in Figure 1. Geographical information for the selected watersheds was extracted from a total of 116 topographic maps at scale 1:24,000 (7.5-minutes) prepared by the U. S. Geological Survey

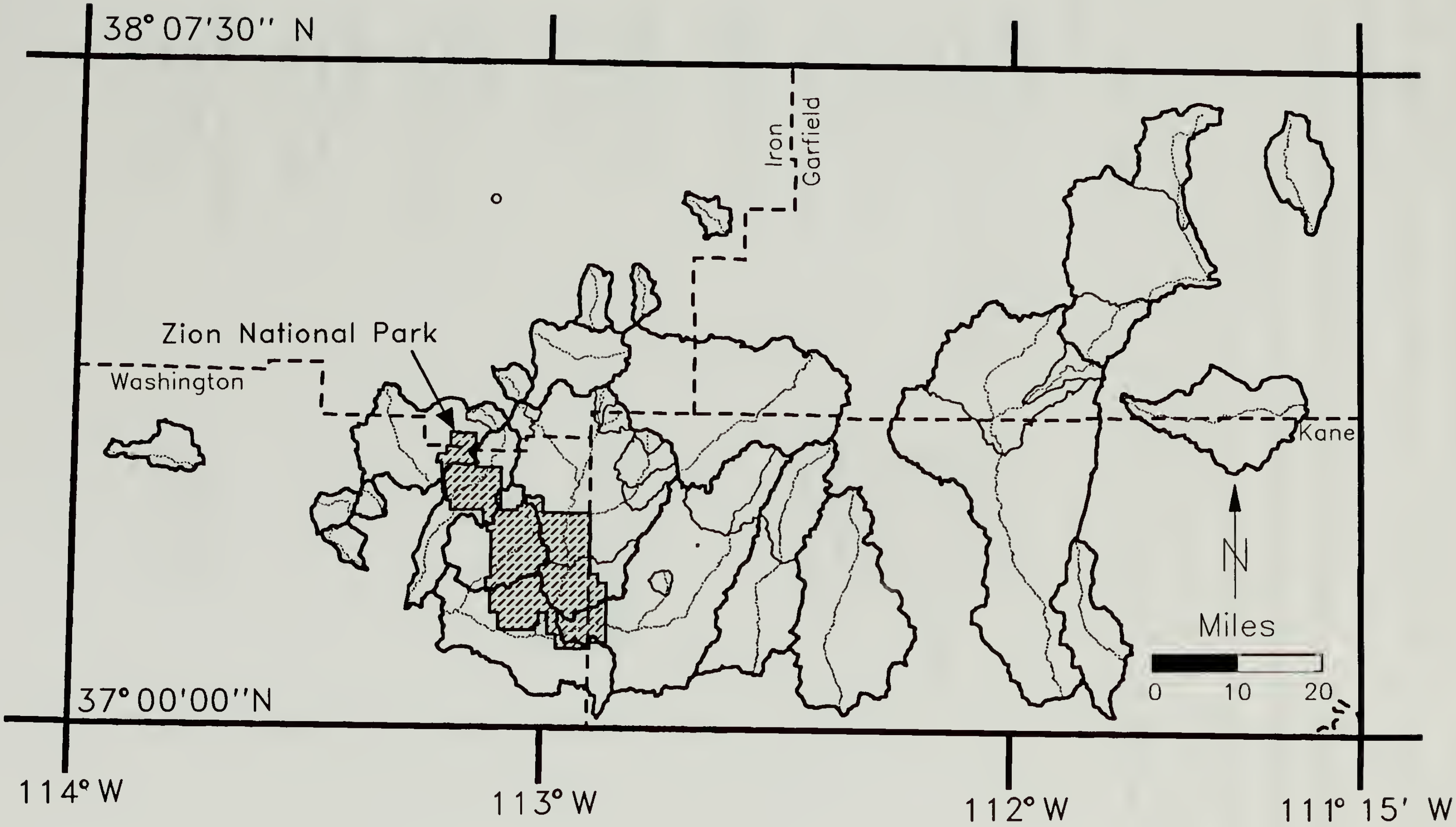

Fig.1 The Study Area, Showing Main Watersheds and Zion National Park

(USGS). An inventory of the topographic maps utilized is provided in Appendix I. Maps names in the appendix are ordered alphabetically, including also their corresponding USGS code-reference number.

Our study region encompasses several of the hydrologic areas of the southern portion of the State as classified by the Utah Division of Water Resources (UDWR, 1983, pp.2). The watersheds of interest were selected based on the availability of peak flows records and some criteria of hydrological homogeneity discussed latter in Section 3. The following lists the state hydrologic areas and all the water courses contained in each area that were included in the study:

▹ Virgin (9-7)
- East Fork of the Virgin River
- North Fork of the Virgin River
- North Creek
- Virgin River
- La Verkin Creek
- Ash Creek
- South Ash Creek
- Crystal Creek
- Deep Creek
- East Fork Deep Creek
- Mineral Gulch
- Leeds Creek
- Santa Clara River
- Moody Wash

▹ Upper Sevier (5-6)
- Sevier River

▹ Escalante (8-4)
- Escalante River
- Pine Creek
- Deer Creek
- Upper Valley Creek
- Twentymile Wash

▹ Paria (9-5)
- Paria River
- Henrieville Creek

▹ Kanab (9-6)
- Kanab Creek
- Johnson Wash

▹ Cedar-Parowan (6-2)
- Coal Creek
- Center Creek
- Summit Creek
- Little Creek
- Shirts Creek

- <u>Wahweep (9-4)</u>
  - Coyote Creek

All the streams listed above have (active) or had (discontinued) USGS surface flow gaging stations. The gaging sites provided the flows records used in the regional flood frequency analysis. Some of the streams have flow records available at more than one location as indicated later in Section 2. A list of the USGS topographic maps used to delineate and study each of the subareas depicted in Figure 1 is included at the end of Appendix I. All basic geographical and hydrological information of the watersheds and the stream network is provided in Section 2.

2.0 PEAK FLOWS AND PRECIPITATION DATA

2.1 Peaks Flows Data

Streamflow data for this study were obtained from the USGS CD-Rom database, named Peak Flows, and through personal communications with the USGS Water Resources Division in Cedar City, Utah (USGS, 1994). Data consist of maximum annual instantaneous flow peaks, expressed in cubic-feet per second (cfs). A preliminary selection of gaging sites included practically all records available within the study area, with the exception of just a few stations having flows strongly affected by human activities. Typically, stations located at relatively high altitudes have short records, while longer records are likely to be available for the larger streams having large drainage areas. This is also the case in the Zion region, where periods of records are of different length for the headwaters than for the lower regions in the Upper Basin of the Virgin River. Nevertheless, due to the characteristics of the methodology of analysis proposed in this study, more is to be gained by using all existing data within an homogeneous region than by arbitrarily discarding stations with short period of records.

2.1.1 Annual Peak Flows Records

Table 1 lists 39 gaging stations that were initially considered suitable for the regional frequency analysis. The first column in Table 1, site no., provides a reference number to help locate the gaging stations in Figure 2, which shows a map with the watersheds of interest and the main drainage network. Station type indicates whether the gaging station was operated as a continuous-record, denoted by 'c', or only as a crest-stage partial record station, denoted as 'p', for which only annual peaks are published. Latitude, longitude and gage elevation (datum) information correspond to the site where the gaging station is located, obtained from USGS records. Drainage area is listed next. Some minor differences in watersheds areas were detected between the values provided by the USGS and those computed by the Geographic Information System (GIS) developed during this study. Base flow levels, established by the USGS to create partial-duration series of peak flows, are

Table 1. Gaging Stations Considered for the Regional Flood Frequency Analysis

Site No.	USGS I.D.	Stat. Type	Station Name	--- Gaging Station --- Latitude	Longitude	Elevat.(ft)	Drainage Area (mi^2)	Base Flow(cfs)	---Period of Record--- 19__	Conti.	Count	Flood Region	Remarks
1	09336400	p	Upper Valley Cr nr Escalante, Ut.	37:44:00	111:43:00	6250.	53.0		59-74	Y	16	LP	
2	09337000	c	Pine Creek nr Escalante, Ut.	37:51:45	111:38:07	6400.	68.1	100.	51-93	N	41	LP	small reg. at headwaters
3	09337500	c	Escalante River near Escalante, Ut.	37:46:41	111:34:26	5670	320.0		10-93	N	38	LP	div.ab.st. for 2300 ac
4	09338900	p	Deer Creek nr Boulder, Ut.	37:51:00	111:21:00	5700.	63.0		59-74	Y	16	LP	
5	09339200	p	Twentymile Wash nr Escalante, Ut.	37:34:00	111:22:00	5080.	140.0		59-68	Y	10	LP	
6	09379800	p	Coyote Creek near Kanab, Ut.	37:08:00	111:45:00	4240.	89.0		59-72	Y	14	LP	
7	09381100	p	Henrieville Cr nr Henrieville, Ut.	37:34:00	111:59:00	5980.	34.0		59-74	Y	16	LP	
8	09381500	p	Paria river near Cannonville, Ut.	37:28:50	112:01:15	5440.	220.0		51-74	N	21	LP	
9	09381800	p	Paria River near Kanab, Ut.	37:04:00	111:53:00	4300.	668.0		59-73	Y	15	LP	
10	09403500	p	Kanab Creek nr Glendale, Ut.	37:17:00	112:29:00	6220.	72.0		59-74	Y	16	LP	
11	09403600	c	Kanab Creek nr kanab, Ut.	37:06:02	112:32:50	5060.	198.0	200.	59-93	N	25	LP	several div.ab.st.
12	09403700	p	Johnson Wash near Kanab, Ut.	37:02:00	112:21:00	5000.	237.0		59-74	Y	16	LP	
13	09404450	c	E.Fk. Virgin River nr Glendale, Ut.	37:20:19	112:36:13	5900.	74.0	90.	67-93	Y	27	LP	few small div.ab.st.
14	09404500	p	Mineral Gulch near Mt. Carmel, Ut.	37:14:00	112:44:00	5620.	7.6		59-74	N	14	LP	
15	09404900	c	E.Fk. Virgin r nr. Springdale, Ut.	37:09:51	112:57:28	3940.	347.8		92-93	Y	2	LP	several small div.ab.st.
16	09405200	c	Deep Creek near Cedar City, Ut.	37:31:18	112:53:01	7680.	6.7		87-93	Y	7	HP	some div.ab.st.
17	09405250	c	E.Fk. Deep Creek nr Cedar City, Ut.	37:30:35	112:52:58	7580.	7.8		87-93	Y	7	HP	some div.ab.st.
18	09405300	c	Crystal Cr nr Cedar City, Ut.	37:31:20	113:01:25	8320.	10.2		57-61	Y	5	HP	
19	09405400	c	N.Fk. Virgin Rv. nr Glendale, Ut.	37:28:30	112:46:42	7530.	5.7	18.	73-78	Y	6	HP	no div.ab.st.
20	09405420	c	N.Fk. Virgin Rv blw Bullock Cnyn, Ut.	37:25:06	112:47:59	6420.	29.6	30.	74-84	Y	11	LP	several div.ab.st.
21	09405450	c	N.Fk. Virgin Rv abv Zion Narrows, Ut.	37:23:26	112:49:30	6000.	42.0	70.	81-84	Y	4	LP	small div.ab.st.
22	09405490	c	N.Fk. Virgin Rv abv Big Bend, Ut.	37:16:43	112:56:38	4400.	311.0		92-93	Y	2	LP	
23	09405500	c	N.Fk. Virgin Rv near Springdale, Ut.	37:12:35	112:58:40	3970.	344.0		13-93	N	70	LP	some div.ab.st.
24	09405900	c	North Creek near Virgin, Ut.	37:14:14	113:09:01	3680.	97.0		85-93	Y	9	LP	two div.ab.st.
25	09406000	c	Virgin River at Virgin, Ut.	37:11:53	113:12:22	3440.	956.0	1600.	10-93	N	77	LP	div.ab.st. for 2800 ac
26	09406150	c	La Verkin Creek near La Verkin, Ut.	37:12:17	113:17:03	3040.	91.0		85-91	Y	7	LP	
27	09406300	c	Kanarra Cr. At Kanarraville, Ut.	37:32:17	113:10:04	5680.	9.9	100.	60-82	Y	23	LP	small div.ab.st.
28	09406500	c	Ash Cr nr new Harmony, Ut.	37:24:45	113:14:10	4450.	132.0		40-47	Y	8	LP	
29	09406700	c	South Ash Cr blw Mill Cr nr Pint., Ut.	37:21:50	113:20:01	5290.	11.0	100.	67-82	Y	16	LP	no div.ab.st.
30	09406800	p	South Ash Cr nr Pintura, Ut.	37:19:50	113:16:50	4100.	14.0		59-74	N	14	LP	
31	09408000	c	Leeds Creek near Leeds, Ut.	37:16:03	113:22:12	4000.	15.5	50.	64-93	Y	30	LP	one domestic div.ab.st
32	09408400	c	Santa Clara River nr Pine Valley, Ut.	37:23:00	113:28:57	6640.	18.7	60.	60-93	Y	34	LP	slight reg/no div.ab.st.
33	09409500	c	Moody Wash near Veyo, Ut.	37:26:00	113:44:30	4800.	33.0	100.	55-69	Y	15	LP	
34	10174500	c	Sevier River at Hatch, Ut.	37:39:04	112:25:46	6870.	340.0	500.	12-93	N	69	LP	no reg/small div.ab.st.
35	10241400	c	Little Cr nr Paragonah, Ut.	37:54:20	112:42:30	6740.	15.8	11.	60-80	Y	21	LP	no reg/diversion ab.st.
36	10241470	c	Center Cr abv Parowan Cr, Ut.	37:47:20	112:48:40	6900.	11.6	30.	65-87	Y	23	LP	no reg/diversion ab.st.
37	10241600	c	Summit Creek nr Summit, Ut.	37:47:10	112:54:50	6313.	24.0	15.	65-87	Y	23	LP	no reg/diversion ab.st.
38	10242000	c	Coal Creek nr Cedar City, Ut.	37:40:20	113:02:02	6000.	80.9	550.	16-93	N	63	LP	slight reg/no div.ab.st.
39	10242100	p	Shirts Creek nr Cedar City, Ut.	37:37:00	113:07:00	5835.	12.8		59-74	N	16	LP	

p: crest-stage station, c: continuous station LP: Low Plateau, HP: High Plateau

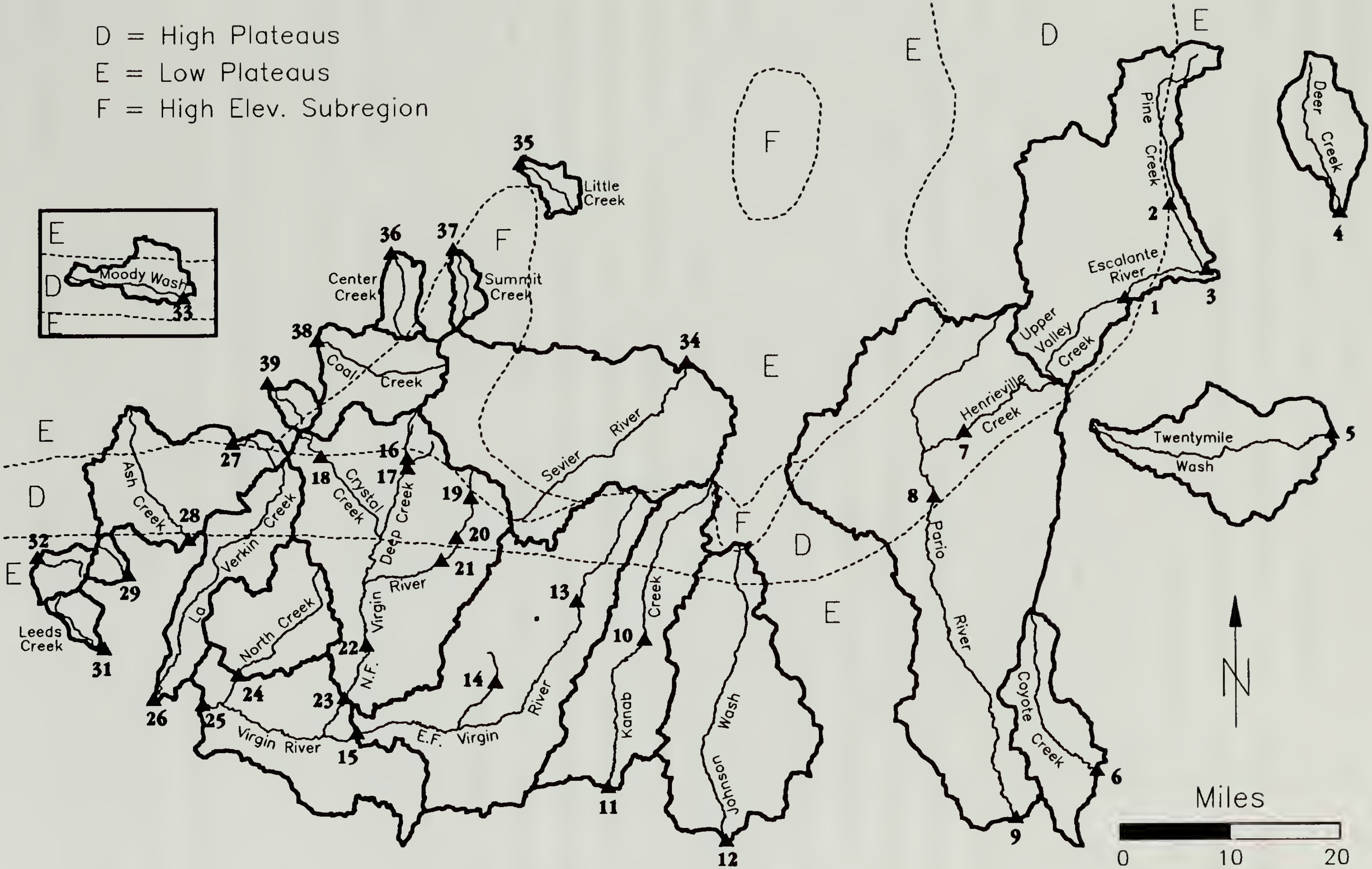

Fig.2 Main Drainage Network, USGS Flow Gaging Stations, and Flood Regions Within the Study Area

provided in Table 1 only for those stations with long and continuous records. Period of record provides the first and last water-year of available data, with 'Y' and 'N' indicating whether a series is continuous or discontinuous during the period, respectively. The number under Count indicates the length of the peak annual series in years. Notice that only 15 out of the 39 stations are still reporting data during water-year 1993. For easy visualization, a bar graph showing graphically the length of usable records is presented in Figure 3.

Table 1 also designates the flood region where each catchment with a gaged site is in. This is based on the Thomas and Lindskov (1983) classification of flood regions for the State of Utah. To determine the flood region, the user needs to estimate the datum and mean basin elevation of the site of interest. The datum is the elevation at the flow gaging site, and the mean basin elevation is determined for the drainage basin which contributes streamflow to the site. Approximate boundaries of the flood regions intersecting the study area are shown in Figure 2. Further discussion of this subject is provided in Section 3.1. Finally, a few remarks are included in Table 1 concerning the degree of water diversion and/or regulation in the streams. The Upper Basin of the Virgin River and adjacent watersheds have not been heavily impacted by human activities; particularly in relation to flood control structures which can drastically reduce the magnitude of flow peaks. However, the lack of accurate and systematic water diversion records prevented us from analyzing the effect of water diversions in the magnitude of flow peaks. Unfortunately, the months with the largest demand for irrigation water, June through September, coincide with the period when flow peaks reach their maximum frequency and intensity, July through September. All available peak flows data were tabulated and included in the report as Appendix II (see values in normal type face). The first group of basic statistics reported at the bottom of the page corresponds to the series of measured peaks.

2.1.2 Extension of Annual Peak Flows Records

The validation of some of the underlying assumptions of the multivariate model to be applied here requires a preliminary estimation of the long-term mean annual peak (MAP) at each gaging site. The difficulty in estimating MAPs arises from the unequal length of the records available. As mentioned before, few records extend over 60 or 70 years, but the

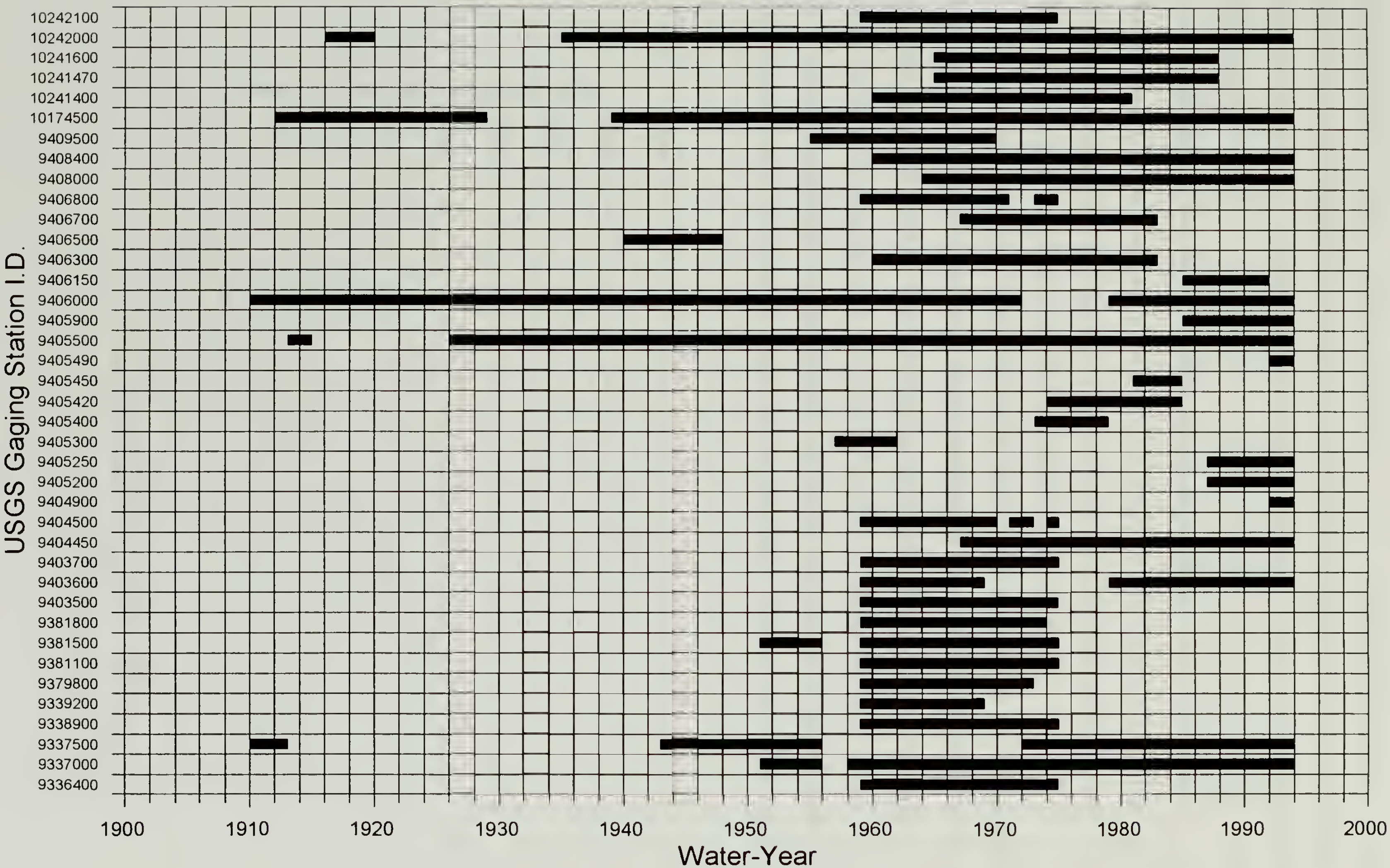

Fig.3 Bar Diagram Showing Period of Record of Annual Peaks

great majority are considered short or very short records. Prior to the estimation of MAPs, it is required that some records be extended to cover a common base-period. This approach makes data more comparable by diminishing the effect that natural cycles in weather conditions may have in those stations with short records. This is a standard procedure utilized by the USGS when applying index-flood methods (Dalrymple, 1960). The base- or common-time period should be chosen as long as possible. The data set available for the region at hand dictates the maximum possible length of the base-period. For instance, observing the bar graph in Figure 3 it is concluded that the base period should extend from 1959 to 1993, since the largest number of records start in 1959.

Simple and multiple linear regression techniques allowed us to fill in missing peaks at several stations. Figure 4 shows a linear correlation between annual peaks at two gaging sites along the Paria River. The correlative association between the two series is typical for the study area when gaging sites are relatively close or along the same water course. For pairs of stations separated a large distance the linear correlation of peaks deteriorates rapidly. In some cases linear correlations could not be detected. This is due to the random

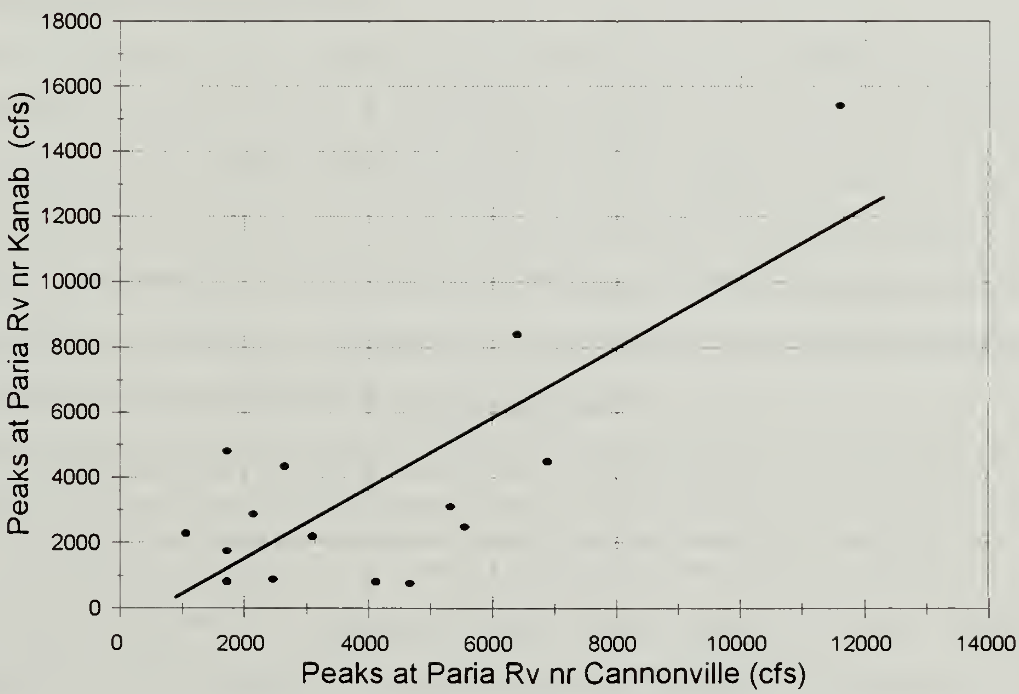

Fig.4 Interstation Correlation of Annual Flow Peaks

occurrence in time and space of storms producing flow peaks, and the low probability of an intense summer storm hitting a particular site, particularly in small catchments. Given the relative low values of correlation coefficients between annual peak series, visual inspection became an important criterion to help determine whether a correlative association between two stations was acceptable or not for the purpose of record extension.

The correlation models finally adopted included random components to help reproducing the full variance of the dependent variable. With only a few exceptions, actual peak measurements were used to fill in data at another station, avoiding the use of previously estimated peaks for further record extension. Whenever possible, records were also extended or filled in prior to 1959. This was done only for stations that showed significant linear correlation with other existing records during the period 1910-1959. The extended data base of peak flows is also presented in Appendix II. Filled in values are highlighted. The original data base was extended from a total of 847 year-station values to 1249 values, a 47.4% increase. Basic statistics for the extended series are also included in Appendix II at the bottom of the page, below the set of statistics for the systematic series.

2.2 Precipitation-Frequency Data

Since precipitation is the primary cause of peak flows, it is imperative that some form of precipitation be part of the regional flood frequency analysis. In New England, where rainfall is fairly uniform, Benson (1962) found that rainfall intensity, though a statistically significant variable, was not one of the most important factors affecting flow peaks. On the other hand, in the southwest where as Benson (1964) says, "... the outstanding characteristic of precipitation is its variability", precipitation is expected to be an important parameter in the determination of mean annual flow peaks in the region.

Heavy summer rains in southern Utah create the peak flows with the largest intensity in the region. According to Woolley (1946), there are two distinct types of storms: (1) the steady or cyclonic storms, which are not very frequent and may result in a large total precipitation but are spread over a protracted period and have relatively small intensities; and (2) thunderstorms, which generally include the violent downpours of brief duration (20 to 30 minutes) and high intensity commonly known as cloudbursts. The great majority of the

cloudburst events occur in July and August, the warmest months, while a few events occur in June and September. Flow peaks induced by cloudbursts can exceed in magnitude the normal spring freshets. They are characterized by very flashy peaks followed by quickly diminishing flows. Most of the cloudburst peaks in the Zion region originate below the 8,000 ft altitude, and mainly in streams exposed to the direction of storm travel. The very local effect of high intensity summer thunderstorms can yield erroneous results when flood frequency analysis is carried out at a single site, particularly if dealing with small drainages and short periods of observation.

There are several indexes of precipitation that can be used in the study regarding the distribution of mean annual peaks in a region. Depending on the meteorological mechanism generating the peaks, different precipitation indexes can be of use. For instance, for snow melt-flood areas, mean annual precipitation has been found significantly correlated with annual peaks (Benson, 1964). On the other hand, for rainfall-induced peaks, a precipitation index involving some form of frequency and duration should be highly correlated with the instantaneous peak discharge of a given frequency. This study considers two indexes from the latter class, the 2yr-24hr precipitation and the 50%-24hr precipitation. Maps of isopluvial lines for both indexes were obtained from the National Weather Service (NOAA, 1973a). Precipitation maps presently available for the State of Utah were generated by the NWS from records compiled from 1910 to 1969. At present, the NWS is in the process of updating the precipitation-frequency maps including information from the last two decades. Isopluvial lines were digitized and incorporated as an additional thematic layer into the regional GIS. A reproduction of one of the precipitation layers is shown in Figure 5.

The two adopted indexes represent different precipitation conditions. The 2yr-24hr precipitation map was generated based on precipitation data from all months of the year, without regard to the type of precipitation: rain, rain and snow mixed or all snow. The 2 year return period for precipitation was chosen to match the expected recurrence interval of mean annual peaks, which in general is estimated to lie between 2 to 3 years. On the other hand, the 0.50 probability-6hr precipitation map considers only precipitation events from the months of May to October. This is equivalent to using a data series made up of precipitation events that are exclusively rain (rainfall only series). Because summer thunderstorms have

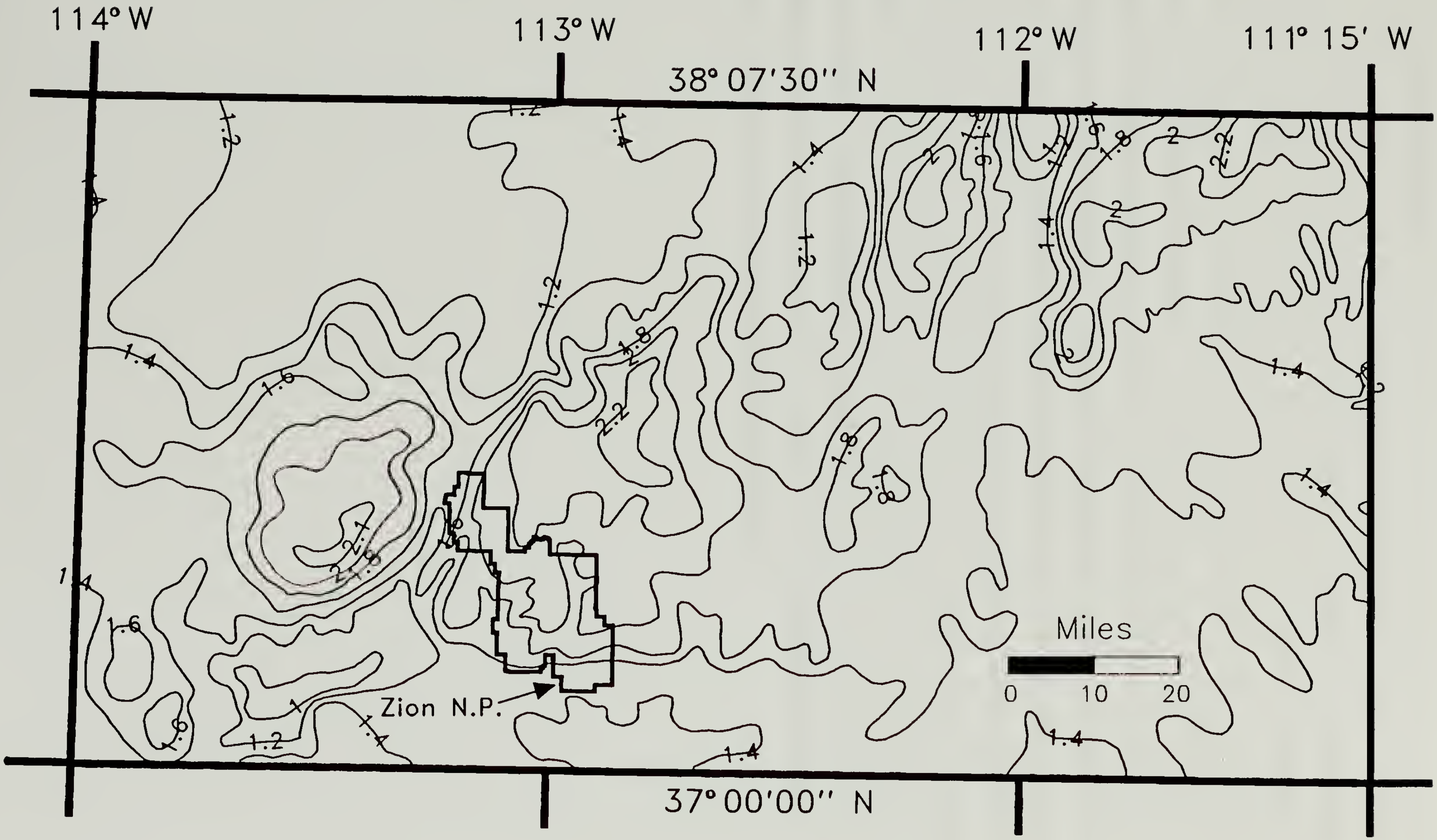

Fig.5 Isopluvials for 2yr-24hr Precipitation in the Study Area, (in inches)

relatively short duration, the precipitation map with the shortest duration available for this series (6-hr) was chosen.

The importance of snow in precipitation-frequency for the region will dictate which of the two indexes will apply better for the purpose of the study. It is known that at very high elevations snow can account for over 50% of the normal annual precipitation. However, that doesn't imply that snow contributes in the same proportion to the annual series of maximum 6hr or 24hr precipitation amounts. A study carried out by the NWS (NOAA, 1973b) for the State of Utah and other Rocky Mountain States analyzed the effect of snow occurrences on the mean annual precipitation. Precipitation-frequency analysis derived from two data sets were compared. One series containing precipitation amounts for each year, regardless of the type of precipitation, and a second series restricted solely to rainfall events. The study concluded that, for 2yr return period and durations of 24hr or less, the contribution of snow amount to precipitation-frequency values in the rainfall only series averages 10 to 15% smaller than the series using all precipitation amounts. Same analysis for the 25yr return period produced differences somewhat smaller. This indicates a tendency for the rare short-duration storm to occur in the warmer months as rain.

3.0 REGIONAL CHARACTERISTICS OF PEAK FLOWS SERIES

3.1 Hydrometeorological Mechanisms Producing Peak Flows

A critical aspect of flood frequency analysis is the understanding of the hydrometeorological mechanisms producing the peaks. Numerous studies in the past were focused in that direction. Specifically for the State of Utah, Thomas and Lindskov (1983) pointed out that annual peak flows at many streams in Utah can result from rainfall, snow melt or rain on snow, and consequently, a statistical flood frequency relation determined from an array of annual peaks from a mixed population usually does not adequately fit the larger peak flows. The two authors carried out an extensive study with the purpose of defining flood regions with unique statistical characteristics. They concluded that the upper altitudinal limit for floods caused by intense thunderstorms increased from North to South in the State. Flood regions were defined based on residual patterns, mean basin elevation of the gaging stations, and on the type of floods that have occurred at the gaging sites (snow melt, thunderstorm, frontal rainfall, or combination thereof). The reader can find a complete map of the State of Utah showing all flood regions in page 12 of the above reference. In an earlier work, Wooley (1946, p.50) also indicated that ".. Most of the cloudburst floods (produced by high intensity, short duration storms) originate in regions below the 8,000 ft altitude, in streams more or less directly exposed to the direction of storm travel".

Boundaries of flood regions intersecting our study area were approximately reproduced in Figure 2. Three flood regions cross the area, they are: the Low Plateau region (LP), the High Plateau region (HP) and the High Elevation subregion. Based on Thomas and Lindskov's classification criteria, only 4 gaging sites are part of the HP region, whereas the remaining 35 sites are contained within the LP region, see Table 1. The four HP sites are located in the North Fork of the Virgin River subbasin, upstream from the Park, next to the watershed divide in the Cascades Spring area. Catchments within the HP region, south of 38° latitude, should have a mean basin elevation greater than 8,000 ft and a study site datum greater than 7,000 ft. This is a mixed population flood area where infrequent thunderstorm floods can have greater magnitude than snow melt floods. Catchments within

the LP region, also south of 38° latitude, must have a mean basin elevation less than 8,000 ft and a study site datum less than 7,000 feet. Summer thunderstorms produce most of the large magnitude floods. Snow melt floods are rare and usually small.

Thomas and Lindskov (1983) flood areas can be interpreted as a stratified classification of the region where different flood producing mechanism are dominant. For instance, for basins south of latitude 39°, flood frequency relation at elevations below 7,000 feet are dominated by thunderstorms. Above 9,000 feet, flood frequency relations will be controlled by snow melt, except for recurrence intervals larger than 100 years where thunderstorms become significant again. The intermediate zone, between 7,000 feet and 9,000 feet, will have a mixed population. Another interesting conclusion from Thomas (1985), who proposes a composite flood-frequency analysis for gaging sites with mixed-populations of peak flows, is that for basins with gages around 6,000 ft in elevation and below (similar to sites of interest in Zion National Park), flood-frequency relations derived from the annual maximum peaks (without a prior disaggregation of populations) is adequate for the commonly used range of recurrence interval of 10 to 100 yrs.

Jarrett (1993) also found latitude-dependent elevation limits for different meteorological mechanisms producing floods in the Rocky Mountains region. Pons (1992) was also concerned with peak flows populations of mixed-origin. During his investigation, Pons selected four areas of the country with uniform hydrometeorological conditions to avoid problems associated with multiple flood producing mechanisms. The segregation of flow records in separate populations to reflect single peak producing mechanisms is certainly an ideal and desirable condition. However, the scarcity of peak flows records available for South-Western Utah precludes that approach for the majority of the gaging sites.

3.2 Seasonal Distribution and Duration of Peak Flows

Although Thomas and Lindskov (1983) when carrying out their multiregression analysis did not explicitly differentiated between snow melt and rainflood peaks (as done for instance by Peterson (1985) who estimates snow melt and thunderstorm flood magnitudes for specific drainages), they have implicitly taken into account the nature of the peak flows by incorporating mean basin elevation (together with drainage area) in the sets of regional

regression equations. The regional classification procedure implemented by Thomas and Lindskov was adopted in this study as a preliminary criterion for selecting gaging sites. It should provide some degree of hydrological homogeneity among peak flows records within the study area.

The objective of this section is to investigate the hypothesis that peaks within the study area are derived from a unique population. Although this is not a basic requirement of the proposed methodology of analysis, it helps remove sources of uncertainty concerning the proper fitting of the regional probabilistic model. Two representative watersheds with long and well established records were selected for comparison. The first watershed corresponds to the North Fork of the Virgin River. This catchment has a large drainage area extending from high elevation headwaters to a low elevation gaging site at 3,970 ft near the town of Springdale (site 23, ID: 09405500). The drainage network is mainly oriented in the north-south direction and subject to a strong gradient of total precipitation that ranges from 29 inches at the headwaters to 15 inches at the outlet per year (see Figure 11 in Diaz and Ismael, 1993). By contrast, the second watershed was chosen among the ones with the highest elevation, and small drainage area. The selected watershed is Coal Creek near Cedar City (site 38, ID: 10242000). It has an area of 81 mi^2, with its outlet at 6,000 ft, and a mean basin elevation of 8,640 ft. The location of the watersheds can be found in Figure 2.

Figure 6 displays the relative magnitude and the time of occurrence of flow peaks registered at sites 23 and 38, top and bottom graphs respectively. The horizontal axis indicates the month of the Julian-year at which a flow peak occurred, showing the empirical distribution of seasonal peak occurrence. The vertical axis plots the ratio between the magnitude of an instantaneous peak to the corresponding mean-daily flow. This graph provides information about the degree of "flashiness" of the peak events and their time of occurrence. There is a clear tendency for the peaks to occur during the summer season, July through September at both watersheds, though peaks also occur year around mostly at low elevation basins (see top graph). Furthermore, visual inspection of the annual hydrographs at Springdale allowed us to ascertain the preponderance of peak flows of rainfall origin over those of snow melt origin. It should be mentioned that partial series of peaks, instead of annual series, were used for creating Figure 6. Partial series include annual series plus

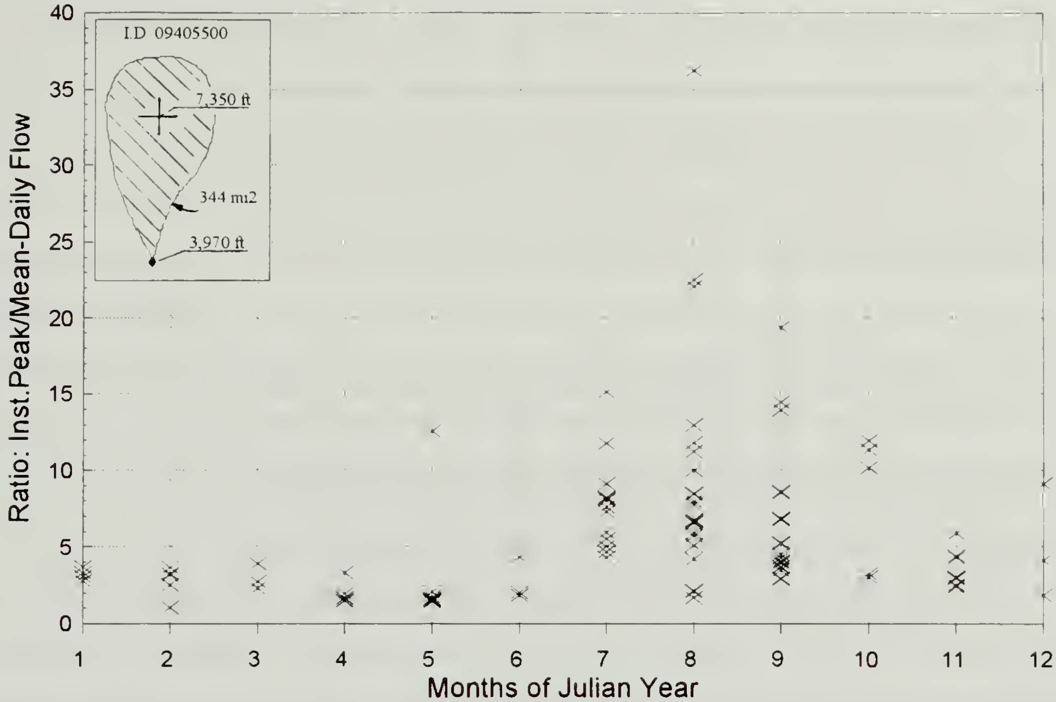

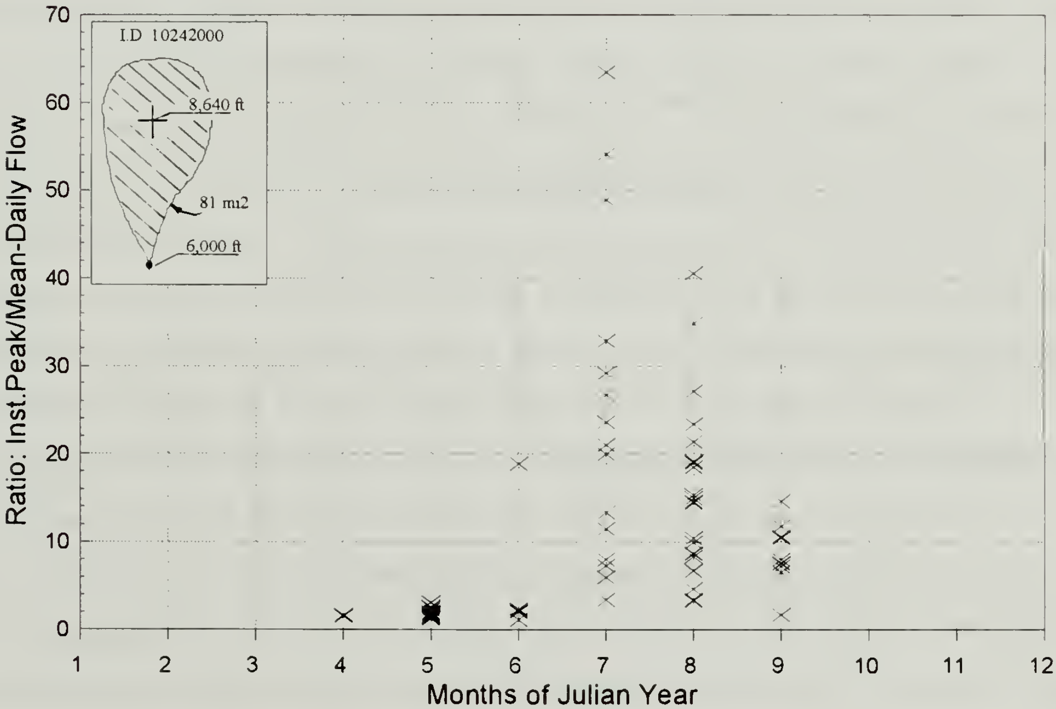

Fig.6 Relative Magnitude and Time of Occurrence of Peak Flows
(top) N. Fk. of the Virgin River near Springdale, and
(bottom) Coal Creek near Cedar

annual secondary peaks above a certain threshold flow ($Q_b = 550$ cfs at site 38 and $Q_b \approx 820$ cfs at site 23). The base flow level is usually selected such as on the average about three secondary peaks per year are included. When comparing the results of the analysis from both types of series it was found that practically the same magnitude of ratios and frequencies were depicted. Hence, partial series were finally adopted because of the larger number of peaks available, yielding more reliable estimates of the relative magnitude and time occurrence of peaks.

The peak-daily flow ratio can be interpreted as an indicator of the duration of the peaks (flashiness). The larger the ratio the shorter the duration of the peak, and vice versa. During the summer months, the ratio reaches magnitudes much larger than during the rest of the year. High intensity and short duration summer storms give rise to a sharp increase and fast decay of the hydrographs, with peaks reaching up to about 35 times the mean-daily flow for the same day at Springdale, and up to about 60 times at Coal Creek. On the other hand, during the snow melt season, usually occurring from late March through June, instantaneous peaks rarely exceed mean-daily flows more than 4 times. Remember that mean-daily flows during the snow melt season are substantially larger than during the rest of the year. This factor is mostly responsible for the low values of the ratios. In turn, peak events with the largest ratios within the snowfall or snow melt seasons correspond mostly to rainfall on snow events, whereas peak events of exclusively snow melt origin are the fewest and have the smallest ratios (close to 1). The repetitive nature of the snow melt peaks is confirmed by the low variance of the ratios during the months of April to June. Conversely, summer peaks display the largest variance as a result of the random nature of the rainfall events.

The peak-flow ratio can also be used to obtain indirect estimates of the expected magnitude of peaks for each season. Consider for instance the month of August at Springdale. The peak-flow ratio for that station during the 8^{th} month ranges from 1.7 to 36.2, with an average value of 9.6. From a previous study we know that base flow during August has a relatively uniform value of 64 cfs. By multiplying the last two figures, a peak flow of 614 cfs is obtained. This constitutes a reasonable estimate for an average rainfall peak to be expected during the month of August. Similar computation for the month of May yields an average peak flow of 500 cfs.

In summary, peak flows in the Zion region display mixed-population characteristics resulting from snow melt and rainfall events, with the latter as the predominant mechanism. The seasonal distribution and duration of peak flows at two stations representative of high and intermediate elevations also show similar characteristics. Peak-daily flow ratios are low and very constant (small variance) during the snow melt season, and large and highly variable during the months with convective summer storms (cloudbursts). There is little evidence of the occurrence of peaks outside the period May-September in high elevation basins (with datum over 6,000 ft). However, as mean basin elevation decreases, in addition to snow melt peaks and summer thunderstorms peaks, flow peaks are also induced by frontal systems moving across the state during the snow accumulation period.

3.3 Seasonal Distribution of the Number of Peaks

Specific environmental studies require information about the probability distribution of the number of peaks occurring at different periods of the year. For this purpose, the effect of seasonality on the occurrence of flow peaks and the underlying probability law have been examined. Zelenhasic (1970) presented a theoretical approach for the analysis of the stochastic properties of flow peaks. This approach considers the number of peaks occurring in a given time interval as well as the time when the peaks occur as random variables. Furthermore, it demonstrates that the probability distribution governing the occurrence of peaks follows a Poisson process.

The above cited methodology has been applied in this study to gain further insight into the probabilistic structure of the seasonal occurrence of peak flows in the Upper Virgin River basin. The gaging station chosen for analysis is Virgin River at Virgin (Site 25, ID: 09406000). This station measures flow peaks from the entire Upper Virgin River basin (956 mi^2). It has the longest flow record available, including a relatively large number of secondary peaks in record. The data are provided in Appendix III. The Virgin River data shows an adequate record of peaks flows, except during the early period 1910 to 1951, when secondary peaks were not tabulated. For the computations, the water-year is divided into nine periods, eight periods 40 days long and one period of 45 days. The beginning and end of the periods were selected to accommodate the observed seasonal distribution of peaks in

the Virgin River basin. Observed frequencies of peaks are obtained from the partial series for all nine periods. Table 2 provides a summary of the computations.

For example, water-year 1961 contains the third largest annual peak on record (13,500 cfs), and the largest number of secondary peaks registered (9 peaks). Six out this nine secondary peaks correspond to the same period. This is reflected in Table 2 (see Period 7) as one case observed ($F_{ob}=1$) when six peaks ($k=6$) occurred during the same period. In addition to the observed frequency, Table 2 provides the theoretical Poisson distribution (F_{th}) of peak occurrences during each period. The Poisson distribution has a single parameter λ

Table 2. Observed and Fitted Poisson Distribution of the Number of Peaks for Nine Periods

Per: 1	Dec 4 - Jan 17	
k	Fob	Fth.
0	144	144.083
1	5	4.835
2	0	0.081
3	0	0.001
4	0	0.000
5	0	
6	0	
Sum:	149	149.000
mean:	0.034	
variance:	0.033	
lambda:	0.00075	

Per: 2	Jan 18 - Feb 26	
k	Fob.	Fth.
0	145	143.158
1	2	5.726
2	2	0.115
3	0	0.002
4	0	0.000
5	0	
6	0	
Sum:	149	149.000
mean:	0.040	
variance:	0.066	
lambda:	0.00101	

Per: 3	Feb 27 - Apr 7	
k	Fob.	Fth.
0	139	138.372
1	9	10.240
2	1	0.379
3	0	0.009
4	0	0.000
5	0	
6	0	
Sum:	149	149.000
mean:	0.074	
variance:	0.082	
lambda:	0.00185	

Per: 4	Apr 8 - May 17	
k	Fob.	Fth
0	137	132.946
1	8	15.156
2	3	0.864
3	1	0.033
4	0	0.001
5	0	0.000
6	0	
Sum:	149	149.000
mean:	0.114	
variance:	0.183	
lambda:	0.00285	

Per: 5	May 18 - Jun 25	
k	Fob.	Fth.
0	144	144.083
1	5	4.835
2	0	0.081
3	0	0.001
4	0	0.000
5	0	
6	0	
Sum:	149	149.000
mean:	0.034	
variance:	0.033	
lambda:	0.00084	

Per: 6	Jun 26 - Aug 5	
k	Fob	Fth
0	123	120.203
1	21	25.815
2	4	2.772
3	1	0.198
4	0	0.011
5	0	0.000
6	0	
Sum:	149	149.000
mean:	0.215	
variance:	0.264	
lambda:	0.00537	

Per: 7	Aug 6 - Sep 14	
k	Fob	Fth
0	114	109.423
1	30	33.782
2	2	5.215
3	2	0.537
4	0	0.041
5	0	0.000
6	1	
Sum:	149	148.997
mean:	0.309	
variance:	0.526	
lambda:	0.00772	

Per: 8	Sep 15 - Oct 24	
k	Fob	Fth.
0	136	136.551
1	13	11.914
2	0	0.520
3	0	0.015
4	0	0.000
5	0	
6	0	
Sum:	149	149.000
mean:	0.087	
variance:	0.080	
lambda:	0.00218	

Per: 9	Oct 25 - Dec 3	
k	Fob.	Fth
0	139	138.396
1	9	10.217
2	1	0.377
3	0	0.009
4	0	0.000
5	0	
6	0	
Sum:	149	149.000
mean:	0.074	
variance:	0.082	
lambda:	0.00185	

(lambda). Its mean and variance are both equal to this parameter. The parameter λ is estimated for each period by the method of moments using information from the available samples. The conformance of the theoretical to the observed distributions was verified by the χ^2-test. The computed χ^2-values were below the critical χ^2-values at the 5% level of significance for each of the nine periods considered. Sample means and sample variances for the number of occurred peaks during the nine periods of the year are given in Table 2. As expected, similar values for the two parameters are obtained at each period. The nine parameters λ, expressed as number of events per day, are plotted in Figure 7 as the abscissas at the center of each time period. The λ values are then fitted by Fourier Series to generate a continuous function. The fitting yields a deterministic periodic function of time, $\lambda(t)$, with a one-year period as shown in Figure 7.

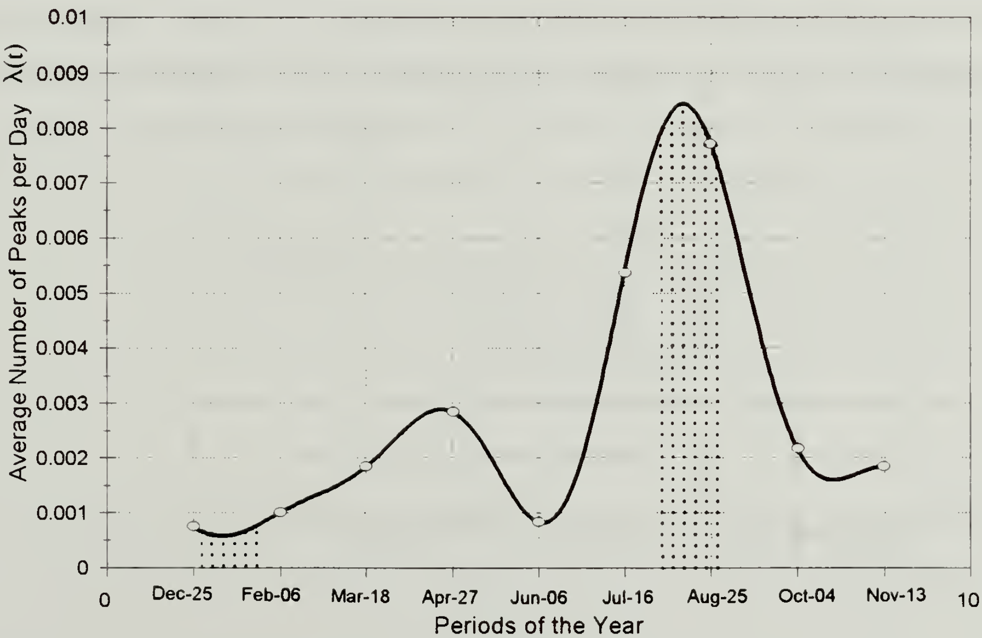

Fig.7 Seasonal Variation of the Average Number of Peaks per Day, $\lambda(t)$

Zelenhasic (1970) expresses the expected value of the number of exceedances $\eta(t)$ during a time interval [0,t] as,

$$E[\eta(t)] = \int_0^t \lambda(s)\, ds = \Lambda(t) \tag{3.1}$$

where $\Lambda(t)$ depends on $\lambda(s)$ which is the periodic nonlinear function portrayed in Figure 7. Then, the probability that exactly k peaks occur in a fixed period [0,t] is estimated by,

$$P[K=k] = \frac{[\Lambda(t)]^k \exp[-\Lambda(t)]}{k!}, \qquad k=0,1,2,\ldots\infty \tag{3.2}$$

Equation (3.2) can also be used to estimate the probability that k peaks will occur in a fixed time interval $[t_1,t_2]$, where t_1 and t_2 correspond for instance to the first and last day of a given month. As an illustration, we will determine the probability that at least two peaks (two or more peaks) will occur during the month of August , the month with the largest occurrence of peaks. From Eq.(3.1) and for the time interval corresponding to the month of August (indicated in Figure 7 with a dotted pattern), the average rate (of arrival) of the Poisson process is $\Lambda_{Aug} = 0.25$. Then,

$$\begin{aligned} P[K \geq 2] &= 1 - P[K<1] = 1 - F_K(1) \\ &= 1 - \frac{\sum_{k=0}^{k=1} e^{-0.25}\, 0.25^k}{k!} \\ &= 0.027 \end{aligned} \tag{3.3}$$

indicates that there is only a 2.7% of probability that two or more peaks above the base discharge (1,600 cfs) will occur at Virgin during August. Similarly, the probability of having at least one peak is equal to 22%, and the probability of not having any peak during August is 78%. For the month with the lowest number of peaks, January, similar computations yield: $\Lambda_{Jan} = 0.02$, a negligible probability for the case of two or more peaks, and 2% and 98% for one and zero peaks, respectively.

3.4 Graphical Estimation of Mean Annual Peaks

As mentioned briefly in Section 2.1.2, estimates of the long-term mean annual peak (MAP) at each gaging site should be determined in order to assess the conditions of hydrological homogeneity in the study area. This task is performed prior to the application of the multivariate flood frequency model. Peaks records were first extended to cover the longest possible common base-period. Then, each extended series of annual peaks were subject to a preliminary single-site frequency analysis. The preliminary analysis consisted on plotting annual peaks discharges versus recurrence intervals for each gaging station. Recurrence intervals were computed by arranging the data in decreasing order of magnitude and assigning a plotting position to the ranked values. The standard Weibull formula was used for this purpose. Although estimated peaks (obtained using the regression procedure) are part of the annual series used to rank the flows, they are not included in the frequency plots. Plots of the single-site frequency curves are included in this report as Appendix IV.

Using the plots in Appendix IV, the MAP at each gaging site is estimated graphically by determining the intersection of a visually fitted frequency curve with the vertical line corresponding to a recurrence interval of 2.7 yr. This recurrence interval approximately to the recurrence of the mean for the lognormal and log-Pearson type-III distributions. Frequency points were carefully fitted in the 1 yr to 10 yr recurrence interval. This graphical procedure to estimate the mean annual flood gives more weight to peaks occurring in the neighborhood of the mean. This approach contrasts with a simple arithmetic average of the peaks which would be heavily biased by infrequent peaks of very large magnitude. This is particularly critical in stations with very short records like the North Fork of the Virgin River below Bullock Canyon (ID: 09405420), for which the graphical mean (200 cfs) represents only 61% of the arithmetic mean (326 cfs). Conversely, for stations with long systematic records the arithmetic average and the graphical mean tend to coincide.

In addition to the MAPs, graphical estimates of flow levels for recurrence intervals of 5 yr and 10 yr were also obtained from the single-site plots. Table 3 provides a summary of all the information graphically derived. Single-sites frequency analysis were conducted for 28 out of the 39 records. Stations with very short records were not considered. The left portion of Table 3 includes basic statistics computed from the systematic records, and the

Table 3. Peak Flows Statistics and Quantiles for Extended Series

Site	USGS	Systematic Record of Annual Peaks									Extended Series of Annual Peaks					
			Flow Domain				Log(e) Domain				Quantiles and Ratios for Extended Series					
No.	I.D.	yrs. rec.	average	std. dev.	coef. var.	skew	average	std. dev.	coef. var.	skew	Yrs Ext.	Q10	Q5	Q2.7	Q10/Q2.7	Q5/Q2.7
1	09336400	16	1147	1299	1.13	2.68	6.6174	0.8758	0.13	0.58	35	3065	2135	1335	2.30	1.60
2	09337000	41	255	251	0.99	1.88	5.1019	0.9873	0.19	-0.33	49	540	370	240	2.25	1.54
3	09337500	38	1037	891	0.86	1.16	6.4941	1.0766	0.17	-0.82	52	2730	2140	1430	1.91	1.50
4	09338900	16	792	999	1.26	1.97	5.7126	1.6196	0.28	-0.52	35	2190	1505	910	2.41	1.65
5	09339200	10	1982	1337	0.67	0.77	7.2996	0.8533	0.12	-0.89						
6	09379800	14	1788	1303	0.73	0.78	7.1170	1.0031	0.14	-1.09	14	4120	2950	1885	2.19	1.56
7	09381100	16	1503	1796	1.19	2.47	6.8034	0.9708	0.14	0.54	43	2635	1780	1165	2.26	1.53
8	09381500	21	3497	2493	0.71	1.80	7.9494	0.6334	0.08	0.38	43	6230	4840	3550	1.75	1.36
9	09381800	15	3697	3694	1.00	2.36	7.8362	0.8545	0.11	0.31	43	6200	4375	2925	2.12	1.50
10	09403500	16	848	625	0.74	0.42	6.2713	1.1844	0.19	-1.10	35	1980	1650	1290	1.53	1.28
11	09403600	25	697	713	1.02	1.73	5.9718	1.1787	0.20	-0.36	35	1960	1375	850	2.31	1.62
12	09403700	16	1207	734	0.61	0.23	6.7473	1.0403	0.15	-1.47	35	2240	1890	1485	1.51	1.27
13	09404450	27	170	184	1.08	1.78	4.6501	0.9625	0.21	0.44	35	470	320	195	2.41	1.64
14	09404500	14	640	873	1.36	2.10	5.2127	1.9636	0.38	-0.56	35	2410	1780	1105	2.18	1.61
15	09404900	2	1220				6.8925									
16	09405200	7	29				2.9336									
17	09405250	7	30				3.0102									
18	09405300	5	770				6.4228									
19	09405400	6	20				2.7057									
20	09405420	11	326	450	1.38	3.23	5.3669	0.7495	0.14	1.94	35	255	220	200	1.28	1.10
21	09405450	4	286				5.5087									
22	09405490	2	1760				7.4548									
23	09405500	70	2184	1619	0.74	1.87	7.4512	0.6920	0.09	0.07	84	4535	3345	2285	1.98	1.46
24	09405900	9	1112	833	0.75	1.20	6.7414	0.7386	0.11	0.28	35	4945	3690	2520	1.96	1.46
25	09406000	77	4925	3933	0.80	1.91	8.2367	0.7231	0.09	0.16	84	10470	7510	5075	2.06	1.48
26	09406150	7	1183				6.5306									
27	09406300	23	251	265	1.05	1.49	4.9603	1.1021	0.22	0.09	34	575	370	220	2.61	1.68
28	09406500	8	991				6.7269									
29	09406700	16	369	458	1.24	2.61	5.2782	1.1808	0.22	-0.20	35	730	475	290	2.52	1.64
30	09406800	14	307	291	0.95	1.32	5.2538	1.0223	0.19	-0.15						
31	09408000	30	716	1026	1.43	2.25	5.4684	1.6933	0.31	-0.26	35	2090	1235	655	3.19	1.89
32	09408400	34	115	140	1.21	3.40	4.3071	0.8870	0.21	0.53	35	255	160	95	2.68	1.68
33	09409500	15	530	618	1.16	1.28	5.3248	1.5575	0.29	-0.10	39	1080	685	400	2.70	1.71
34	10174500	69	654	315	0.48	0.69	6.3628	0.5052	0.08	-0.24	69	1160	960	720	1.61	1.33
35	10241400	21	93	116	1.24	1.29	3.6277	1.4131	0.39	0.29	35	250	170	100	2.50	1.70
36	10241470	23	100	102	1.02	1.30	4.0837	1.0257	0.25	0.32	35	265	185	110	2.41	1.68
37	10241600	23	177	253	1.43	1.81	4.2931	1.2891	0.30	0.59	35	495	300	160	3.09	1.88
38	10242000	63	1120	1047	0.93	1.63	6.6014	0.9592	0.15	-0.20	63	2580	1820	1150	2.24	1.58
39	10242100	16	346	257	0.74	1.67	5.6036	0.6951	0.12	0.13	35	780	610	430	1.81	1.42
Average		22	997	964	1.00	1.70	5.8188	1.0479	0.19	-0.05					2.21	1.55
Std Dev					0.26	0.74	1.3783	0.3295	0.08	0.65					0.44	0.17

right gives flow levels for three different quantiles. The significance of the ratios $Q_{10/2.7}$ and $Q_{5/2.7}$ will be discussed latter in Section 3.5.

Only systematic records of peak flows were considered for the frequency analysis. This study recognizes the importance of historic flows in the computation of flood frequency analysis. For instance, Webb and Baker (1987) analyzed the effect of incorporating estimated historic floods (floods not included in the systematic record) in the computation of the flood frequency on the Escalante River (site 3 in our study). However, the addition of historic peaks (with very high return periods, around and over 100 yr) practically doesn't change the distribution of peaks for low return periods (in the 1 to 5 yr range), as it can be inferred from Webb and Baker's study. Furthermore, a basin-wide effort to detect and estimate historical peak flows is beyond the scope of this study.

3.5 Langbein's Homogeneity Test

A customary reference to analyze hydrological homogeneity for a regional flood frequency analysis is the test developed by W.B. Langbein of the U.S. Geological Survey. Langbein conceived an statistical test based on comparing the slope of frequency curves from individual streams within a study region. The underlying assumption is that if individual streams having a wide range of drainage areas have frequency curves of about equal steepness, the records of peaks will be homogeneous with respect to the flood-producing mechanism. The variation of these slopes can be tested to see whether the spread could occur by chance among samples from the same population due simply to sample variability. The problem is then to calculate the spread to be expected, and to set limits to the spread that is acceptable. Details of the formulation of Langbein's test can be found in Dalrymple (1960).

In Langbein's test the slope of the frequency curves is measured by the ratio of the 10 yr to the 2.33 yr flood (the Gumbel distribution is used by Langbein to represent extreme events). In our study mean annual peaks are associated with a slightly different recurrence interval, 2.7 yr. The acceptable spread of the ratio is associated with the standard deviation of the reduce variate of the Gumbel distribution. Typically 2 standard deviations are adopted. This implies that the permissible range should contain 95% of the possible

observations. The 10 yr flood has been used to compute the slope since this is the longest recurrence interval for which many records will give dependable estimates. Flood ratios have been computed for 27 out of the 39 gaging sites based on the extended series of peak flows. The remaining 12 stations have records too short to be considered for this analysis. Sequential steps of the computational procedure are included in Table 4. The last two columns in Table 4 provide the plotting coordinates for the stations in Langbein's test chart. Tr is the recurrence interval estimated from the single-site frequency curve for a flow level given by the product of $Q_{2.7}$ times the average ratio. The adjusted period of record is computed as the length of the systematic record plus half the length of the extended portion of the record.

Table 4. Data for Langbein's Homogeneity Test

Site No.	USGS I.D.	Mean Ann. Q2.7	Ratio Q10/Q2.7	Q2.7 x Avg. Rat	Tr for prev. column	Adjusted Per. Rec.
1	09336400	1335	2.30	2739	8.0	26
2	09337000	240	2.25	492	8.5	45
3	09337500	1430	1.91	2934	12.9	45
4	09338900	910	2.41	1867	7.3	26
6	09379800	1885	2.19	3867	8.7	14
7	09381100	1165	2.26	2390	8.3	30
8	09381500	3550	1.75	7284	14.0	32
9	09381800	2925	2.12	6001	9.1	29
10	09403500	1290	1.53	2647	60.0	26
11	09403600	850	2.31	1744	7.8	30
12	09403700	1485	1.51	3047	80.0	26
13	09404450	195	2.41	400	7.2	31
14	09404500	1105	2.18	2267	8.3	25
23	09405500	2285	1.98	4688	11.5	77
24	09405900	2520	1.96	5170	12.0	22
25	09406000	5075	2.06	10412	10.0	81
27	09406300	220	2.61	451	6.8	29
29	09406700	290	2.52	595	7.1	26
31	09408000	655	3.19	1344	5.4	33
32	09408400	95	2.68	195	6.9	35
33	09409500	400	2.70	821	6.5	27
34	10174500	720	1.61	1477	50.0	69
35	10241400	100	2.50	205	6.4	28
36	10241470	110	2.41	226	7.3	29
37	10241600	160	3.09	328	5.5	29
38	10242000	1150	2.24	2359	8.2	63
39	10241000	430	1.81	882	14.2	26
Average Ratio			**2.21**			

The test chart in Figure 8 displays the set of test curves that show within what range of recurrence intervals an estimate of the 10 yr flood should be for a specified length of record. Stations that plot within the two bounds can be considered to be homogeneous according to Langbein's criterion, and therefore can be considered as potential candidates for regional flood frequency analysis. Only three stations, sites 10, 12 and 34 lay outside the confidence bands. The three stations have flood ratios noticeably lower than the average ratio (2.21) for the entire set. This is also reflected by the marked downward curvature of their frequency curves presented in Appendix IV. A close examination of the annual series of flow peaks at site 34, Sevier River at Hatch, help us explaining the large departure in plotting position of this site from the rest of the stations. It was observed that 74% of the 69 registered peaks occurred from late March to early June, the snow melt season (most of them during May). This finding certainly contradicts the initial supposition of rainfall being the dominant mechanism producing floods. The other two stations, sites 10 and 12, showed a more balanced partition between snow melt and rainfall peaks, however, the short records available at both sites prevent us from further examination.

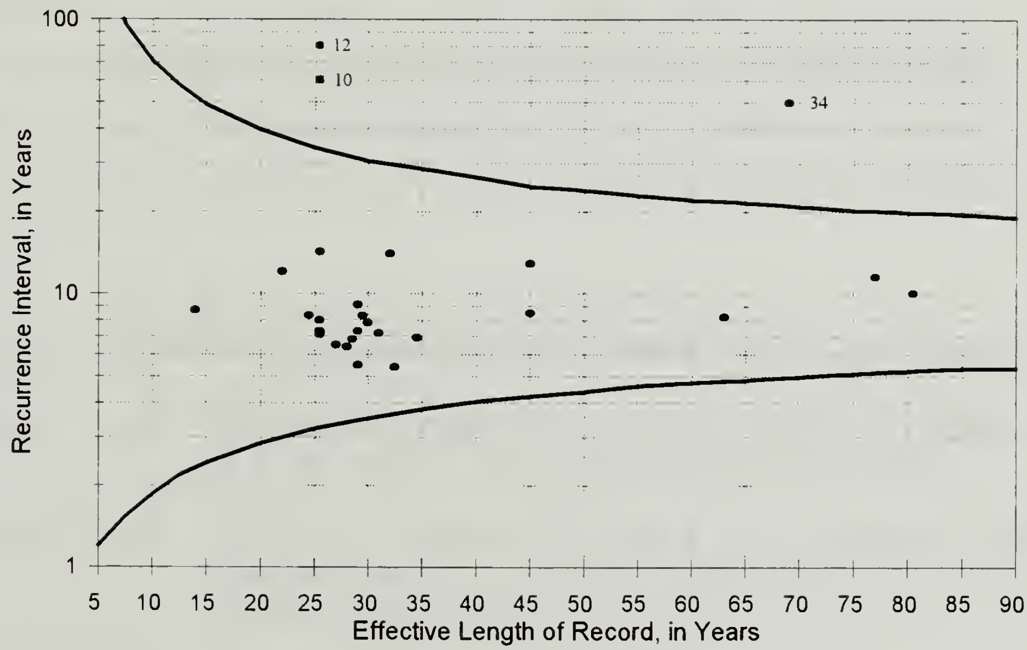

Fig.8 Langbein's Homogeneity Test Chart

3.6 Regional Prediction of Mean Annual Peak

Abundant literature can be found since the early 1960's that analyzes the statistical relation between mean annual floods estimated at several sites in an homogeneous region and explanatory hydrological variables. The procedure consists on regionalizing the peaks data on the basis of physiographic characteristics of river catchment, characteristics of precipitation, or other meteorological characteristics of various types. This approach is also part of the Generalized Least-Square Method, currently being used by the USGS for regional flood frequency analysis, where different return period quantiles are related to basin characteristics via multiple regression. Based on results from previous investigations, this study has identified a set of hydrologic variables that may affect the occurrence of floods in the region where Zion National Park is located. An important requirement for the selection of the independent variables was that they have to be readily obtainable from topographic and meteorological maps. Compilation of the hydro-meteorological characteristics for all the watersheds was a tedious and time consuming task despite the use of the GIS developed for the study region. Several maps of the watersheds generated during this stage of the work are included in Appendix V. The maps show: boundaries of the watersheds, general drainage network and the adopted main water-course (to measure channel length and slope), location of the basin centroid and flow gaging site, and isopluvials of precipitation intensity. Table 5 contains a summary of the compiled geographical and meteorological information for all watersheds with the exception of site 30 (site 30 was only used for peaks data extension purposes).

A brief description of the hydrological characteristics listed in Table 5 follows:

Gage Datum (D) — indicates the elevation of the terrain where the USGS gaging station is or was located. Data obtained from USGS records.

Watershed Centroid — indicates the location of the centroid of the watershed. Latitude and longitude coordinates expressed in degree-minute-second. Data obtained from the GIS.

Drainage Area (A) — gives the areal extent of the watershed contributing to peak discharge,expressed in square miles. Data obtained from the GIS.

Table 5. Geographical and Meteorological Characteristics of Watersheds

USGS Gaging Station			Watershed Centroid		Drainage	Mean Basin	Channel Characteristics				Channel	50%-6hr	2yr-24hr
Site No.	I.D.	Datum (ft)	Latitud	Longitud	Area (GIS) (mi2)	Elevation (ft)	El.@ 10%L (ft)	El.@ 85%L (ft)	10-85%Len (mi)	Total Lngth (mi)	Slope (ft/mi)	Precip.Int. (inches)	Precip.Int. (inches)
1	09336400	6250	37 41 52	111 48 34	54.79	7620	6400	7350	9.48	12.64	100.2	1.07	1.59
2	09337000	6400	37 59 34	111 39 29	66.43	8890	6420	9960	13.60	18.14	260.2	1.17	1.95
3	09337500	5670	37 50 48	111 44 21	317.44	8030	5780	7210	17.24	22.99	82.9	1.07	1.76
4	09338900	5700	37 57 50	111 22 52	65.79	7680	5800	8920	12.59	16.79	247.8	1.05	1.70
5	09339200	5080	37 32 39	111 31 55	145.55	6170	5160	6670	24.38	32.51	61.9	0.90	1.39
6	09379800	4240	37 10 55	111 49 40	90.73	5110	4290	5380	16.36	21.81	66.6	0.95	1.30
7	09381100	5980	37 37 08	111 52 56	21.75	7120	6220	7300	11.27	15.02	95.9	1.05	1.52
8	09381500	5440	37 37 15	112 00 14	200.95	6890	5590	7640	19.32	25.76	106.1	1.03	1.46
9	09381800	4300	37 26 50	111 59 40	649.03	6390	4410	6550	48.35	64.46	44.3	0.96	1.38
10	09403500	6220	37 23 58	112 27 19	73.51	7250	6240	7480	14.74	19.65	84.1	1.19	1.78
11	09403600	5060	37 15 53	112 30 30	192.64	6670	5130	7060	29.07	38.76	66.4	1.12	1.62
12	09403700	5000	37 12 39	112 21 02	245.92	6300	5200	6560	25.71	34.28	52.9	1.05	1.48
13	09404450	5900	37 24 50	112 35 09	74.30	7300	6030	7140	10.12	13.49	109.7	1.17	1.75
14	09404500	5620	37 15 23	112 44 43	5.57	6110	5610	5950	2.56	3.42	132.8	1.12	1.68
15	09404900	3940	37 15 59	112 42 10	343.48		4200	6760	36.06	48.08	71.0	1.11	1.56
16	09405200	7680	37 33 34	112 52 35	6.84	8484	7780	9080	3.58	4.78	363.0	1.42	2.22
17	09405250	7640	37 31 52	112 51 02	9.33	7818	7720	8650	3.03	4.03	307.3	1.45	2.24
18	09405300	8320	37 31 38	113 02 41	10.22	7592	8420	9580	3.15	4.21	367.8	1.32	2.04
19	09405400	7530	37 29 46	112 46 37	5.65		7650	8560	2.22	2.95	410.6	1.42	2.22
20	09405420	6420	37 27 58	112 47 13	29.51		6590	8150	5.58	7.44	279.6	1.37	2.04
21	09405450	6000	37 26 56	112 46 59	45.35	8010	6120	7940	8.00	10.67	227.5	1.35	2.04
22	09405490	4400	37 26 17	112 54 09	288.18		4550	7580	19.35	25.80	156.6	1.29	1.97
23	09405500	3970	37 24 30	112 54 11	343.42	7350	4250	7330	24.47	32.62	125.9	1.28	1.94
24	09405900	3680	37 18 54	113 05 41	95.12	6542	3810	6350	12.15	16.21	209.0	1.12	1.76
25	09406000	3440	37 18 10	112 52 30	956.40	6400	3580	6610	38.54	51.39	78.6	1.24	1.82
26	09406150	3040	37 22 52	113 10 01	96.28		3160	6200	23.80	31.73	127.7	1.06	1.66
27	09406300	5680	37 31 54	113 07 13	9.84	7950	5880	8040	4.60	6.13	470.0	1.12	1.85
28	09406500	4450	37 29 34	113 15 41	132.98		4750	7030	12.80	17.07	178.1	0.99	1.58
29	09406700	5290	37 22 54	113 22 03	11.13	7210	5430	7200	3.55	4.74	498.5	1.22	1.90
30	09406800	4100				6720							
31	09408000	4000	37 18 42	113 24 51	15.56	6360	4220	6640	6.35	8.46	381.2	1.08	1.69
32	09408400	6640	37 22 06	113 26 35	18.67	8720	6730	9120	4.73	6.31	505.3	1.31	2.14
33	09409500	4800	37 27 53	113 48 35	33.96	6070	5140	6380	9.29	12.39	133.4	1.02	1.57
34	10174500	6870	37 34 09	112 36 41	332.32	8480	6920	8170	22.07	29.42	56.6	0.98	1.54
35	10241400	6740	37 52 46	112 39 12	16.04	7470	6910	8100	5.33	7.38	223.1	0.97	1.59
36	10241470	6900	37 44 36	112 47 42	14.05	8450	6850	10040	5.93	7.91	537.9	1.13	1.87
37	10241600	6313	37 43 59	112 53 56	23.75	8230	6740	9200	7.08	9.44	347.5	1.08	1.58
38	10242000	6000	37 37 53	112 56 21	80.39	8640	6200	8290	11.08	14.77	188.6	1.14	1.75
39	10242100	5835	37 35 26	113 03 57	12.94	8032	5910	8030	4.22	5.62	502.7	1.19	1.97
Max.		8320			956.40	8890			48.35	64.46	537.9	1.45	2.24
Min		3040			5.57	5110			2.22	2.95	44.3	0.90	1.30

Mean Basin El. (E) measures the median elevation of the watershed, in feet. It can be interpreted as an index of the orographic effect in the type of precipitation in the basin. Data obtained from the USGS and GIS.

Channel Length (L) measures the length of the main water course from the watershed outlet to the basin divide, in miles. The selected channel is not necessarily the one with the longest path, but the stream suspected to be the larger contributor of peaks. Data obtained from the GIS.

Channel Slope (S) indicates the average rate of change in elevation of the main channel, in feet per mile, measured from the 10th to the 85th percentile of the

		total channel length upstream from the gage. This is an indirect measure of the basin gradient. Data obtained from the GIS.
Precip. Inten. (50%-6hr)	(P_6)	a precipitation-frequency index based exclusively on rainstorms with a 50% exceedanceprobability and a 6-hour duration. The value of the variable, in inches, is associated with a point probability at the basin centroid. Derived from NWS map using the GIS.
Precip. Inten. (2yr-24hr)	(P_{24})	a precipitation-frequency index representing the occurrence of all precipitation events with a recurrence interval of 2-years and 24-hour duration. P_{24} was obtained in the same form as P_6.

Figure 9 shows descriptive plots where $Q_{2.7}$, the explained variable, is individually related to six of the hydrological factors (explanatory variables) affecting the magnitude of peaks. They are: drainage area, gage datum, mean basin elevation, channel length, channel slope and precipitation intensity. Overall, the six bivariate correlations (in the logarithmic domain) give satisfactory results. In particular, log-Area, log-Slope, log-Length and Log-Datum depict strong correlative associations with log-$Q_{2.7}$. Mean basin elevation and precipitation intensity show somewhat larger scatter than the previous four variables, but still clear relationships can be noted. It is hoped that when the NWS releases the new precipitation maps for south-western Utah the P_{24} relation can be improved. The relation between log-$Q_{2.7}$ and log-P_6 (not shown) was observed to be the weakest. The same simple correlation task was conducted using log-MAP as the dependent variable. Results were similar to those found for $Q_{2.7}$, except that a larger number of sites, 38 instead of 28, were include in the latter analysis. The log-domain is used for the plots in Figure 9 to reflect the same type of relations used in the regional multivariate model to be introduced in Section 4.

It should be pointed out that the basin characteristics mentioned above are not independent among themselves. Several of them are significantly interrelated such as drainage area and channel length, channel slope and gage datum, etc. Related hydrologic characteristics should not be used together for predicting purposes. Our objective now is to identify the most efficient combination of hydrological factors in explaining the variations in the mean of peak flows within the study region. There is a statistically defined limit to the number of variables necessary to relate the mean annual peaks to basin characteristics.

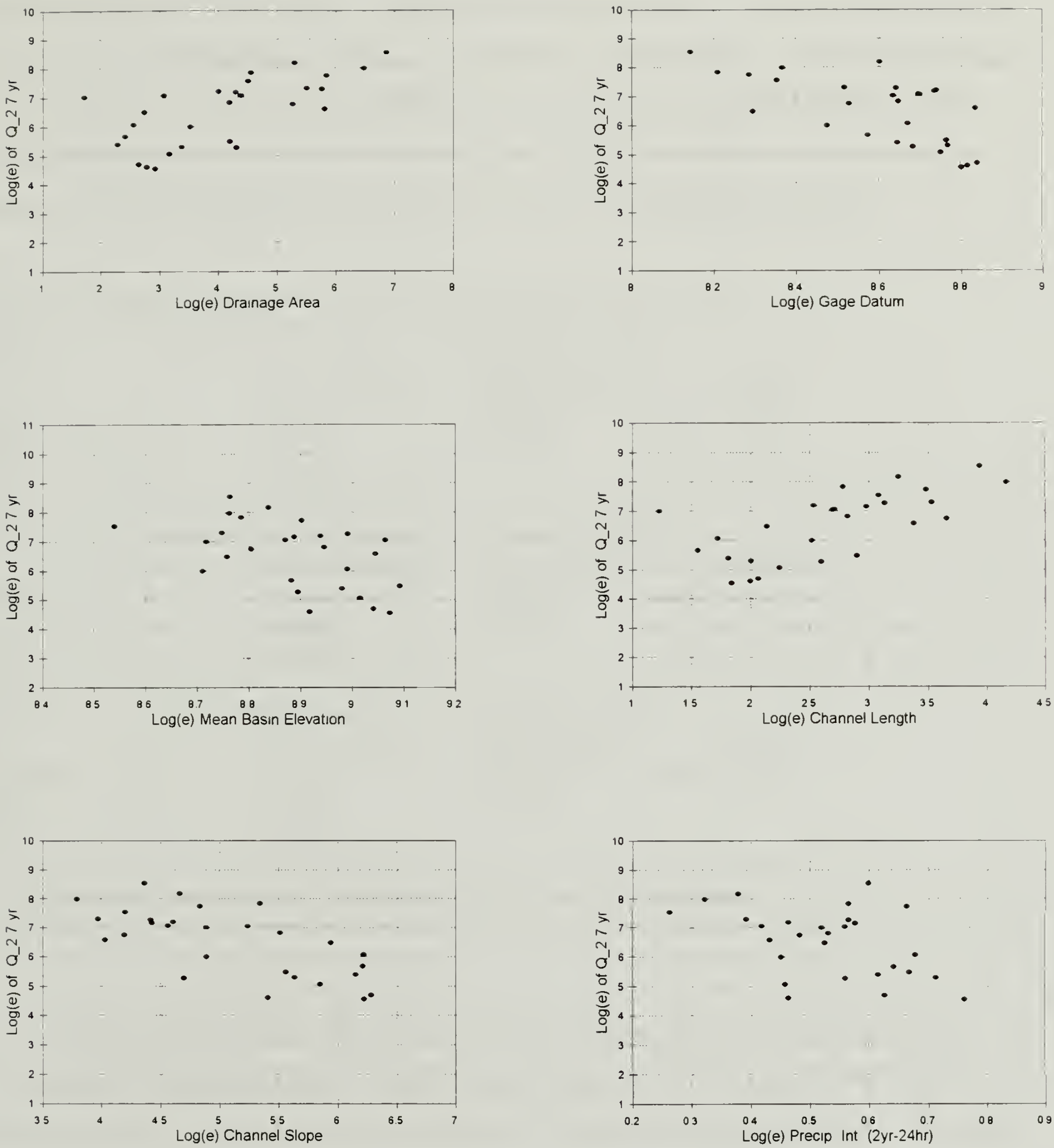

Fig.9 Descriptive Plots of Mean Annual Peaks ($Q_{2.7}$) vs. Hydrological Factors

The independent variables are selected using multiple linear regression analysis with stepwise technique. Variables are included in the order determined by the amount of contribution to variance reduction. The F-value is the criterion used to decide the inclusion of a hydrologic characteristic in the regression equation. Variables are added one by one to the model and the F-statistic for a variable to be added must be significant at a predefined level. The stepwise process ends when none of the variables outside the model has a significant F-statistic. Table 6 provides a summary of the results of the stepwise procedure.

Table 6. Summary of Stepwise Procedure for Dependent Variable MAP

Step 1	Variable AREA Entered		R-square = 0.63		
	DF	Sum of Squares	Mean Square	F	Prob > F
Regression	1	46.2338	46.2338	60.47	0.0001
Error	36	27.5241	0.76456		
Total	37	73.7579			
Step 2	Variable DATUM Entered		R-square = 0.67		
	DF	Sum of Squares	Mean Square	F	Prob > F
Regression	2	49.6594	24.8297	36.06	0.0001
Error	35	24.0985	0.68853		
Total	37	73.7579			
Step 3	Variable PRE24 Entered		R-square = 0.70		
	DF	Sum of Squares	Mean Square	F	Prob > F
Regression	3	51.6040	17.2013	26.40	0.0001
Error	34	22.1539	0.65159		
Total	37	73.7579			
No other variable met the 0.150 significance level for entry into the model					

Notice in Table 6 that 70% of the regional variance of the mean of log-peaks is explained by the first three factors entered into the model, with log-area as the single dominating factor. All variables in the model are significant at the 0.150 level. No other variable met the 0.150 significance level for entry into the model. This finding represents a typical result. However, A, D and P_{24} should not be interpreted as the only variables affecting flow peaks, but rather they represent the most efficient subset of basin character-

istics available to predict peaks. In fact, when the stepwise procedure was repeated to predict $Q_{2.7}$, this time only two variables were entered to form the predictive model, S and D, explaining 71% of the $Q_{2.7}$ regional variance. Figure 10 is another way to represent the results of the multiple regression analysis by plotting observed versus predicted log-mean annual peaks (graphical estimate $Q_{2.7}$). Figure 10 shows an acceptable scatter of the points around the 45° line. The predicting capability of the model can still be improved if limitations are imposed on the range of those basin characteristics considered in the regressions, in other words, if a more homogeneous region is defined. In summary, four hydrologic factors were identified as potential predictors of mean annual peaks in the Zion region, they are: drainage area, gage elevation, channel slope and precipitation intensity. More details about the final form of the model adopted to represent mean-annual peaks are given in Sections 4.1 and 5.3.

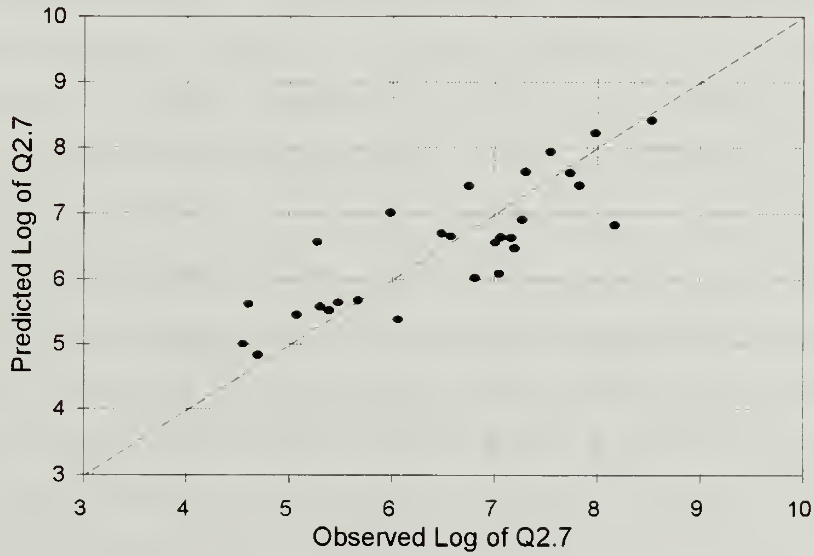

Fig.10 Observed vs. Predicted Log of Mean Annual Peaks ($Q_{2.7}$)

4.0 MULTIVARIATE LOGNORMAL MODELS

4.1 Regional Multivariate Lognormal-2 Model

Many hydrologic variables are measured from the base zero and have no upper bound. This causes their distributions to be asymmetrical. It has been found through extensive experience (Yevjevich, 1982) that the lognormal probability distribution fits well these positively skewed distributions in hydrology, including frequency of floods. The lognormal distribution has been widely used in its univariate form for flood frequency modeling. Specifically within the study area, frequency analysis at a single site showed the log-Pearson type III and lognormal distributions equally suitable for representing maximum annual peaks at the N. Fk. Virgin River near Springdale (ID: 09405500) (Diaz, 1992). The similar fitting of these two distributions should be expected since watersheds in the proximity of Zion National Park are located in a region of the country where the generalized skew coefficient for peak flows series is practically zero (U.S. Water Resources Council, 1981).

Although alternative distributions have been found in some cases even more appropriate than the lognormal distribution for flood frequency modelling, they are very difficult to deal with in their multivariate forms. This study applies the outcome of a recent research project, Pons (1992), who developed a methodology for regional flood frequency analysis based on multivariate lognormal models. Pons chose the multivariate lognormal distribution with 2 and 3 parameters, MLN2 and MLN3 respectively, because they have a relatively simple form while still maintaining the most important characteristics needed for flood frequency analysis. The following sections present excerpts from Pons' dissertation, including the models formulation and parameter estimation procedures. The interested reader should consult the aforementioned reference for a thorough description and discussion of the definition and testing of the models.

4.1.1 MLN2 - Model Formulation

Basically, the lognormal distribution represents the normal distribution of the logarithms of a selected random variable, in this case, annual peaks. That is, if the

logarithms of annual peaks $y=\ln(x)$ are normally distributed, then the variable x is considered to be logarithmic-normally distributed. Distribution theory provides the following properties of the marginals of the multivariate lognormal-2 distribution,

$$Y_j = \ln(X_j) \sim N\left(\mu_j(y), \sigma_j^2(y)\right) \tag{4.1}$$

$$\mu_j(x) = e^{\mu_j(y)+\frac{1}{2}\sigma_j^2(y)} \tag{4.2}$$

$$\sigma_j^2(x) = e^{2\mu_j(y)+\sigma_j^2(y)}\left(e^{\sigma_j^2(y)}-1\right) \tag{4.3}$$

$$\eta_j^2(x) = e^{\sigma_j^2(y)}-1 \tag{4.4}$$

$$\gamma_j(x) = \eta_j^3(x)+3\,\eta_j(x) \tag{4.5}$$

where $\mu_j(x)$ is the mean at site j, $\sigma_j^2(x)$ is the variance at site j, $\eta_j(x)$ is the coefficient of variation at site j and $\gamma_j(x)$ is the coefficient of skewness at site j of the untransformed flood variable. Likewise, $\mu_j(y)$ is the mean of the log-transformed variable at site j and $\sigma_j^2(y)$ is the variance of the log-transformed variable. From Eqs.(4.4) and (4.5) we can see that if two marginals at different sites have equal values of the parameter $\sigma_j^2(y)$, they will have equal coefficient of variation and equal coefficient of skewness. This constitutes a restriction imposed by this distribution, characterized by a fixed relationship between the coefficient of variation and the coefficient of skewness.

Similar to other existing methodologies dealing with regional floods analysis, the formulation of this model assumes that the mean of maximum annual peak series can be related to geographic and climatological characteristics of the catchments. The decision as to which basin characteristics to consider has been investigated in Section 3.6. It is based on the contribution of each added parameter to the reduction of error variance in the regression equations for the mean and the basin characteristics . Pons relates the mean of peak flows to basin characteristics by building a regression model for the mean $\mu_j(y)$ of log-transformed peak flows at site j in the following manner,

$$\mu_j(x) = e^{\mu_j(y) + \frac{1}{2}\sigma_j^2(y)} = C\, A_j^a\, S_j^s\, P_j^p \tag{4.6}$$

where three of the four hydrologic factors identified in Section 3.6 were chosen: A_j is the drainage area at site j, S_j is the main channel slope at site j and P_j is the precipitation intensity at site j. It should be noted that the addition of extra physical characteristics to the model translates into additional parameters. Adopting the assumption that $\sigma_j^2(y)$ is constant for the region and equal to $\sigma^2(y)$, Eq.(4.6) can be written as

$$\mu_j(y) = c + a \ln(A_j) + s \ln(S_j) + p \ln(P_j) \tag{4.7}$$

As indicated earlier, the assumption of a constant value of the parameter $\sigma_j^2(y)$ for the region implies that also the coefficient of variation and the coefficient of skewness should be constant throughout the region. In addition, in a hydrological region where the flood producing mechanism is basically unique, a relationship between the cross correlation coefficients of the logs of peak flows data and the inter-gaging station distances can be built. Pons (1992) uses a negative exponential function of the form,

$$\rho_{ij}(y) = e^{-b\, d_{ij}} \tag{4.8}$$

where b is a regional parameter and d_{ij} is the distance between stations i and j. Though not included here, Pons demonstrates that the cross correlation between the transformed series and the cross correlation between the untransformed series are functionally related with the regional variance of the logs $\sigma^2(y)$. All the above assumptions permitted Pons justify the following form of the lognormal-2 multivariate model,

$$f(\underline{y}) = (2\pi)^{-\frac{m}{2}} |V|^{-\frac{1}{2}} e^{-\frac{1}{2}(\underline{y}-\boldsymbol{\mu}(y))' V^{-1} (\underline{y}-\boldsymbol{\mu}(y))} \tag{4.9}$$

where V and $\boldsymbol{\mu}(y)$ are defined below, and ' denotes the transpose of the vector,

$$
\underline{\mu}(y) = \begin{Bmatrix} \mu_1(y) \\ \mu_2(y) \\ \vdots \\ \vdots \\ \mu_m(y) \end{Bmatrix} = \begin{Bmatrix} c + a\ln(A_1) + s\ln(S_1) + p\ln(P_1) \\ c + a\ln(A_2) + s\ln(S_2) + p\ln(P_2) \\ \vdots \\ \vdots \\ c + a\ln(A_m) + s\ln(S_m) + p\ln(P_m) \end{Bmatrix} \tag{4.10}
$$

and

$$
V = \begin{bmatrix} \sigma^2(y) & e^{-b d_{12}}\sigma^2(y) & e^{-b d_{13}}\sigma^2(y) & \dots\dots & \dots\dots & e^{-b d_{1m}}\sigma^2(y) \\ & \sigma^2(y) & e^{-b d_{23}}\sigma^2(y) & \dots\dots & \dots\dots & e^{-b d_{2m}}\sigma^2(y) \\ & & \sigma^2(y) & \dots\dots & \dots\dots & e^{-b d_{3m}}\sigma^2(y) \\ & & & & & \vdots \\ & & & & & \sigma^2(y) \end{bmatrix} \tag{4.11}
$$

where m is the number of gaging stations. In conclusion, the untransformed series of peak flows will be multivariate lognormal with marginal distributions having the mean expressed as a function of basin characteristics, a common coefficient of variation, and a common coefficient of skewness.

4.1.2 MLN2 - Preliminary Estimation of Parameters

The parameters of the model: c, a, s, p, b and $\sigma^2(y)$, are ultimately estimated using the maximum likelihood procedure presented in Section 4.1.3. However, since the equations derived from that procedure cannot be solved explicitly, the optimization algorithm set up to search for the optimum set of parameters needs to be initialized with a set of initial estimates of the searched parameters. This is a feasible task since all parameters have a statistical meaning. For instance:

- initial estimates for c, a, s and p are obtained from a multiple linear regression of the mean of log-transformed peak flows, $\underline{\mu}(y)$, as the dependent variable, versus the logarithm of area, logarithm of slope, and logarithm of precipitation intensity as the independent variables.

- parameter b is estimated as the slope of the regression line of the cross correlation coefficients of the log-transformed peaks versus inter-station distances, forcing the intercept through zero to equal one.
- the variance of the log-transformed peak flows $\sigma^2(y)$ is initially estimated as the weighted average of the individual variances of the log transformed data, with weights equal to the lengths of the individual records.

4.1.3 MLN2 - Maximum Likelihood Estimation of Parameters

Maximum likelihood estimation produces estimates that posses desirable characteristics such as consistency, and also of efficiency and asymptotic normality under certain regularity conditions. For the MLN2 model these regularity conditions are satisfied, allowing the derivation of the asymptotic distribution of the estimators based on the density function given by Eq.(4.9). For the most general case of unequal samples size and when the observations are multivariate in space and independent in time, the likelihood function is obtained as the product of the likelihood of the individual observations (annual peaks recorded at multiple stations). After taking logarithms of the likelihood function and factorizing $\sigma^2(y)$ out of the variance covariance matrix, Pons gives the following log-likelihood LL function,

$$\begin{aligned} LL(parameters; \underline{Y}) = -\sum_{t=1}^{n} \frac{m_t \ln(2\pi)}{2} - \frac{1}{2}\left[\sum_{t=1}^{n}\left(m_t \ln\sigma^2(y) + \ln|E_t|\right)\right] - \\ \frac{1}{2\sigma^2(y)} \sum_{t=1}^{n} (\underline{y}_t - \underline{\mu}_t(y))' E_t^{-1} (\underline{y}_t - \underline{\mu}_t(y)) \end{aligned} \tag{4.12}$$

where

$$E_t = \begin{bmatrix} 1 & e^{-bd_{12}} & e^{-bd_{13}} & \cdots\cdots & e^{-bd_{1m}} \\ & 1 & e^{-bd_{23}} & \cdots\cdots & e^{-bd_{2m}} \\ & & & & \vdots \\ & & & & \vdots \\ & & & & 1 \end{bmatrix} \tag{4.13}$$

and:

m_t	number of stations observed in year t
$\underline{\mu}_t(y)$	vector of means of the m_t stations present in year t
E_t	matrix of cross correlations among the m_t stations present in year t

The method of maximum likelihood consist in estimating the parameters c, a, s, p, b and $\sigma^2(y)$ such that LL is maximized. As indicated earlier, maximization of the log-likelihood function in Eq.(4.12) can not be solved explicitly. The Powell optimization algorithm is utilized to search for the location of the maximum of LL, thus yielding the maximum likelihood estimates of the parameters of the model.

4.2 Multivariate Lognormal-3 Model

As indicated in Section 4.1.1, the fixed relationship between the coefficient of variation and the coefficient of skewness for MLN2 may become an unacceptable condition for some hydrologic regions. The problem can be circumvented by the MLN3 distribution, which offers a greater flexibility at the expense of the complexity and difficulty in estimating parameters.

4.2.1 MLN3 - Model Formulation

When the lower bound of the empirical distribution of peaks is not zero, it is necessary to modify the lognormal distribution function by introducing a new parameter, the lower boundary. Typically, the lower boundary is not known a priori, therefore, the relations for parameters given for MLN2 cannot be applied directly. From distribution theory, the properties of a marginal of the MLN3 distribution are known as,

$$Y_j = \ln(X_j - \tau_j) \sim N(\mu_j(y), \sigma_j^2(y)) \tag{4.14}$$

$$\mu_j(x) = \tau_j + e^{\mu_j(y) + \frac{1}{2}\sigma_j^2(y)} \tag{4.15}$$

$$\sigma_j^2(x) = e^{2\mu_j(y)+\sigma_j^2(y)}\left(e^{\sigma_j^2(y)}-1\right) \tag{4.16}$$

$$\eta_j(x) = \frac{\left(e^{\sigma_j^2(y)}-1\right)^{\frac{1}{2}}}{1+\dfrac{\tau_j}{e^{\mu_j(y)+\frac{\sigma_j^2(y)}{2}}}} \tag{4.17}$$

$$\gamma_j(x) = \frac{e^{3\sigma_j^2(y)} - 3e^{\sigma_j^2(y)}+2}{\left(e^{\sigma_j^2(y)}-1\right)^{\frac{3}{2}}} \tag{4.18}$$

where $\sigma_j^2(x)$, $\eta_j(x)$ and $\gamma_j(x)$ are as defined in Section 4.1.1, and $\mu_j(x)$ denotes the mean at site j of the untransformed series. The additional parameter per marginal distribution, denoted by τ_j, is shown in the set of equations above. This parameter can not be regionalized since it represents the lower bound of each marginal distribution. However, by assuming a constant variance $\sigma^2(y)$ and a constant coefficient of variation $\eta(x)$ throughout the region, τ_j can be estimated by,

$$\tau_j = \frac{\left[\left(e^{\sigma^2(y)}-1\right)^{\frac{1}{2}}-\eta_x\right]\mu_j(x)}{\left(e^{\sigma^2(y)}-1\right)^{\frac{1}{2}}} = \left(1-\frac{\eta_x}{\left(e^{\sigma^2(y)}-1\right)^{\frac{1}{2}}}\right)\mu_j(x) \tag{4.19}$$

While the mean of the log-transformed peaks are related to basin characteristics for MLN2, in MLN3 instead, the mean of peak flows in the original domain is utilized. The same form of model shown in Eq.(4.6) is used. Furthermore, the lag-zero cross correlation of the untransformed peak flows can also be represented by the same relationship used for the previous model, Eq.(4.8). Under all these assumptions, Pons proposes the following form of the MLN3 model,

$$\underline{Y} = \ln(\underline{X}-\underline{\tau}) \sim MVN(\underline{\mu}(y), V) \tag{4.20}$$

where

$$\underline{\mu}_y = \begin{Bmatrix} \mu_1(y) \\ \mu_2(y) \\ \vdots \\ \vdots \\ \mu_m(y) \end{Bmatrix} = \ln \underline{\tau} + \left\{ \ln \eta(x) - \frac{1}{2}\sigma^2(y) - \ln\left[(e^{\sigma^2(y)} - 1)^{\frac{1}{2}} - \eta(x) \right] \right\} \begin{Bmatrix} 1 \\ 1 \\ \vdots \\ \vdots \\ 1 \end{Bmatrix} \tag{4.21}$$

and

$$V = \begin{bmatrix} \sigma^2(y) & e^{-bd_{12}}\sigma^2(y) & e^{-bd_{13}}\sigma^2(y) & \cdots\cdots & \cdots\cdots & e^{-bd_{1m}}\sigma^2(y) \\ & \sigma^2(y) & e^{-bd_{23}}\sigma^2(y) & \cdots\cdots & \cdots\cdots & e^{-bd_{2m}}\sigma^2(y) \\ & & \sigma^2(y) & \cdots\cdots & \cdots\cdots & e^{-bd_{3m}}\sigma^2(y) \\ & & & & & \vdots \\ & & & & & \sigma^2(y) \end{bmatrix} \tag{4.22}$$

where m is the number of stations. In conclusion, the untransformed series of peak flows will be multivariate lognormal-3 with marginal distributions having the mean expressed as a function of basin characteristics, a common coefficient of variation, and a common coefficient of skewness.

4.2.2 MLN3 - Preliminary Estimation of Parameters

The parameters of the model: $c, a, s, p, b, \sigma^2(y)$ and $\eta(x)$ are estimated using a pseudo-maximum likelihood procedure. Similar to the procedure implemented for the MLN2 model, initial estimates of the parameters are necessary prior to the implementation of the pseudo-maximum likelihood estimator. Parameters are initially computed as follows:

- c, a, s and p are obtained as for MLN2, except that in this case the log of the mean annual peaks at each station are used.
- parameter b is estimated from the cross correlation coefficients of the untransformed observations. Since τ_j is initially unknown, data transformation is not possible.
- the variance of the transformed peaks is obtained from a weighted mean of sample coefficients of skewness. After obtaining the weighted coefficient of skewness,

$\sigma^2(y)$ is computed from Eq.(4.18).

- the coefficient of variation $\eta(x)$ is obtained from a weighted average of the sample coefficients of variation of the untransformed peaks.

4.2.3 MLN3 - Pseudo Maximum Likelihood Estimation of Parameters

In the lognormal-3 distribution each location parameter τ_j has to be smaller than the lowest observed value at the corresponding site j. In other words, the range of the distribution is constrained by one of the parameters. This violates one of the regularity conditions needed to obtain the asymptotic properties of maximum likelihood estimators. Most of the asymptotic properties of the MLN2 are lost since a full maximum likelihood estimation procedure for the MLN3 is not feasible. Nevertheless, the method still consists of finding the parameter set that maximizes the log-likelihood function, though this time constrained on one of the parameters. From there comes the name of pseudo maximum likelihood estimator. Following same previous notation, the density function of the MLN3 model is given by,

$$f(\underline{x}) = (2\pi)^{-\frac{m}{2}} |V|^{-\frac{1}{2}} e^{-\frac{1}{2}[\ln(\underline{x}-\underline{\tau})-\underline{\mu}(y)]' V^{-1} [\ln(\underline{x}-\underline{\tau})-\underline{\mu}(y)]} \prod_{i=1}^{m} \frac{1}{(x_j-\tau_j)} \tag{4.23}$$

where $\ln(\underline{x}-\underline{\tau})$ is the vector of elements $\ln(x_j-\tau_j)$, and the other terms are as previously defined. For the case of unequal sample sizes, Pons (1992) provides the log-likelihood function for the MLN3 model,

$$\begin{aligned} LL(parameters\,;\underline{X}) = & -\sum_{t=1}^{n} \frac{m_t \ln(2\pi)}{2} - \frac{1}{2}\left[\sum_{t=1}^{n}\left(m_t \ln\sigma^2(y) + \ln|E_t|\right)\right] \\ & - \frac{1}{2\sigma^2(y)}\sum_{t=1}^{n}[\ln(\underline{x}_t-\underline{\tau}_t)-\underline{\mu}_t(y)]' E_t^{-1} [\ln(\underline{x}_t-\underline{\tau}_t)-\underline{\mu}_t(y)] \\ & - \sum_{t=1}^{n}\sum_{j=1}^{m_t} \ln(x_{jt}-\tau_j) \end{aligned} \tag{4.24}$$

where m_t, $\underline{\mu}_t(y)$ and E_t are as defined below Eq.(4.13). Finally, the method of maximum likelihood consists in estimating the parameters $c, a, s, p, b, \sigma^2(y)$ and $\eta(x)$ such that LL is maximized. As indicated earlier, the location parameters of the marginal distributions need to be constrained so the maximum values they can take correspond to the minimum observed values at the gaging station. Since lower bounds τ_j are not explicitly defined as parameters of the model, they become constraints to the rest of the parameters during the optimization process. Again the Powell algorithm, but this time with some modifications to accommodate for the constrained system, is implemented to search for the maximum of the log-likelihood function.

5.0 MODELS APPLICATION

5.1 Validation of Underlying Assumptions

The formulation of the MLN2 and MLN3 regional models is based on two major assumptions: 1) the variance of the log-transformed peaks $\sigma^2(y)$ is constant throughout the study region, which in turn implies a constant coefficient of variation $\eta(x)$ and a constant coefficient of skewness $\gamma(x)$ for the region, and 2) the regional cross-correlation (space correlation) of maximum annual peaks between pairs of stations can be represented by an exponentially decaying function. All these assumptions are being graphically examined in the following sections.

5.1.1 Regional Characteristics of the Coefficient of Variation

Several studies from the early 1960's to the present have assumed the coefficient of variation of annual peak series to be a constant within a region. On the other hand, Benson (1962) argues that the coefficient of variation depends on basin characteristics such as drainage area, channel slope and many others. Pons (1992), in line with the outcomes from the latest studies, avoided an explicit formulation of the coefficient of variation in his multivariate models (see Section 4.1.1 and 4.2.1.). In order to comply with Pons' assumptions it is necessary that we test the hypothesis indicating the relationship between the coefficient of variation and hydrological characteristics of the watersheds as non-existent or at least negligible within the region. No analytical procedure is introduced for this purpose, only judgment based on graphical observations is presented.

Figure 11 shows four descriptive plots of the coefficient of variation of the untransformed peak series (from Table 3) versus: a) drainage area, b) stream gage elevation, c) channel slope and d) precipitation intensity (from Table 5). This is the same set of hydrologic variables that yielded the most efficient correlative association with the mean annual peaks (see Section 3.6). Note in Figure 11 that C_v values in all four plots are widely scattered over the whole range of the hydrological variables. The visual analysis indicates that the coefficient of variation is independent of the analyzed hydrological characteristics, and therefore C_v can be assumed approximately constant within the region. Any small

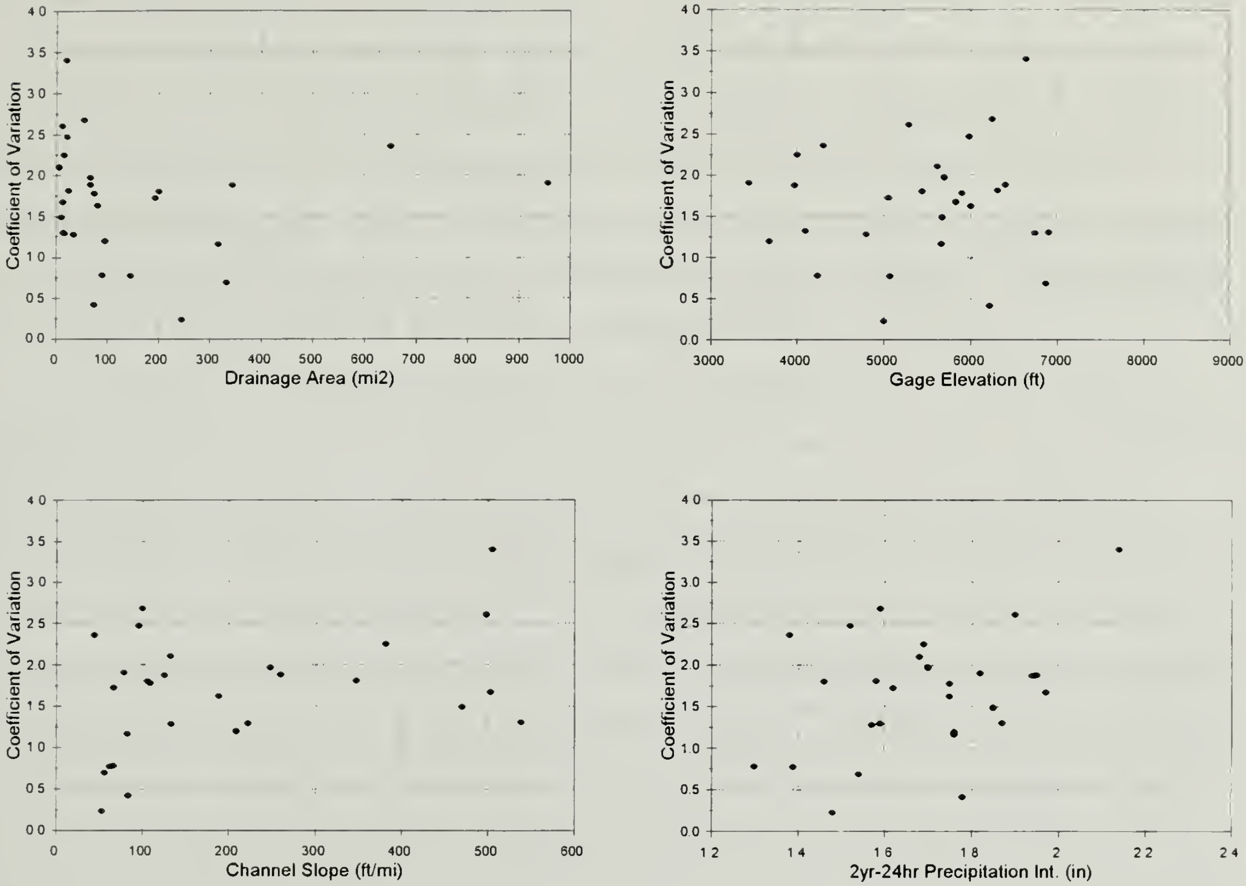

Fig.11 Coefficient of Variation versus Hydrological Characteristics
a) Drainage Area, b) Gage Datum, c) Channel Slope, d) Precipitation Intensity

dependance of the coefficient of variation on basin characteristics such as for channel slope can be considered negligible. The size of watersheds included in the analysis can be properly limited to avoid any dependence of C_v with geographical variables.

5.1.2 Regional Characteristics of the Coefficient of Skewness

The typical large variance found on the estimation error of the skewness coefficient has prompted many investigators to regionalize this high order statistical property of the annual series of peaks. The idea of assuming a regional coefficient of skewness has also been proposed by the U.S. Water Resources Council in their log-skew regionalization

procedure presented in Bulletin 17B (1981). Bulletin 17B suggests regionalization of the skewness coefficient when the sample length is below a certain threshold level. The majority of the stations within and around Zion National Park have short records that would require a regionalization of the skewness coefficient. For the purpose of regionalization the Bulletin provides a generalized skew coefficient map derived from multiple long-term records. It should be pointed out that Bulletin 17B makes no distinction between annual series with snow melt or rainfall peaks for the derivation of the generalized skew coefficient. The importance of this consideration within the Zion region has been discussed in Section 3.1.

Coefficients of skewness estimated from the log-transformed systematic records at several gaging sites are shown in Figure 12 (see Log-skew data in Table 3). Two clusters of points can be distinguished. A first group for stations 1 to 14 and a second group for stations 23 to 39. The two groups of points display different degree of scatter around a constant value very close to zero (-0.05). The group on the left, with the larger scatter, represents stations located east of the Park. Stations in this group have short and very short systematic records which is reflected by their larger variance. Contrarily, the stations in the second group, in close vicinity to the Park, show a smaller variability around the average value. This group contains the four longest records available in the region, sites 23, 25, 34, and 38. A third group of stations, sites 15 through 22, have not been plotted for having very short records.. These are stations located mostly in the headwaters of the North Fork of the Virgin River.

It is important to emphasize the critical effect that the length of a record has in the estimation of a log-skew coefficient. Notice for that purpose the plotting position of stations with long records, sites 2, 23, 25, 34 and 38, all marked with encircled points. These five stations represent a wide range of watershed sizes, from 15 to 956 mi^2, with gages located within an also wide range of elevations, from 6,400 to 3,440 ft. The five stations are among the closest points to the constant average, suggesting that as more long records become available, stations than now depart from the constant average will tend to converge toward the center of the plot. In summary, it is concluded that long-term skew coefficients in the Zion area are better described by a regional constant value rather than by at-site estimates.

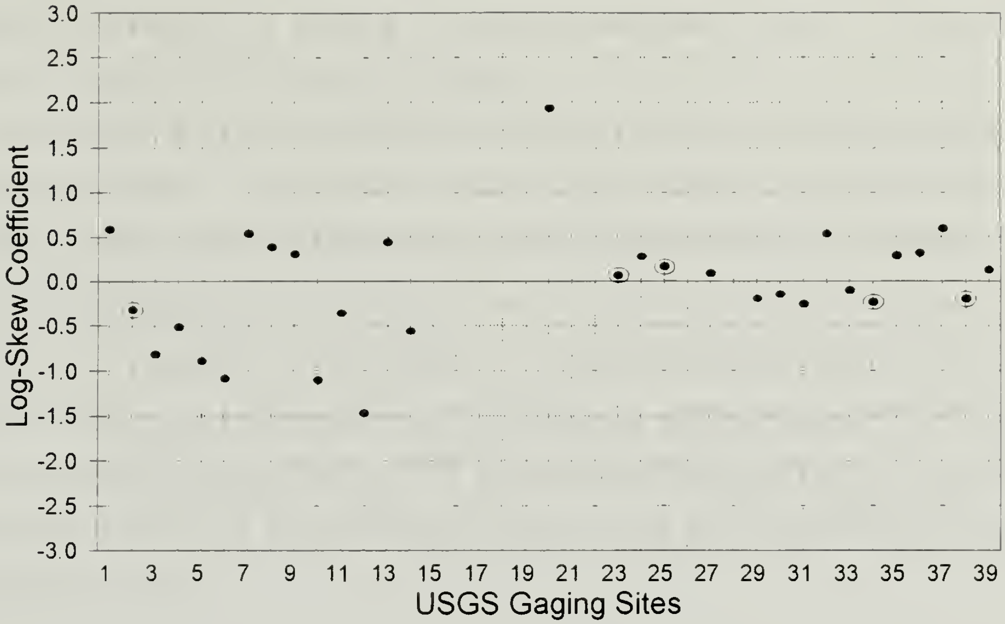

Fig.12 Log-skew Coefficients in the Zion Region

5.1.3 Regional Characteristics of the Cross-Correlation

The relation of the cross-correlation coefficient of annual hydrologic series to inter-station distance has been extensively studied by other investigators, see for instance Berndtsson (1987). Meteorological events that have a noticeable impact on hydrological series are regional in nature. For instance, extreme precipitation events and their corresponding peak flows is a typical example of this type of phenomenon. Sometimes weather systems moving over a region create response patterns that, because of the vast coverage and motion of the system, the hydrological response vary smoothly over the area affected by the event. Several examples of this regional conditions can be identified in the Zion region. For instance, the cloudburst storm that caused the flood of December 6th 1966 in Southwestern Utah was a slow moving system traveling eastward across the state. Record 24-hour amounts of precipitation were measured at Alton, Orderville and Kanab (Butler, 1972). Peak discharge of Virgin River at Virgin (site 25), the highest of record, reached 22,800 cfs. Peak discharges were also the highest of record at five other neighboring gaging sites as a result of the same storm, sites 23, 25, 29, 30, 32 and 33. Obviously, under this

conditions, the customary assumption of independence of flood events is not satisfied. This emphasizes the importance of utilizing a model that addresses the effect of interstation correlation for regional flood frequency analysis.

Estimation of the cross-correlation coefficient is carried out between pairs of stations with concurrent records. Unfortunately, records rarely coincide in lengths and/or initiation dates, hence yielding highly variable estimates of the cross-correlation coefficients. Figure 13 shows intersite dependance of peak flows derived from ten sites in the region. The sites are: 3, 11, 16, 17, 23, 24, 27, 28, 32 and 37. They were selected to cover a wide range of interstation distances. As expected, the cross-correlation approaches one for very close stations, and decreases exponentially as the interstation distance increases. The exponent 'b' defines the rate of decay of the exponential function, being pre-estimated by the model using the Least-square method.

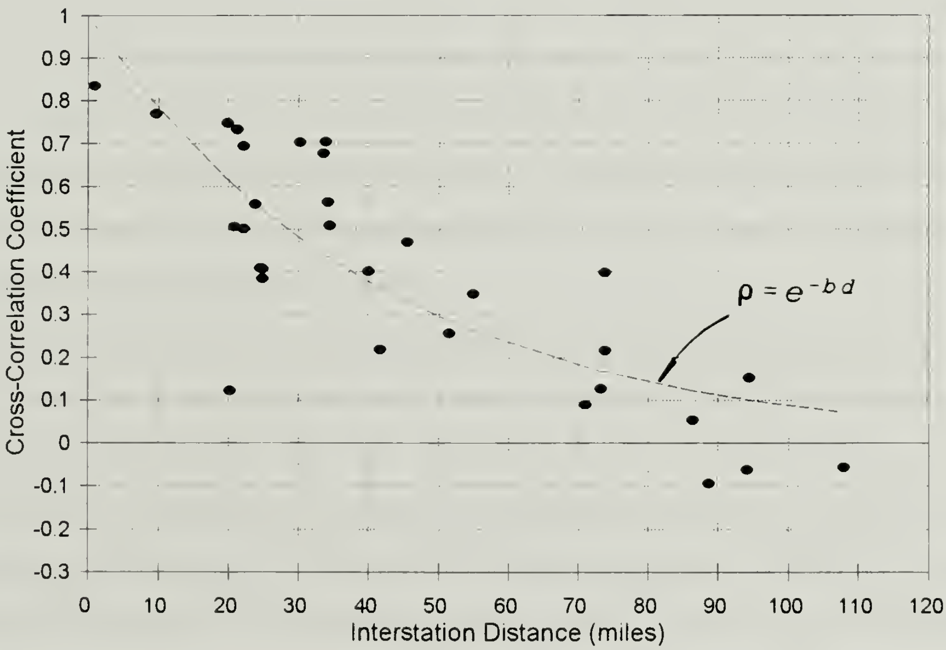

Fig.13 Cross-correlation vs. Distance Relationship for 10 Selected Stations

The level of cross-correlation between stations in a region defines the effectiveness of a multisite/regional approach. For instance, if all stations in a region were perfectly

correlated, $\rho_{i,j} = 1$ for all pairs of stations i, j (and of equal record length), there would be no additional information to be extracted from neighboring stations to increase the reliability of a quantile estimate at a given site. Conversely, if there were no cross-correlation of peaks among the sites, the effective data set can be expanded from that at the single site to the entire region. In practice the gain due to regionalization will lie somewhere between no gain and the full gain possible obtainable only when there is no cross-correlation and a strong assumed structure among site parameters (NRC, 1988).

5.2 Selecting an Homogenous Region Based on Preserving the Model Structure

The first criterion used in this study for selecting flow gaging sites for the regional analysis was following Thomas and Lindskow (1983) classification of flood regions for the State of Utah, see Section 3.1. Later in Section 3.5, the early homogeneity test used in conjunction with index flood methods was implemented. Basically, Langbeins' homogeneity test checks for similarly shaped flood frequency curves. Based on Langbeins' criterion, only three out of the 39 sites originally selected from Thomas' Low Plateau region were found unfit for the regional analysis. More recent regionalization studies have focused on the idea that hydrologically homogeneous regions need to be delineated in terms of hydrologically meaningful basin characteristics and flood statistics as well as in terms of geographic locations, see for instance Wiltshire (1986).

This section proposes an alternative approach to select an homogeneous region. It is based on the observed series of peaks, and consist in analyzing the effect that the series have in the assumed regional structure of peaks flows as defined in Sections 4.1.1 and 4.2.1. In his work Pons (1992) analyzed three types of errors that can cause the maximum likelihood (ML) procedure to yield improper values of the model parameters. They are: 1) errors in the definition of the mean of log-transformed peaks $\sigma^2(\mathrm{m})$, 2) errors on the assumption of constant variance of log-peaks $\sigma^2(\mathrm{v})$, and 3) errors on the assumption of a fixed relationship of cross-correlation versus distance $\sigma^2(\mathrm{r})$. After comparing these three types of errors, Pons determined that deviations from the assumed relationship between the mean of log-peaks and basin characteristics have the most detrimental effect on the maximum likelihood estimation procedure.

The limitation mentioned above can be circumvented if deviations from the assumed regional structure of peaks are minimized. In other words, we should find a group of stations that satisfy the level of homogeneity needed for the ML procedure to perform satisfactorily. The procedure implemented for this purpose consists in running the model repeatedly, dropping one station at a time. The station being removed from the set at each step is the one that grants the largest reduction of the variance of the error term under consideration. Since there are three error terms to minimize, the procedure is repeated entirely for each one of them. Figure 14 shows the results of the series of runs. The three curves display the error terms variance as a function of the number of stations remaining on the set. In general the three curves display a smooth decrease of the error terms. Only $\sigma^2(v)$ decreases more rapidly during the removal of the first six stations.

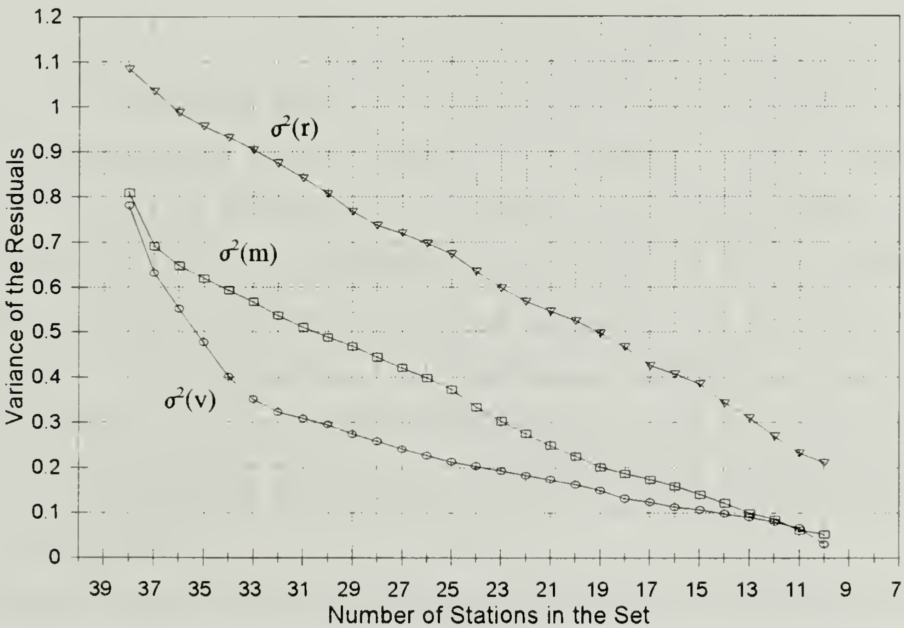

Fig.14 Decrease in $\sigma^2(m)$, $\sigma^2(r)$ and $\sigma^2(v)$ as a Function of Number of Stations

It should be mentioned that the structure of the cross-correlation function was also investigated using the interdistance between watersheds centroids instead of gaging sites. No improvement in the relation was detected. Intergage distance was finally adopted since it is a type of data more readily available. The relation of the mean of log-peaks was investigated

using two alternative sets of hydrological factors: [A, S, P] and [A, D, P]. Again, the results showed no significant differences. The set [A, D, P] was finally adopted since gage elevation (datum) is easier to obtain than channel slope.

The curves in Figure 14 show how the variance of the three errors decrease as stations are progressively removed from the model. However, they do not indicate specifically which stations remain in the set at each level. They only tell us that for instance, by reducing the number of stations from 38 to 15, $\sigma^2(m)$ drops from 0.84 to 0.14. The additional information is provided by Table 7 which classifies the sites based on their contribution to the errors variance. A station displaying a dark area indicates that its presence on the set contributes to reduce the variance of the respective error. Conversely, a clear area indicates that the presence of the station drastically increases the error term. Intermediate cases are also indicated.

The results in Table 7 were used to select the most desirable subset of stations necessary to compose the regional model. The relative goodness of the regional structure is judged based on the variance of the three errors $\sigma^2(m)$, $\sigma^2(r)$ and $\sigma^2(v)$ when considered simultaneously. Although, as indicated earlier, reducing $\sigma^2(m)$ has the highest priority. From Table 7 we can conclude that, in general, the model rejected first the stations located the farthest from the Park, as indicated by the larger number of clear areas at the top and bottom of the table. A cluster of the most desirable stations (darker areas all across) is found in the center of the table, from sites 16 to 25. The stations in this last group are the closest to the Park. There are also a few other potential good sites in terms of reducing the errors variance, like sites 28 and 32.

The concept of areal independence was another criterion for selecting the final subset of stations for the flood regional analysis. Gaging sites are considered areally independent when areas assigned to specific gaging sites do not overlap, i.e., individual stations represent mutually exclusive areas. Some of the stations used in our study allow for partial overlapping of the contributing drainages. See for instance gages at sites 19, 20, 21, 22, 23, all located along the same water course. Area overlap was restricted to a maximum of one third of the larger catchment. In summary, based on the error analysis described above, the length of records available, and the areal independence of the watersheds; a subset with ten

Table 7. Classification of Gaging Stations Based on Their Contribution to Errors Variance

Site No.	Station I.D.	Station Name	Record Length (yr)	--- Deviations from Model Structure -- x-correl.	variance	mean	Selected Station
1	9336400	Upp.Vally	16				
2	9337000	Pine Cr	41				
3	9337500	Escalante	38				
4	9338900	Deep Cr	16				
5	9339200	Twentym.	10				
6	9379800	Coyote Cr	14				
7	9381100	Henrievi.	16				
8	9381500	Paria /Ca	21				
9	9381800	Paria /Ka	15				
10	9403500	Kanab /Gl	16				
11	9403600	Kanab /Ka	25				X
12	9403700	Johnson	16				
13	9404450	EFVR /Gle	27				
14	9404500	Mineral	14				
15	9404900	EFVR /Spr	2				
16	9405200	Deep Cr	7				X
17	9405250	EF Deep C	7				X
18	9405300	Crystal	5				
19	9405400	NFVR /Gle	6				X
20	9405420	NFVR /Bul	11				
21	9405450	NFVR /Zio	4				X
22	9405490	NFVR /BBe	2				
23	9405500	NFVR /Spr	70				X
24	9405900	North Cr	9				X
25	9406000	Virgin Rv	77				X
26	9406150	La Verkin	7				
27	9406300	Kanarra	23				
28	9406500	Ash Cr/Ha	8				X
29	9406700	S.Ash/Mil	16				
31	9408000	Leeds Cr	30				
32	9408400	Santa Cla	34				X
33	9409500	Moody Wa.	15				
34	10174500	Sevier Rv	69				
35	10241400	Little Cr	21				
36	10241470	Center Cr	23				
37	10241600	Summit Cr	23				
38	10242000	Coal Cr	63				
39	10242100	Shirts Cr	16				

Lowest Error Variance
Intermediate Error Variance
Highest Error Variance

gaging stations was selected for estimating the parameters of the regional models . The ten stations are marked with a cross in Table 7. They cover a wide range of drainage areas, from 7 to 956 mi^2, as well as mean basin elevations, with gaging sites ranging from 3,500 to 7,689 ft in elevation. In the case of site 11, although it exhibits unfavorable conditions for reducing $\sigma^2(v)$, it was still included in the subset given its proximity and similar topographic characteristics with site 15 (ungaged site). The selected subset of stations have specific common properties that distinguish the subregion from the neighboring area. In other words, from the point of view of the structure of the regional model, the subregion can be considered homogeneous. The reader should notice that the selected ten stations encircle several potential sites, within and outside the Park, where frequencies of peak flows may need to be estimated.

5.3 Estimation of the Parameters of the Models

The maximum likelihood estimation procedure, briefly described in Sections 4.1.3 and 4.2.3, was applied to the subset of stations selected in the previous section. Multiple runs were carried out to explore the performance and sensitivity of the ML parameter estimation procedure. The goodness of fit of the MLN2 and MLN3 models was judged by graphically comparing the resulting regional flood frequency curves with the empirical frequency distributions at the stations. Three stations were selected for validating the regional models: sites 13, 23 and 25. They were chosen due to the good quality of the data, extended period of record (particularly sites 23 and 25), and wide range of watersheds areas and elevations. Only one station, site 13, was not part of the subset of stations used for parameters estimation. The authors recognize that the validation of the models with stations not participating in the parameter estimation procedure would have been preferable. However, the scarcity of stations with long records around Zion made that approach virtually impossible. Results of the computations are presented in Table 8. Table 8.A lists eight of the selected ten stations (and their corresponding watershed characteristics) that were ultimately used for estimating the parameters of the models (sites 17 and 28 were removed). It also shows the standard errors $\sigma^2(m)$, $\sigma^2(r)$ and $\sigma^2(v)$ as estimated initially by the model. The three error values can be compared with the curves presented in Figure 14.

Table 8. Summary of Results from ML Procedure

8.A Hydrological Characteristics of Selected Watersheds

Stat No.	Map No.	USGS ID	Name	Area	Datum	Ppt24	Latitude	Longitude
1	11	9403600	Kanab /Ka	192.64	5060.	1.62	37.1003	112.5483
2	16	9405200	Deep Cr	6.84	7680.	2.22	37.5217	112.8833
3	19	9405400	NFVR /Gle	5.65	7530.	2.22	37.4717	112.7794
4	21	9405450	NFVR /Zio	45.35	6000.	2.04	37.3903	112.8250
5	23	9405500	NFVR /Spr	343.42	3970.	1.94	37.2100	112.9778
6	24	9405900	North Cr	95.12	3680.	1.76	37.2369	113.1506
7	25	9406000	Virgin Rv	956.40	3500.	1.82	37.1981	113.2075
8	32	9408400	Santa Cla	18.67	6640.	2.14	37.3839	113.4819

Sd.Dev Residuals for Mean of Peaks : 0.358
Sd.Dev Residuals for Cross Correlation : 0.316
Sd.Dev Residuals for Variance of Peaks : 0.293

8.B Estimated Parameters, ML Procedure

Param.	Description	Lw.Bnd	Up.Bnd	-------MLN2------- Initial	Final	--------MLN3------- Initial	Final
P(1)	Constant	-6.00	45.00	25.849	32.6451	23.909	23.9790
P(2)	Coef Ln(Area)	-6.00	12.00	0.706	0.4999	0.647	0.5755
P(3)	Coef Ln(Datum)	-6.00	12.00	-2.855	-3.5118	-2.473	-2.4326
P(4)	Coef Ln(Ppt24)	-6.00	12.00	1.774	1.3766	0.755	0.7476
P(5)	Var. LN(peaks)	0.001	6.00	0.720	0.6333	0.324	0.5808
P(6)	Coef X-Correla	0.001	0.10	0.022	0.0473	0.030	0.0405
P(7)	Coef of Variat	0.001	10.00	0.879	0.9167		
No.Iterations :					28		5
No.Function Evaluations :					4186		896
Value Log-Likelihood :					253.5		1598.5

Table 8.B provides a summary of the computations of the parameters estimated by the ML procedure for the two regional models. Figure 15 (top graph) shows the type of fitting achieved with MLN2 and MLN3 at site 23. The dots represent the empirical frequency distribution of the measured annual peaks, whereas the fitted models are as indicated by the legend on the graph. Both regional models, MLN2 and MLN3, provide very good and similar fitting of the available data. Also the single-site fitting of the data using a univariate lognormal-2 model is provided for comparison. The regional models give an improved fitting compared to the univariate model for recurrence intervals greater than 10 years. For

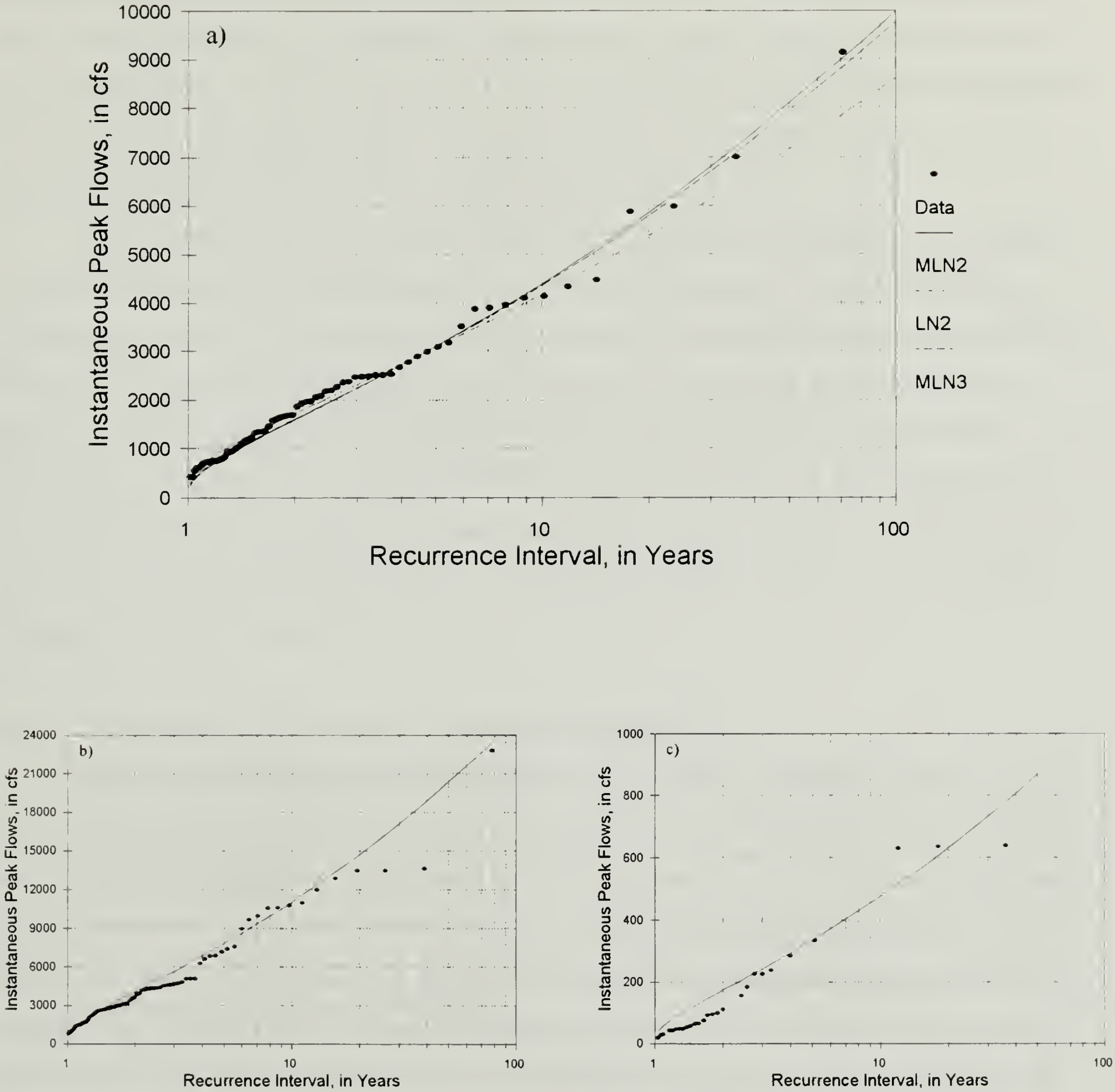

Fig.15 Regional and Univariate Fitting of Annual Peaks
a) at Site 23, N.Fk. Virgin River nr Springdale, b) at Site 25, N.Fk. Virgin River at Virgin, c) at Site 13, E.Fk. Virgin River nr Glendale

recurrences smaller than 7 years the fittings by the univariate and multivariate models are almost identical. Similarly good results were obtained when evaluating the performance of the regional model for sites 13 and 25, see graphs 15 b) and c), where the fitting by the MLN2 model is shown. The extended series of peaks at site 13 were used to estimate the plotting positions. It should be mentioned that the use of other short records for validation of the models is of questionable value. Empirical frequency distributions made up of short records typically have their plotting positions highly distorted.

The validation process presented above assures the good performance of the models for sites located in the intermediate and lower reaches of the upper Virgin River system. Unfortunately, there isn't any station with long records in the headwaters upstream from the Park (site 13 has only 27 years of record). The lack of long records in the headwaters prevent us from presenting a full validation of the models including the high elevation catchments. Nevertheless, it is expected that the regional character of the models plus the inclusion of sites with very high mean basin elevation during the calibration stage (sites 16, 19 and 21), despite of their short records, will yield acceptable results even for watersheds located at very high elevation.

5.4 Application of the Models to Ungaged Watersheds

One of the main purposes for developing a regional flood frequency model is to be able to estimate flood frequency curves at ungaged sites. As demonstrated in the previous two sections, the parameters of the model should be derived from a set of stations adjacent to the ungaged site in order to preserve as much as possible the underlying structure of the probability model. Furthermore, it is recommended that the basin characteristics of the ungaged site be similar to the watershed characteristics of the sites used for estimating the parameters of the model. The procedure for applying the regional models at ungaged sites within Zion National Park and vicinity areas is as follows:

1. Define the set of stations to be used for estimating the parameters of the model. This task has been completed and the results presented in Section 5.2.
2. Estimate the parameters of the model using the maximum likelihood procedure. This task has also been completed and the results presented in Section 5.3.

3. Determine the basin characteristics of the ungaged watershed. They are: drainage area (in square miles), terrain elevation of the selected river site (in feet), and the 2yr-24hr precipitation intensity (in inches) estimated at the centroid of the catchment.

4. Compute the mean $\mu_j(y)$, the standard deviation $\sigma_j(y)$, and lower bound τ_j (the latter only for MLN3) of the marginal distribution j based on the estimated parameters of the regional model:

- for MLN2:

$$\mu_j(y) = c + a\ \ln(A_j) + s\ \ln(S_j) + p\ \ln(P_j)$$

$$\sigma_j(y) = \sqrt{\sigma^2(y)}$$

- for MLN3:

$$\mu_j(x) = e^{[c + a\ln(A_j) + s\ln(S_j) + p\ln(P_j)]}$$

$$\sigma_j(y) = \sqrt{\sigma^2(y)}$$

$$\tau_j = \left(1 - \frac{\eta(x)}{(e^{\sigma^2(y)} - 1)^{\frac{1}{2}}}\right)\mu_j(x)$$

$$\mu_j(y) = Log_e[\mu_j(y) - \tau_j] - \frac{1}{2}\sigma^2(y)$$

5. Compute the frequency distribution of peak flows at the ungaged site as,

- for MLN2:

$$Y_T = \mu_j(y) + t\ \sigma_j(y)$$

$$X_T = e^{Y_T}$$

- for MLN3:

$$X_T = \tau_j + e^{[\mu_j(y) + t\ \sigma_j(y)]}$$

where t is the standard normal deviate obtainable from tables of the area under the normal curve or using a polynomial approximation..

Site 15, in the East Fork of the Virgin River near Springdale, was chosen to demonstrate the capability of the models to estimate percentiles of the frequency distribution at an ungaged location. Site 15 can be considered ungaged since only two years of record

are available. The computations indicated in points 3, 4 and 5 were carried out using a spreadsheet. Results of the spreadsheet computations are presented in Table 9. The spreadsheet is provided with this report to facilitate the final computations to the user. The estimated frequency distribution at site 15 is shown graphically in Figure 16. The two regional models provide very similar estimations of the frequency distribution.

It is interesting to compare the results of the estimated flood frequency curve at site 15 with one of the two annual peaks measured at the site so far. For instance, a peak of considerable magnitude was observed during water-year 1993. If we enter the frequency curve in Figure 16 with the value of the maximum instantaneous discharge for that water-year, estimated in 1,940 cfs, we can determine that the measured peak has an estimated frequency of occurrence close to 3-years. Frequency estimates at regular recurrence intervals can be read directly from Table 9, or estimated from the curves in Figure 16.

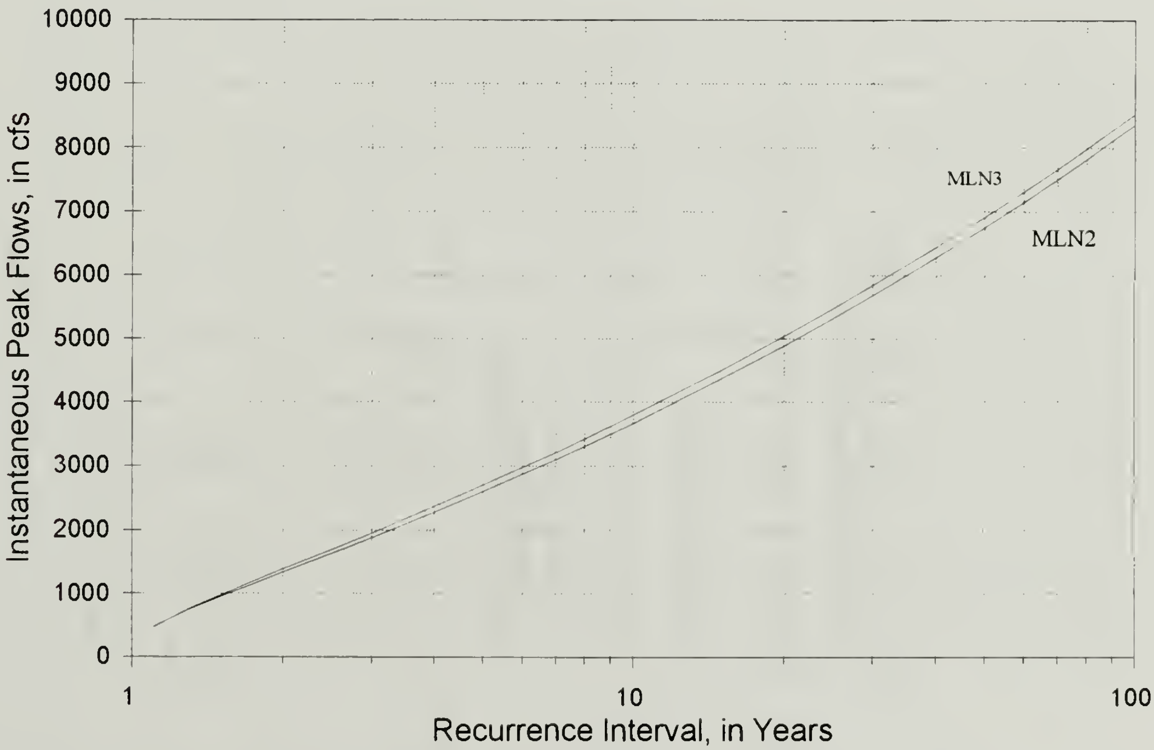

Fig.16 Estimated Frequency at Ungaged Site, E.Fk. Virgin River near Springdale

Table 9. Estimation of Flood Quantiles at an Ungaged Site Using Regional Models

UNGAGED SITE: E.F. Virgin River nr Springdale - 09404900

Basin Characteristics

Area (mi2)	Datum (ft)	Precip (in)
347.8	3940	1.56

MLN2 Model Parameters

Coef. 'c'	Coef. 'a'	Coef. 's'	Coef. 'p'	Sigma2 y	'b'
33.930	0.4575	-3.604	0.9707	0.6185	0.050

Derived from MLN2 Model Parameters

mean (y)	Sigma (y)
7.2015	0.7864

MLN3 Model Parameters

Coef. 'c'	Coef. 'a'	Coef. 's'	Coef. 'p'	Sigma^2 (Y)	'b'	Cv
23.979	0.5755	-2.4326	0.7476	0.5808	0.041	0.92

Derived from MLN3 Model Parameters

mean(x)	low.bnd(x)	skewness	sigma(y)	mean(y)
1881	-69	3.36	0.7621	7.2854

Estimated Flood Frequency Distribution

Ret.Per.	Exc.Prob	---Normal Deviate---		------ MLN2 Fit --------		MLN3 Fit
(yr)		w	t	Y(t)	X(t)	X(t)
100.0	0.010	3.0349	2.3268	9.0314	8361	8523
90.0	0.011	2.9999	2 2870	9.0001	8104	8267
80.0	0.013	2.9604	2.2418	8.9646	7821	7985
70.0	0.014	2.9150	2.1898	8.9236	7507	7672
60.0	0.017	2.8616	2.1285	8.8754	7154	7318
50.0	0.020	2.7971	2.0542	8.8170	6748	6912
40.0	0.025	2.7162	1.9604	8.7432	.6268	6430
30.0	0.033	2.6081	1.8343	8.6441	5677	5835
25.0	0.040	2.5373	1.7511	8.5786	5317	5472
20.0	0.050	2.4477	1.6452	8.4954	4892	5042
15.0	0.067	2.3273	1.5014	8.3823	4369	4512
10.0	0.100	2.1460	1.2817	8.2095	3676	3806
7.0	0.143	1.9728	1.0676	8.0411	3106	3222
5.0	0.200	1.7941	0.8415	7.8633	2600	2701
4.0	0.250	1.6651	0.6742	7.7317	2279	2370
3.0	0.333	1.4823	0.4303	7.5399	1882	1956
2.5	0.400	1.3537	0.2529	7.4004	1637	1700
2.0	0.500	1.1774	-0.0000	7.2015	1341	1390
1.7	0.588	1.3321	-0.2226	7.0264	1126	1162
1.5	0.667	1.4823	-0.4303	6.8631	956	982
1.3	0.769	1.7125	-0.7361	6.6226	752	763
1.1	0.909	2.1899	-1.3354	6.1513	469	458

6.0 SUMMARY AND CONCLUSIONS

The main outcome of this study was the implementation of a regional flood frequency analysis for Zion National Park and vicinity areas. It is based on a multivariate lognormal model that explicitly accounts for the cross correlation among the series of annual peaks in the region. This distinctive characteristic of the model is critical in the Zion region where the highest peaks have been recorded during the same year at several stations. This finding precludes the use of traditional Index-flood methodologies since the basic requirement of independence of events is violated. Another major obstacle for the analysis is the limited database of annual peaks available. This restricts the applicability of another technique, the Generalized Least Square method, that as proved by other investigators (Pons, 1992), becomes unreliable when the number of available stations with long records decreases.

Two regional flood frequency models with the statistical characteristics explained in Section 4 were implemented, named MLN2 and MLN3. They will allow the user to estimate flow quantiles (maximum instantaneous peaks) at ungaged river sites based on readily available geographical and meteorological information. The models can also be used to increase the reliability of estimated flow quantiles at sites with very short records like in the case of headwater catchments.

This study used Thomas and Lindskov (1983) classification of flood regions in the State of Utah to preselect gaging sites with approximately uniform hydrologic characteristics. Additional analysis and testing, including Langbein's homogeneity test, provided further insight into the hydrological characteristics of the annual series of flow peaks in the region. It was found that peak series display mixed-population characteristics resulting from snow melt and rainfall events, with the latter as the predominant mechanism. The ratios of maximum instantaneous peaks over mean daily flows for the same day (an indicator of the degree of flashiness of the stream) are low and very constant during the snow melt season, and large and highly variable during the months with convective thunderstorms. High intensity and short duration summer storms give rise to sharp increases and fast decay of the hydrographs, with peaks reaching up to about 30 to 60 times the mean-daily flow depending

on the mean elevation of the catchment. On the other hand, during the snow melt season, usually occurring from late March through June, instantaneous peaks rarely exceed mean-daily flows more than 4 times. The probability distribution of the number of peaks occurring at different times of the year was also examined. A distinctive seasonal pattern was observed. The study provides a methodology for the estimation of the probability of occurrence of any number of peaks during any given period of the year.

The parameters of MLN2 and MLN3 were estimated (using the maximum likelihood procedure) based on the observed series of peaks from a subset of stations that are known to preserve the assumed structure of the regional models. The selected subset of stations have specific common properties that distinguish the subregion from the neighboring area. In other words, from the point of view of the structure of the regional model, the subregion can be considered homogeneous. The mean of peak flows in the region can be in great part explained by basin characteristics, among them: basin area, channel slope, gage elevation and precipitation intensity.

Both regional models, MLN2 and MLN3, showed very good and similar fitting capabilities when compared with empirical frequency distributions at three selected stations. The three stations are representative of catchments at low, intermediate and high elevation areas of the Upper Virgin River Basin. The model validation process assured the reliability of the regional models when used for sites located at intermediate and lower reaches of the Upper Virgin River system. The performance of the models at high elevation sites could not be thoroughly verified given the lack of long records for headwaters stations. Nevertheless, we expect MLN2 and MLN3 to yield reasonable estimates of flood quantiles even for watersheds at very high elevation. A spreadsheet is provided with this report to facilitate the final computations for estimating percentiles of the frequency distribution curves at ungaged locations. It is recommended to compute and compare frequency curves obtained from both models, MLN2 and MLN3. In case of a noticeable difference between the two models it is suggested to select the curve provided by MLN2 which has consistently provided more accurate fittings.

7.0 LITERATURE CITED

Benson, M. A., 1962. " Factors Influencing the Occurrence of Floods in a Humid Region of Diverse Terrain". U.S. Geological Survey, Water-Supply Paper 1580-B.

Benson, M. A., 1964. "Factors Affecting the Occurrence of Floods in the Southwest". U.S. Geological Survey, Water-Supply Paper 1580-D.

Berndtsson, R., 1987. "On the Use of Cross Correlation Analysis in Studies of Patterns of Rainfall Variability". Journal of Hydrology, 93, 113-134.

Butler, E., 1972. "Developing a State Water Plan - Cloudburst Floods in Utah, 1939-1969". U.S. Geological Survey, in Cooperation with the Utah Dept. of Natural Resources, Division of Water Resources, Cooperative-Investigations Report No.11.

Dalrymple, T., 1960. "Flood-Frequency Analyses". U.S.Geological Survey, Water-Supply Paper 1543-A.

Diaz, G. E., 1992. "Streamflow Characterization at Zion National Park, Utah". Technical Report presented to the National Park Service, Water Resources Division - WRB, Fort Collins, Colorado

Diaz, G. E. and T. Ismael, 1993. "Precipitation-Runoff Relationship at the Upper Basin of the Virgin River, Utah". Technical Report presented to the National Park Service, Water Resources Division - WRB, Fort Collins, Colorado.

Jarrett, D. R., 1993. "Flood Elevation Limits in the Rocky Mountains". In Engineering Hydrology, edited by C.T. Kuo, Proceedings of the ASCE Engineering Hydrology Symposium, San Francisco, California, July 25-30.

National Research Council, 1978. "Estimating probabilities of Extreme Floods". Committee on Techniques for Estimating Probabilities of Extreme Floods. National Academy Press, Washington D.C.

N.O.A.A., 1973a. "Precipitation-Frequency Atlas of the Western United States". Atlas 2, Vol IV - Utah.

N.O.A.A., 1973b. "Precipitation-Frequency Atlas of the Western United States". Atlas 2, Vol III - Colorado.

Peterson, R. V., 1985. "Regional Insights in Determining Extreme Flood Magnitudes". In Delineation of Landslide, Flash Flood, and Debris Flow Hazards in Utah, pp.395-403. Proceedings of a Specialty Conference held at Utah State University, Logan Ut, June 14-15.

Pons, A. F., 1992. "Regional Flood Frequency Analysis Based on Multivariate Lognormal Models". Ph.D. Dissertation presented to the Dept. of Civil Engineering, Colorado State University, Fort Collins, Colorado.

Resh, V.H. and several other authors, 1988. "The Role of Disturbance in Stream Ecology". In Journal of the North American Benthological Society, 7(4):433-455.

Thomas, B. E. and K. L. Lindskov, 1983. "Methods for Estimating Peak Discharge and Flood Boundaries of Streams in Utah". U.S.G.S. Water-Resources Investigations Report 83-4129.

Thomas, B. E., 1985. "Problems with Statistical Flood-Frequency Analyses in Streams in Utah". In Delineation of Landslide, Flash Flood, and Debris Flow Hazards in Utah, pp.379-393. Proceedings of a Specialty Conference held at Utah State University, Logan Ut, June 14-15, 1984.

U.D.W.R., 1983. "Hydrologic Inventory of the Virgin and Kanab Study Units", Utah Division of Water Resources - Comprehensive Water Planing Program.

U.S. Geological Survey, 1994. Personal Communication with Mr Terry Lockner, Water Resources Division, Cedar City, Utah.

U.S. Water Resources Council, 1981. "Guidelines for Determining Flood Flow Frequency". Bulletin 17, Hydrologic Committee - Water Resources Council, Washington D.C.

Yevjevich, V., 1982. "Probability and Statistics in Hydrology". Water Resources Publication, P.O. Box 2841, Littleton, Colorado.

Webb R. H. and V. R. Baker, 1987. "Changes in Hydrologic Conditions Related to Large Floods on the Escalante River, South-Central Utah". In Regional Flood Frequency Analysis, pp.309-323. Edited by V. P. Singh. Publisher D. Reidel Publishing Co.

Woolley, R. R., 1946. "Cloudburst Floods in Utah, 1850-1938". U.S. Geological Survey, Water-Supply Paper 994.

Zelenhasic, E, 1970. "Theoretical Probability Distributions for Flood Peaks". Hydrology Paper No.42, Colorado State University, Fort Collins, Colorado.

Appendix I : List of USGS 1:24000 (7.5 minute) Topographic Maps

No.	Map Name	USGS	Code
1	Alton	D4	37112
2	Antimony	A8	38111
3	Asay Bench	E5	37112
4	Bald Knoll	C4	37112
5	Barker Reservoir	H7	37111
6	Big Lake	A6	38111
7	Boulder Town	H4	37111
8	Brian Head	F7	37112
9	Bridger Point	A7	37111
10	Bryce Point	E2	37112
11	Bryce Canyon	F2	37112
12	Bull Valley Gorge	D1	37112
13	Butler Valley	D7	37111
14	Calf Creek	G4	37111
15	Calico Peak	C8	37111
16	Canaan Creek	F6	37111
17	Canaan Peak	E7	37111
18	Cannonville	E1	37112
19	Carcass Canyon	E5	37111
20	Cedar City	F1	37113
21	Cedar Mountain	E1	37113
22	Central West	D6	37113
23	Clear Creek Mountain	C7	37112
24	Cogswell Point	D8	37112
25	Collet Top	D4	37111
26	Cottonwood Mountain	H6	37112
27	Cutler Point	B4	37112
28	Dave Canyon	F5	37111
29	Death Ridge	E6	37111
30	Deer Spring Point	C2	37112
31	Deer Creek Lake	A4	38111
32	Deer Range Point	C1	37112
33	Eightmile Pass	B1	37112
34	Elephant Butte	A7	37112
35	Escalante	G5	37111
36	Fivemile Valley	B8	37111
37	Flanigan Arch	F8	37112
38	George Mountain	E4	37112
39	Glendale	C5	37112
40	Grass Lakes	H8	37111
41	Grass Valley	D4	37113
42	Griffin Point	G7	37111
43	Hatch	F4	37112
44	Haycock Mountain	F5	37112
45	Hebron	F7	37113
46	Henrie Knolls	E6	37112
47	Henrieville	E8	37111
48	Hildale	A8	37112
49	Horse Mountain	D6	37111
50	Horse Flat	C7	37111
51	Hurricane	B3	37113
52	Jacobs Reservoir	A5	38111
53	Johnson Lakes	A3	37112
54	Kanab	A5	37112
55	Kanarraville	E2	37113
56	King Bench	G3	37111
57	Kolob Reservoir	D1	37112
58	Kolob Arch	D2	37112
59	Little Creek Mountain	A2	37112
60	Long Valley Junction	D5	37112
61	Lower Coyote Spring	B7	37111
62	Lower Bowns Reservoir	A3	38111
63	Maple Ridge	D7	37113
64	Mount Carmel	B6	37112
65	Navajo Lake	E7	37112
66	Nephi Point	B2	37112
67	New Harmony	D3	37113
68	Nipple Butte	B6	37111
69	Orderville	C6	37112
70	Page Ranch	E4	37113
71	Panquitch Lake	F6	37112
72	Paragonah	H7	37112
73	Parowan	G7	37112
74	Parowan Gap	H8	37112
75	Petes Cove	D5	37111
76	Petrified Hollow	A2	37112
77	Pine Hollow Canyon	A1	37112
78	Pine Point	B3	37112
79	Pine Lake	F8	37111
80	Pintura	C3	37113
81	Podunk Creek	D3	37112
82	Pollywog Lake	A7	38111
83	Posy Lake	H6	37111
84	Rainbow Point	D2	37112
85	Roger Peak	H5	37111
86	Seep Flat	E4	37111
87	Signal Peak	C4	37113
88	Skutumpah Creek	C3	37112
89	Slickrock Bench	D8	37111
90	Smith Mesa	C2	37112
91	Smithsonian Butte	A1	37113
92	Springdale West	B1	37112

No.	Map Name	USGS	Code
93	Sringdale East	B8	37112
94	Steep Creek Bench	H3	37111
95	Stoddard Mountain	E3	37113
96	Straight Canyon	D7	37112
97	Strawberry Point	D6	37112
98	Summit	G8	37112
99	Sweetwater Creek	G8	37111
100	Temple of Sinawava	C8	37112
101	The Guardian Angels	C1	37112
102	The Barracks	B7	37112
103	Thompson Pass	A4	37112

No.	Map Name	USGS	Code
104	Tropic Canyon	F1	37112
105	Tropic Reservoir	E3	37112
106	Upper Valley	F7	37111
107	Virgin	B2	37112
108	Webster Flat	E8	37112
109	West Clark Bench	A8	37111
110	White Tower	B5	37112
111	Wide Hollow Reservoir	G6	37111
112	Wilson Peak	F3	37112
113	Yellowjacket Canyon	A6	37112

No.	Additional Maps	USGS	Code
114	Fivemile Ridge	G5	37112
115	Little Creek Peak	H5	37112
116	Red Creek Reservoir	G6	37112
117	Sunset Flat	E3	37111

Watershed with Outlet at Site No.	USGS 7.5' Topographic Maps
1	16, 42, 79, 106
2	6, 35, 52, 83, 85, 111
3	<1>, <2>, 5, 40, 99
4	7, 31, 62, 56, 94
5	17, 19, 25, 28, 29, 75, 86, 117
6	9, 15, 36, 50, 61, 68
7	17, 79, 47, 106
8	<7>, 10, 11, 12, 18, 89, 104
9	<7>, <8>, 9, 13, 15, 32, 33, 36, 50, 61, 77, 81, 84,105, 109
10	1, 4, 38, 39, 60, 81
11	<10>, 27, 54, 64, 110, 113
12	1, 4, 27, 53, 66, 76, 78, 81, 88, 103
13	1, 39, 60, 69, 97
14	23, 64, 69, 102
15	<13>, <14>, 34, 93, 96, 110, 113
16	65, 108
17	<16>
18	21, 57
19	65, 96, 97
20	<19>
21	<19>
22	<16>, <17>, <19>, 23, 24, 69, 100, 101
23	<22>, 92, 93, 102
24	58, 90, 92, 101, 107
25	<13>, <14>, <23>, <24>, 34, 48, 91, 93, 110, 113
26	51, 57, 58, 80, 90, 101, 107
27	21, 55
28	<27>, 41, 57, 58, 67, 70, 95
29	41, 67, 80, 87
31	80, 87
32	41, 87
33	22, 45, 63
34	1, 3, 8, 38, 43, 44, 46, 60, 65, 71, 96, 97, 105
35	26, 114, 115, 116
36	8, 73
37	8, 37, 73, 98
38	8, 20, 21, 37, 43, 108
39	21

Note: <x> indicates that all maps from watershed 'x' are also included in the current watershed

Appendix II: Recorded and Extended Series of Annual Peak Flows, Basic Statitics

Water Year	Upp.Valley 09336400	Pine Cr 09337000	Escalante 09337500	Deer Cr 09338900	Twentymil 09339200	Coyote 09379800	Henrieville 09381100	Paria Can. 09381500	Paria Kan. 09381800	Kanab Gle. 09403500	Kanab Kan. 09403600	Johnson 09403700	EFVR n. Gl 09404450	Mineral 09404500	EFVR Spr. 09404900	Deep Cr 09405200	EF Deep Cr 09405250	Crystal 09405300	NFVR Gle 09405400
	Gaging Stations																		
1910			385																
1911			810																
1912			557																
1913																			
1914																			
1915																			
1916																			
1917																			
1918																			
1919																			
1920																			
1921																			
1922																			
1923																			
1924																			
1925																			
1926																			
1927																			
1928																			
1929																			
1930																			
1931																			
1932																			
1933																			
1934																			
1935																			
1936																			
1937																			
1938																			
1939																			
1940																			
1941																			
1942																			
1943		275	1750																
1944		107	1970																
1945		124	840																
1946		246	540																
1947		156	1110																
1948		308	315																
1949		603	2790																
1950		146	189																
1951		285	1560				455	2040	1625										
1952		325	1980				1716	1400	3184										
1953		153	3450				1445	2910	1839										
1954		108	544				544	1600	2115										
1955		102	2980				1922	3260	3082										
1956							1427	3645	3234										
1957							1053	2439	1945									387	
1958		288	1966				1232	3016	2562									863	
1959	5560	53	763	1350	1590	419	1740	6890	4500	83	160	1520	408	262				1300	
1960	185	74	1660	148	230	980	2350	5550	2490	120	2100	120	266	190				182	
1961	670	947	2780	3820	1500	2250	7360	5320	3100	1300	3030	1180	42	1340				1120	
1962	420	448	2134	2140	560	600	1440	1060	2300	710	1400	1030	624	7					
1963	1970	423	1767	455	4620	1680	4010	11600	15400	1600	1310	1540	152	3210					
1964	590	428	838	680	1220	630	220	1730	4800	500	600	1000	511	710					
1965	270	1000	2055	240	1940	95	700	1730	818	250	640	61	154	400					
1966	590	24	477	145	1260	760	600	2460	903	320	360	1200	298	25					
1967	300	1010	3230	149	3340	3300	800	2150	2880	1190	1230	2000	635	315					
1968	305	250	1566	100	3560	3800	360	2650	4330	2100	1300	1150	65	5					
1969	2450	197	1520	930		1820	670	4680	773	630	1887	1950	238	20					
1970	1090	180	1710	1680		2000	475	4120	827	1700	1193	2750	30	1011					
1971	1600	340	2642	28		2110	1900	1730	1740	1370	2704	2100	66	1760					
1972	750	11	179	8		4590	270	3100	2200	530	1838	240	630	147					
1973	970	193	2530	730			290	6400	8400	1140	1450	520	184	297					30
1974	630	51	170	74			860	1050	1055	29	1110	950	44	570					10
1975	1198	108	224	1910			1728	4616	4273	1274	466	1769	58	1474					15
1976	2833	63	1090	1266			591	948	352	949	991	1128	640	1404					8
1977	906	52	760	343			1070	2493	2003	1608	465	1400	112	1337					6
1978	1282	66	23	942			1885	5120	4811	1785	216	534	96	1930					52
1979	2295	153	257	2156			1188	2873	2410	998	190	1353	285	816					
1980	1465	131	1400	340			2386	6737	6540	1694	1060	956	334	865					
1981	1977	713	2750	351			1727	4611	4267	531	220	2327	156	271					
1982	1118	100	204	1872			1507	3901	3508	1501	327	1606	93	405					
1983	1912	187	192	135			1936	5285	4988	892	148	480	226	1114					
1984	1553	126	1000	331			1388	3518	3099	1935	1130	1351	100	2190					
1985	229	111	1350	278			2091	5784	5521	966	376	1790	48	960					
1986	1056	162	1210	804			1090	2556	2070	991	350	1948	76	1379					
1987	195	217	512	1533			1663	4405	4047	541	55	251	48	1443		13	9		
1988	1502	122	421	982			1418	3615	3203	1333	511	2462	49	831		23	32		
1989	2006	33	89	204			546	803	197	1666	340	1122	55	1266		10	14		
1990	523	364	870	521			1101	2594	2112	1961	49	1934	20	1909		24	11		
1991	500	101	777	169			607	1000	407	1067	40	1808	29	1801		7	10		
1992	660	383	710	1409			1422	3628	3216	2350	65	1416	44	2045	500	15	31		
1993	1588	376	900	962			1636	4318	3954	1401	430	735	226	510	1940	110	103		

Basic Statistics for Measured Peak Flows Series

Count......	16	41	38	16	10	14	16	21	15	16	25	16	27	14	2	7	7	5	6
Mean	1147	255	1037	792	1982	1788	1503	3497	3697	848	697	1207	170	640	1220	29	30	770	20
Std.Dev....	1299	251	891	999	1337	1303	1796	2493	3694	625	713	734	184	873					
Coef.Var...	1.13	0.99	0.86	1.26	0.67	0.73	1.19	0.71	1.00	0.74	1.02	0.61	1.08	1.36					
Skew......	2.68	1.88	1.16	1.97	0.77	0.78	2.47	1.80	2.36	0.42	1.73	0.23	1.78	2.10					

Basic Statistics for Extended Peak Flows Series

Count	35	49	52	35	10	14	43	43	43	35	35	35	35	35	2	7	7	5	6
Mean	1233	254	1240	834	1982	1788	1414	3519	3188	1115	850	1305	201	978	1220	29	30	770	20
Std.Dev	1020	238	918	824	1337	1303	1167	2050	2534	603	757	669	193	755					
Coef.Var	0.83	0.94	0.74	0.99	0.67	0.73	0.83	0.58	0.79	0.54	0.89	0.51	0.96	0.77					
Skew	2.30	1.92	0.69	1.61	0.77	0.78	3.31	1.50	2.79	-0.04	1.18	-0.02	1.28	0.75					

Gaging Stations

NFVR Bul. 09405420	NFVR Narr 09405450	NFVR B.B. 09405490	NFVR Spr 09405500	North Cr. 09405900	Virgin Vlr. 09406000	La Verkin 09406150	Kanarra 09406300	Ash Cr 09406500	So. Ash Mil 09406700	So. Ash Pin 09406800	Leeds Cr 09408000	Santa Clara 09408400	Moody Was 09409500	Sevier Rv 10174500	Little Cr 10241400	Center Cr 10241470	Summit Cr 10241600	Coal Cr 10242000	Shirts Cr 10242100
			1674		2770														
			4266		10600														
			2839		5100									1210					
			920		12000									502					
			1460		2500														
			3689		4360									770					
			3750		4350									1040				480	
			2501		2610									982				390	
			1438		5100									550				500	
			1701		1240									504				500	
			5880		11000									1130					
			1259		2650									803					
			772		3400									1490					
			3923		5100									826					
			1059		3100														
			974		1660									689					
			710		2770									643					
			1200		4300														
			750		2600									536					
			3900		4200														
			428		3000														
			2370		3550														
			2500		9000														
			3000		2350														
			940		1550														
			1980		1760													840	
			4480		6300													2910	
			2540		1920													830	
			7000		13500													491	
			2900		10000									835				1850	
			4110		4370			1500						580				1630	
			3100		2980			1400						1140				800	
			1180		3150			495						780				533	
			734		919			985						524				1250	
			1370		1070			385						672				765	
			1690		844			1440						480				816	
			558		1700			290						366				208	
			3520		2080			1430						607				410	
			798		1400									488				408	
			1100		1010									1060				346	
			2680		6620									317				211	
			833		2800									248				112	
			2520		4840									827				456	
			1660		12900									455				1750	
			2480		4690									410				1000	
			3960		10600								532	343				1570	
			956		2260								145	254				214	
			668		1430								185	626				651	
			2270		7410								396	833				2360	
196			2070	2573	4420				325	189	729	114	25	328	62	81	172	1210	109
167			430	172	2190		28		169	200	467	45	39	259	160	170	141	477	144
217			5880	6340	13500		528		829	200	1580	340	1400	816	351	195	277	2000	460
207			1870	1454	3100		107		210	130	535	63	546	989	37	171	42	1040	370
206			4340	4781	4550		555		386	190	833	142	28	285	10	212	75	1600	273
194			1350	1674	4630		232		210	28	2980	63	26	628	38	64	249	1750	1070
226			5990	6764	6890		99		250	48	2060	81	199	795	282	353	99	2340	144
183			1620	1458	3930		88		158	938	565	40	791	450	75	23	22	344	75
294			9150	10057	22800		344		1910	890	2710	776	1810	572	23	274	70	3340	440
172			1930	1337	6840		800		500	210	213	49	31	644	330	300	600	2440	470
206			3880	4434	13660		307		872	54	386	139	1800	975	12	56	795	4620	340
163			1350	1344	2660		1000		615	580	94	27	285	320	8	36	122	313	212
177			2390	1803	2880		600		98		1290	30	292	236	152	24	858	278	790
212			2200	2275	4369		96		395		198	115	486	1260	6	25	8	85	150
180			1970	1918	6790		223		158	510	84	206	695	958	40	94	355	1820	220
1740			776	192	3640		65		52	125	8	19	266	487	92	109	20	2400	265
178			4140	4195	11044		57		16		80	82	411	498	290	258	37	4440	526
174			1240	1064	5267		34		175		27	48	333	403	7	36	22	358	68
225			749	912	7207		94		100		15	28	287	487	6	116	21	70	486
95			1325	1415	7198		64		245		403	132	525	528	9	32	42	570	501
204			1670	2032	7600		43		326		570	175	624	1180	17	19	53	899	275
222			3190	3664	10830		100		281		892	139	541	1210	16	20	86	515	640
80	128		2190	2798	3650		19		41		43	95	441	406	30	67	39	376	431
204	242		2780	3454	9700		296		113		278	84	415	739	140	16	73	651	358
272	214		2490	2569	4740		305		606		802	240	773	1380	88	57	515	1480	529
188	560		2090	2091	4580		216		149		712	36	305	650	133	191	129	695	330
160			1050	304	2920	116	221		176		12	48	333	626	151	28	28	3840	670
157			610	346	1620	249	213		134		811	29	289	614	114	12	20	364	241
160			1010	1630	7200	305	225		194		1170	56	351	341	343	146	51	840	440
167			1580	950	2690	2820	335		756		4420	307	926	616	141	74	264	603	344
156			624	530	1500	948	209		114		62	20	269	181	63	36	448	2500	125
155			734	590	3020	2730	209		116		125	21	271	207	71	155	67	140	237
155			726	756	1490	1110	214		138		27	31	294	253	94	145	354	176	74
177		2090	2520	2890	4270		229		216		83	66	374	296	45	54	85	950	343
179		1429	1700	2010	3920		265		398		358	147	560	1220	160	188	269	750	419

Basic Statistics for Measured Peak Flows Series

11	4	2	70	9	77	7	23	8	16	14	30	34	15	69	21	23	23	63	16
326	286	1760	2184	1112	4925	1183	251	991	369	307	716	115	530	657	93	100	177	1120	346
450			1619	833	3933		265		458	291	1026	140	618	316	116	102	253	1047	257
1.38			0.74	0.75	0.80		1.05		1.24	0.95	1.43	1.21	1.16	0.48	1.24	1.02	1.43	0.93	0.74
3.23			1.87	1.20	1.91		1.49		2.61	1.32	2.25	3.40	1.28	0.66	1.29	1.30	1.81	1.63	1.67

Basic Statistics for Extended Peak Flows Series

35	4	2	84	35	84	7	34	8	35	14	35	35	39	69	35	35	35	63	35
230	286	1760	2245	2365	5056	1183	248	991	327	307	732	115	469	657	103	110	186	1120	359
262			1604	2074	3846		219		348	291	962	138	410	316	102	91	218	1047	214
1.14			0.71	0.88	0.76		0.88		1.07	0.95	1.31	1.20	0.87	0.48	0.99	0.83	1.17	0.93	0.60
5.71			1.67	1.90	1.81		1.79		2.99	1.32	2.28	3.44	2.01	0.66	1.26	0.98	1.76	1.63	1.13

Appendix III: Partial Series of Peak Flows for Virgin River at Virgin

Wat-Yr	Month	Day	Year	Peak (cfs)
1910	1	1	10	2770
1911	9	30	11	10600
1912	7	31	12	5100
1913	10	27	12	12000
1914	7	30	14	2500
1915	9	3	15	4360
1916	7	26	16	4350
1917	10	6	16	2610
1918	3	12	18	5100
1919	9	3	19	1240
1920	8	19	20	11000
1921	8	22	21	2650
1922	8	31	22	3400
1923	7	22	23	5100
1924	9	10	24	3100
1925	8	25	25	1660
1926	10	5	25	2770
1927	9	13	27	4300
1928	10	31	27	2600
1929	7	31	29	4200
1930	8	4	30	3000
1931	11	17	30	3550
1932	2	9	32	9000
1933	9	8	33	2350
1934	7	28	34	1550
1935	4	8	35	1760
1936	7	31	36	6300
1937	5	8	37	1920
1938	3	3	38	13500
1939	9	6	39	10000
1940	9	17	40	4370
1941	5	6	41	2980
1942	10	13	41	3150
1943	3	9	43	919
1944	5	12	44	1070
1945	5	3	45	844
1946	8	12	46	1700
1947	10	29	46	2080
1948	9	16	48	1400
1949	9	8	49	1010
1950	7	8	50	6620
1951	8	29	51	2800
1952	12	30	51	4840
	4	28	52	2230
	5	4	52	2620
	6	3	52	2330
1953	8	1	53	12900
	7	19	53	3200
	7	30	53	2080
1954	9	12	54	4690
	7	25	54	3280
	8	4	54	1820
1955	8	25	55	10600
	10	8	54	4250
	7	21	55	1670
	8	4	55	3220
	8	8	55	2260
	8	12	55	2220
	8	24	55	3390
1956	1	27	56	2260
1957	6	10	57	1430
1958	9	3	58	7410
	11	3	57	3140
	2	25	58	3190
	3	16	58	2190
	4	23	58	1680
	5	11	58	3510
	7	23	58	2780
	9	12	58	5500
1959	8	3	59	4420
	8	18	59	2440
	8	19	59	3970
1960	9	1	60	2190

Wat-Yr	Month	Day	Year	Peak (cfs)
1961	9	17	61	13500
	11	6	60	2410
	7	4	61	2800
	8	3	61	2490
	8	10	61	2960
	8	11	61	2490
	8	22	61	2960
	8	23	61	2860
	8	24	61	1920
	9	8	61	2980
1962	2	12	62	3100
	2	9	62	2380
	9	28	62	2150
1963	9	18	63	4550
	8	5	63	3770
	8	18	63	2110
	8	19	63	1750
1964	8	12	64	4630
	10	18	63	2150
	8	4	64	1820
1965	9	5	65	6890
1966	11	23	65	3930
	11	25	65	1630
	12	30	65	2290
	7	30	66	2190
1967	12	6	66	22800
	9	24	67	7220
1968	8	7	68	6840
	7	30	68	3210
	8	2	68	1800
1969	1	25	69	13660
	1	21	69	2550
	2	25	69	1710
	4	23	69	2110
	5	2	69	1960
	5	9	69	2010
1970	8	18	70	2660
	8	4	70	2230
1971	8	21	71	2880
	8	22	71	2220
	8	23	71	2070
1979	3	28	79	7600
	5	6	79	4260
	5	20	79	3210
	8	12	79	1630
1980	9	10	80	10830
	1	14	80	2130
	4	21	80	1730
1981	7	15	81	3650
	4	19	81	2110
1982	8	23	82	9700
	3	12	82	1990
1983	11	30	82	4740
	12	23	82	3290
	3	14	83	2470
	4	30	83	1830
	5	9	83	1820
	5	28	83	2910
	9	24	83	3580
1984	9	10	84	4580
	7	22	84	2510
1985	7	19	85	2920
1986	3	8	86	1620
1987	7	20	87	7200
	8	7	87	2550
1988	11	5	87	2690
	4	21	88	1810
	8	1	88	1820
	8	6	88	2260
1989	7	28	89	1500
1990	8	15	90	3020
	9	23	90	1686
1991	9	6	91	1490
1992	8	23	92	4270
	5	29	92	1790
1993	2	20	93	3920

Appendix IV: Single-site Frequency Analysis of Annual Peaks Series Within the Study Area

Upper Valley Cr nr Escalante - 9336400

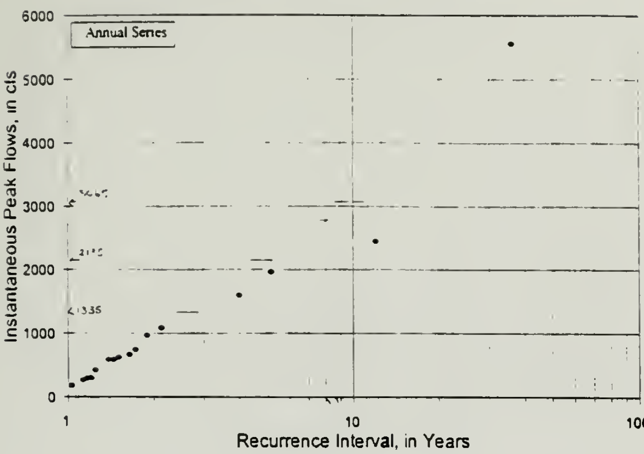

Pine Creek nr Escalante - 9337000

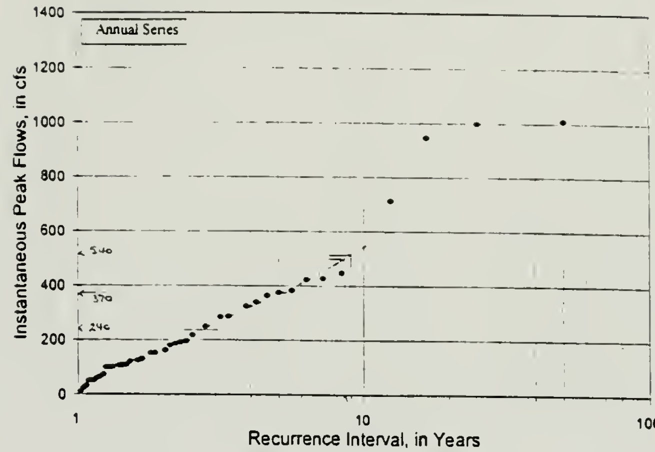

Escalante Rv. nr Escalante - 09337500

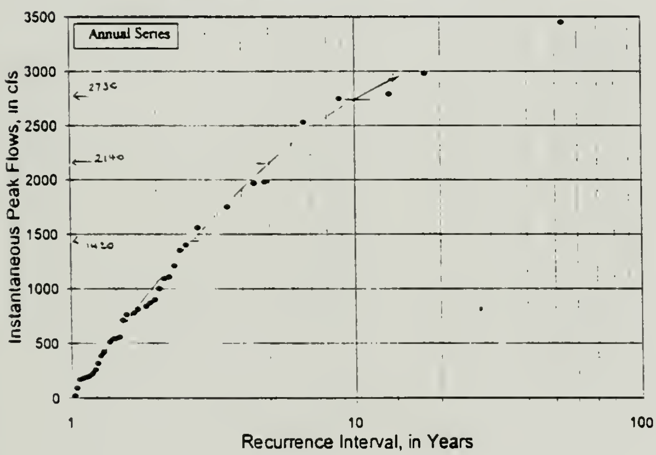

Deer Creek nr Boulder - 9338900

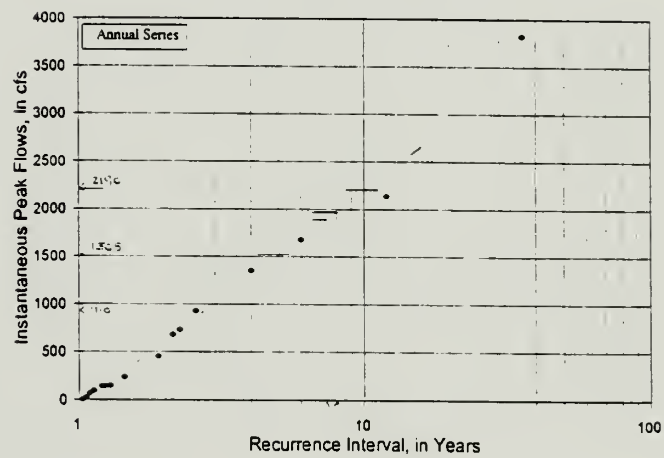

Coyote Creek nr Kanab - 09379800

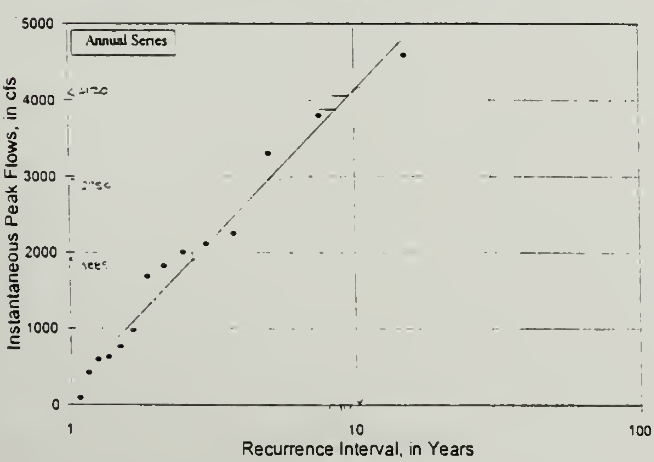

Henrieville Cr nr Henrieville- 9381100

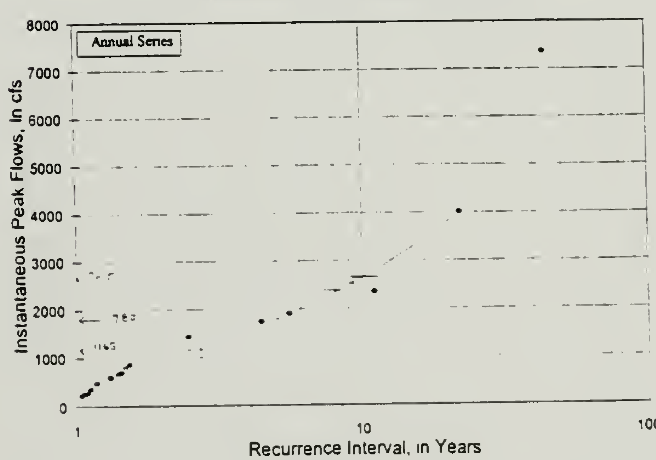

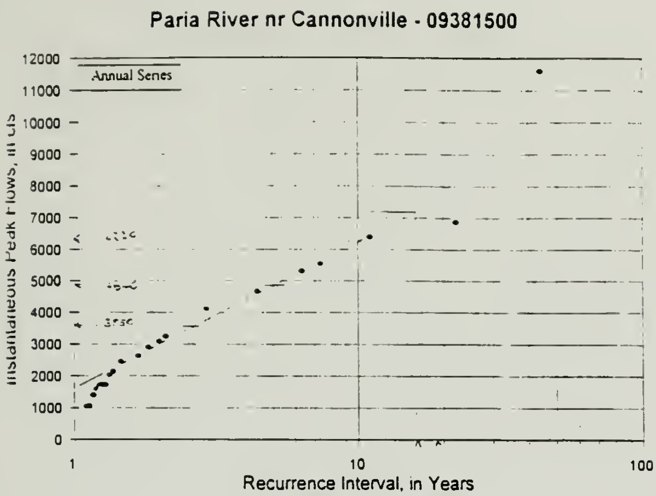
Paria River nr Cannonville - 09381500
Annual Series
Recurrence Interval, in Years

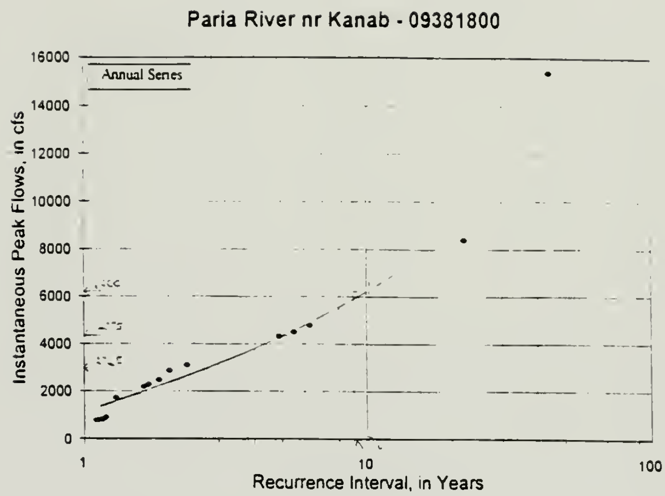
Paria River nr Kanab - 09381800
Annual Series
Instantaneous Peak Flows, in cfs
Recurrence Interval, in Years

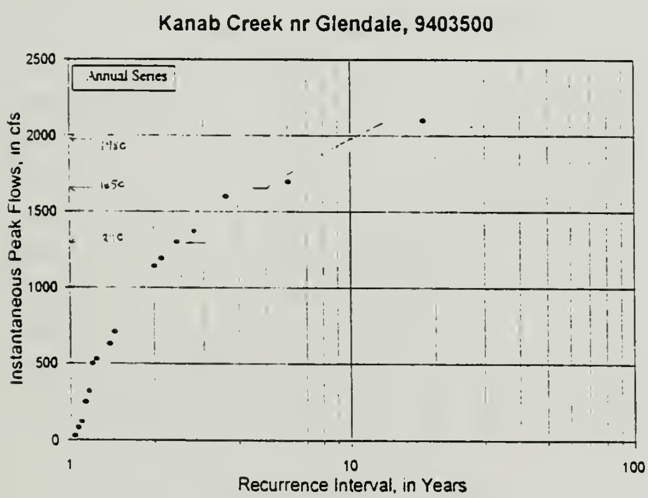
Kanab Creek nr Glendale, 9403500
Annual Series
Instantaneous Peak Flows, in cfs
Recurrence Interval, in Years

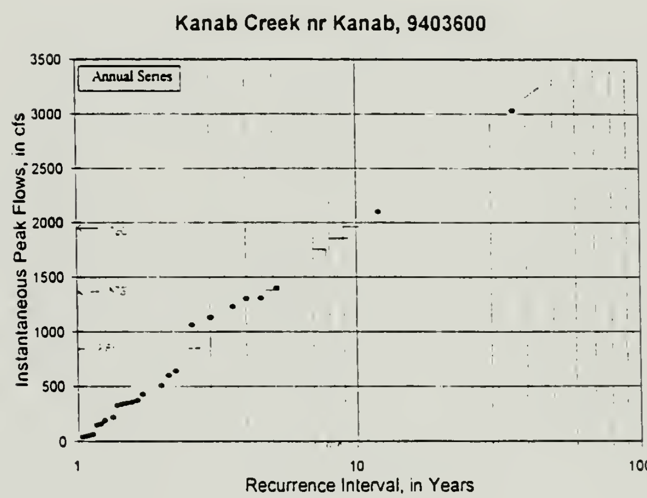
Kanab Creek nr Kanab, 9403600
Annual Series
Instantaneous Peak Flows, in cfs
Recurrence Interval, in Years

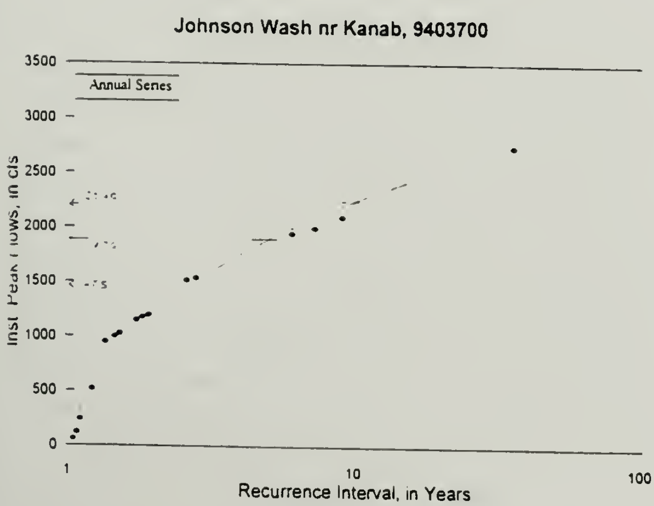
Johnson Wash nr Kanab, 9403700
Annual Series
Recurrence Interval, in Years

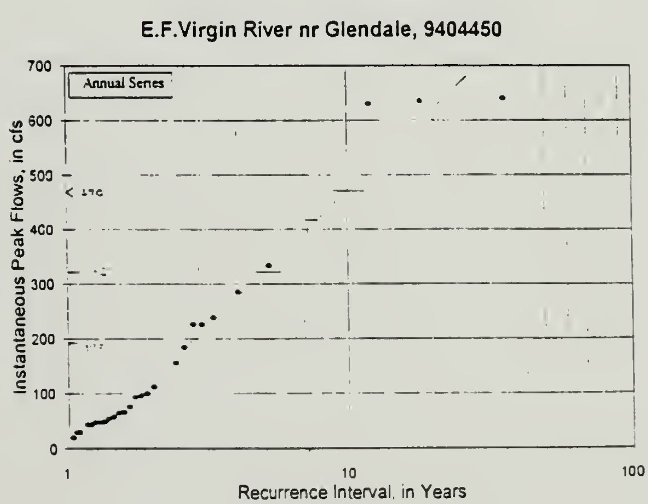
E.F.Virgin River nr Glendale, 9404450
Annual Series
Instantaneous Peak Flows, in cfs
Recurrence Interval, in Years

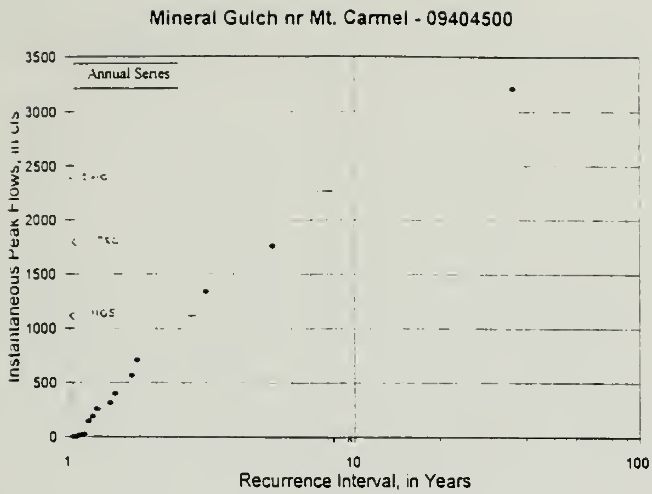

Mineral Gulch nr Mt. Carmel - 09404500
Annual Series
Instantaneous Peak Flows, in cfs
Recurrence Interval, in Years

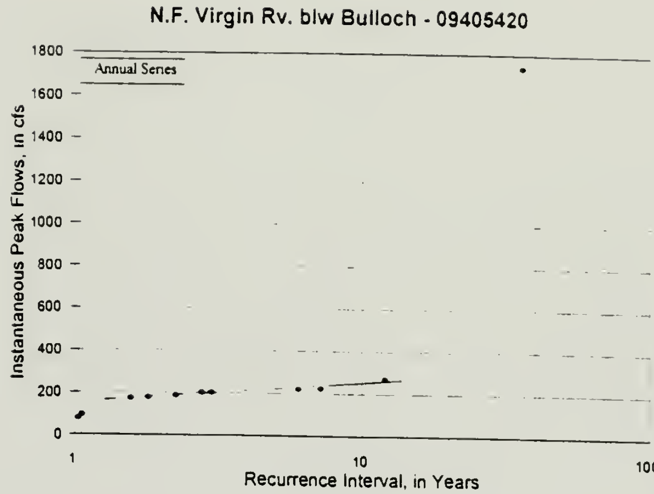

N.F. Virgin Rv. blw Bulloch - 09405420
Annual Series
Instantaneous Peak Flows, in cfs
Recurrence Interval, in Years

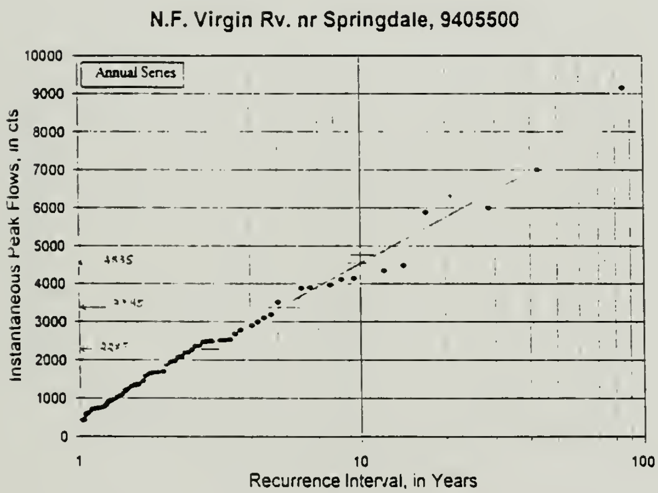

N.F. Virgin Rv. nr Springdale, 9405500
Annual Series
Instantaneous Peak Flows, in cfs
Recurrence Interval, in Years

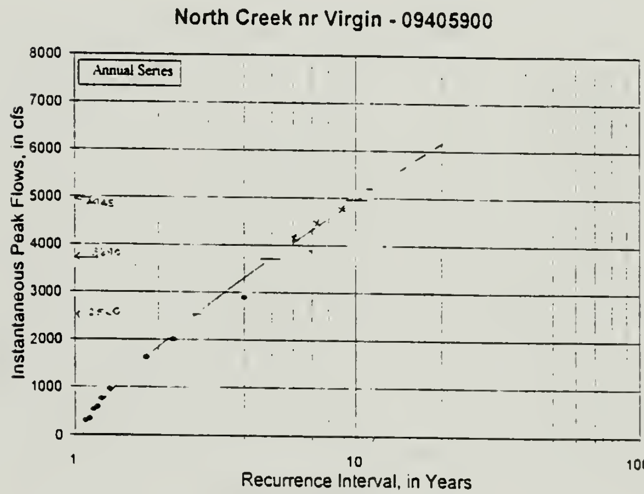

North Creek nr Virgin - 09405900
Annual Series
Instantaneous Peak Flows, in cfs
Recurrence Interval, in Years

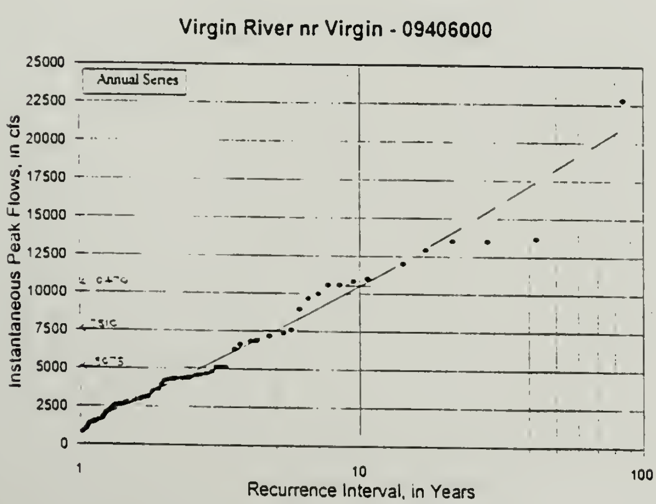

Virgin River nr Virgin - 09406000
Annual Series
Instantaneous Peak Flows, in cfs
Recurrence Interval, in Years

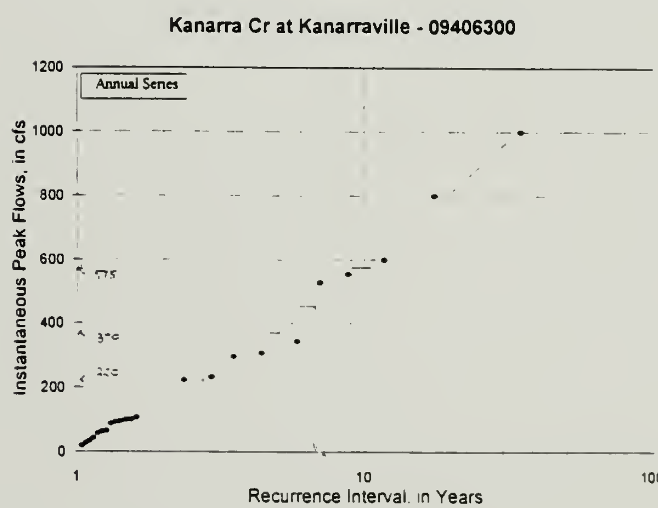

Kanarra Cr at Kanarraville - 09406300
Annual Series
Instantaneous Peak Flows, in cfs
Recurrence Interval, in Years

South Ash Creek blw Mill Cr - 09406700

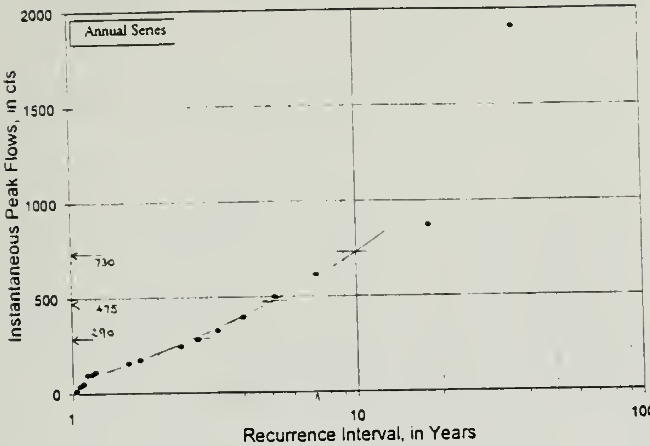

Leeds Creek nr Leeds, 9408000

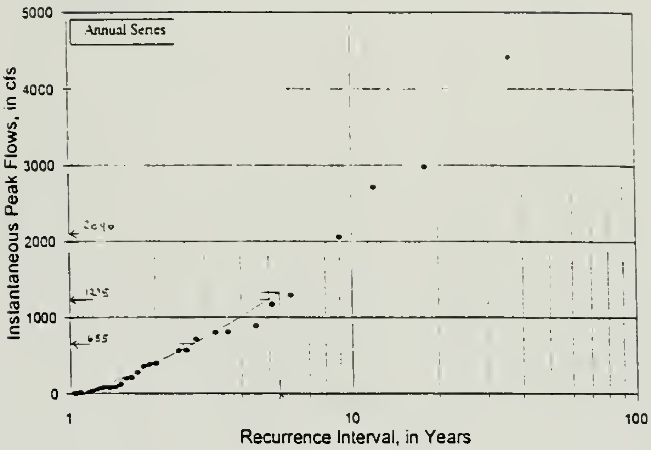

Santa Clara Rv nr Pine Valley, 9408400

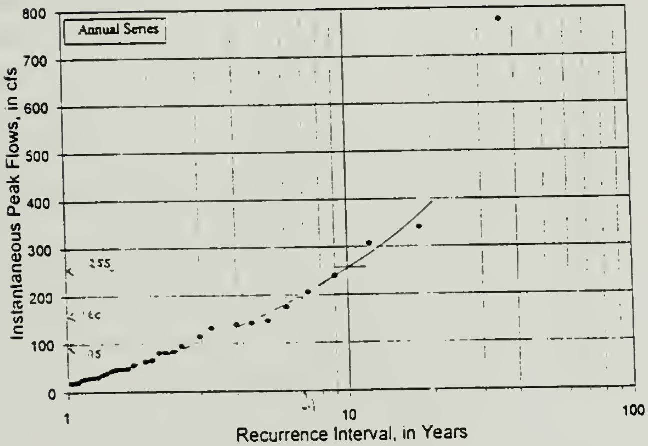

Moody Wash nr Veyo - 09409500

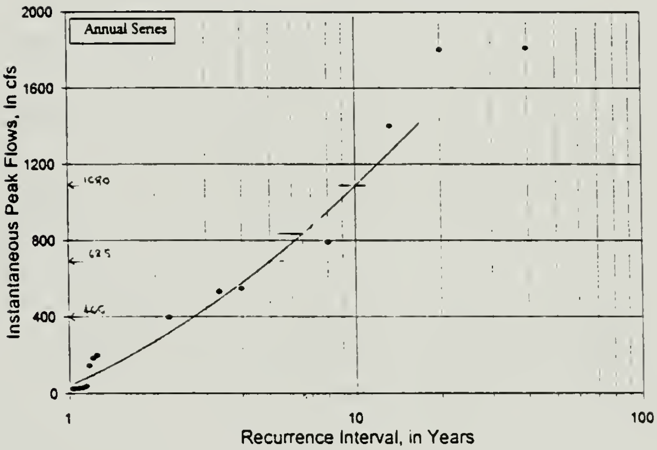

Sevier River at Hatch - 10174500

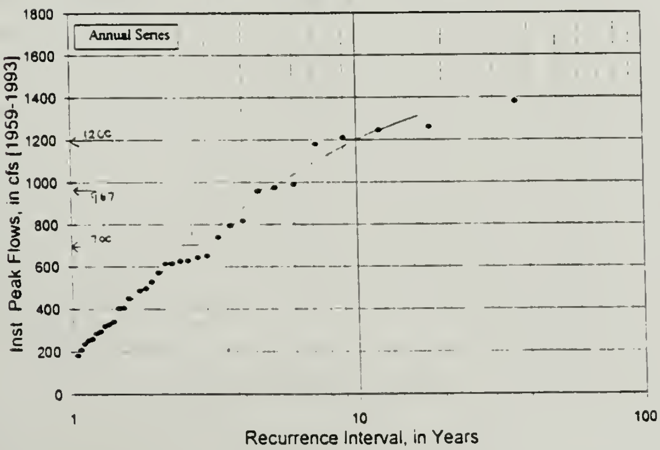

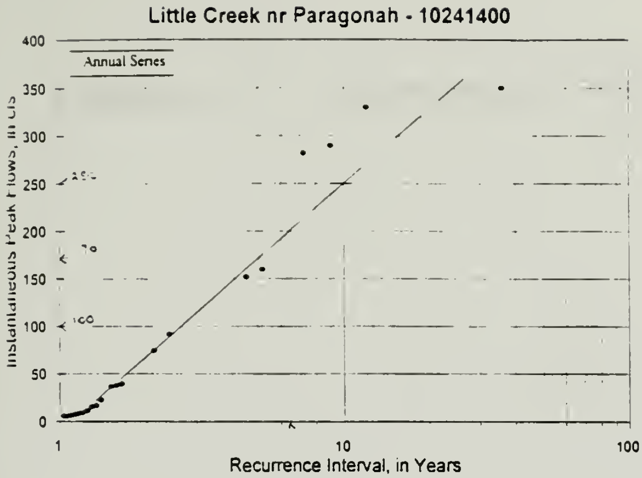
Little Creek nr Paragonah - 10241400
Annual Series
Recurrence Interval, in Years

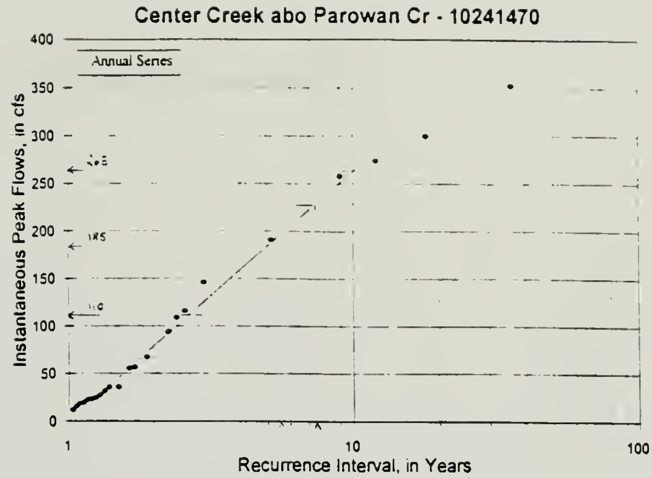
Center Creek abo Parowan Cr - 10241470
Annual Series
Instantaneous Peak Flows, in cfs
Recurrence Interval, in Years

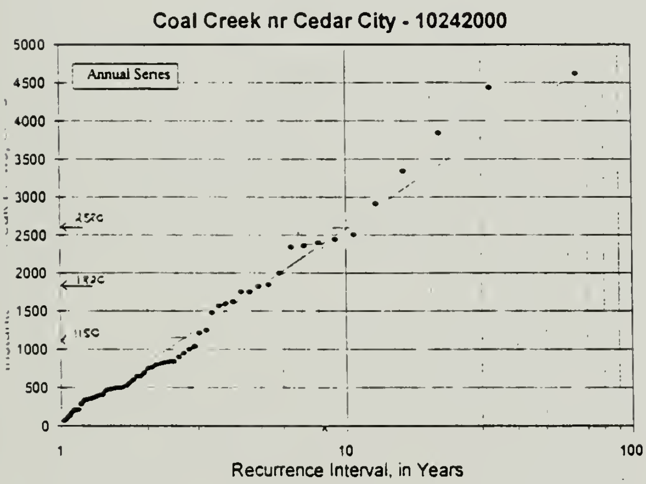
Coal Creek nr Cedar City - 10242000
Annual Series
Recurrence Interval, in Years

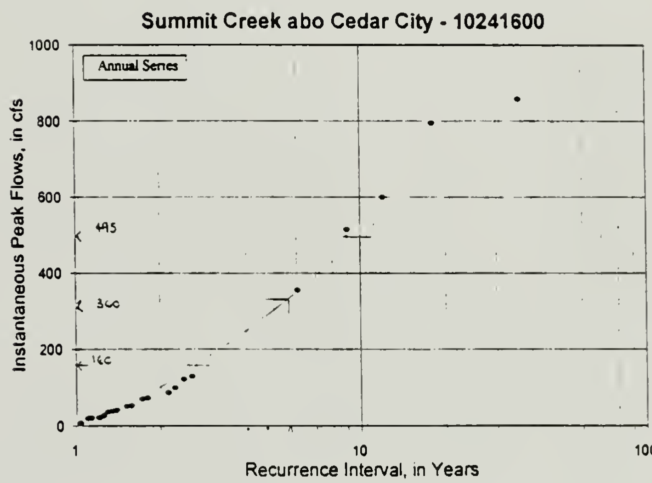
Summit Creek abo Cedar City - 10241600
Annual Series
Instantaneous Peak Flows, in cfs
Recurrence Interval, in Years

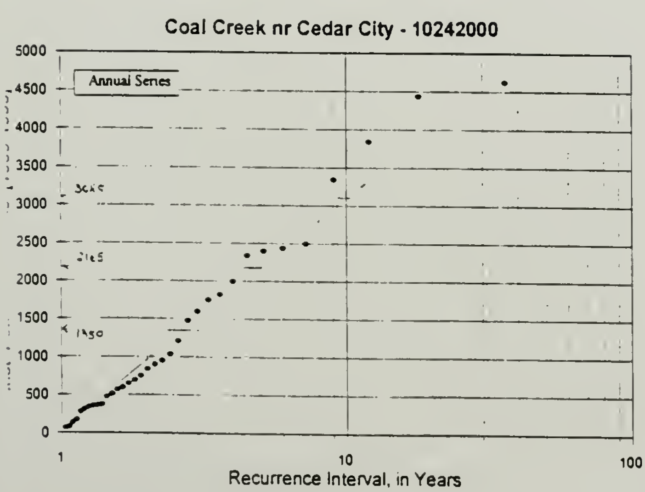
Coal Creek nr Cedar City - 10242000
Annual Series
Recurrence Interval, in Years

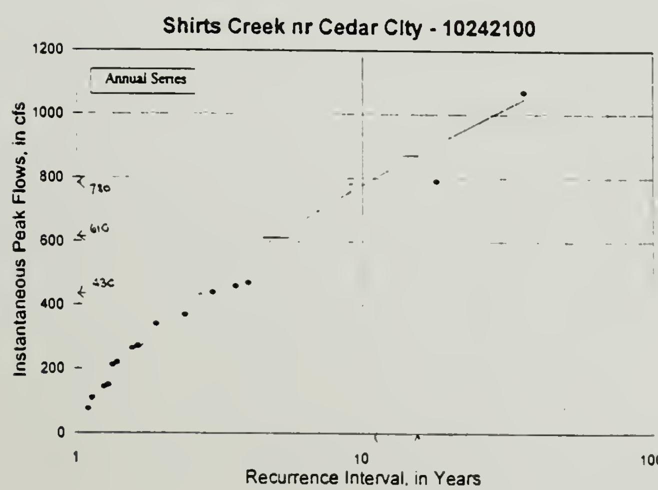
Shirts Creek nr Cedar City - 10242100
Annual Series
Instantaneous Peak Flows, in cfs
Recurrence Interval, in Years

Appendix V: Hydrological Characteristics of Watersheds

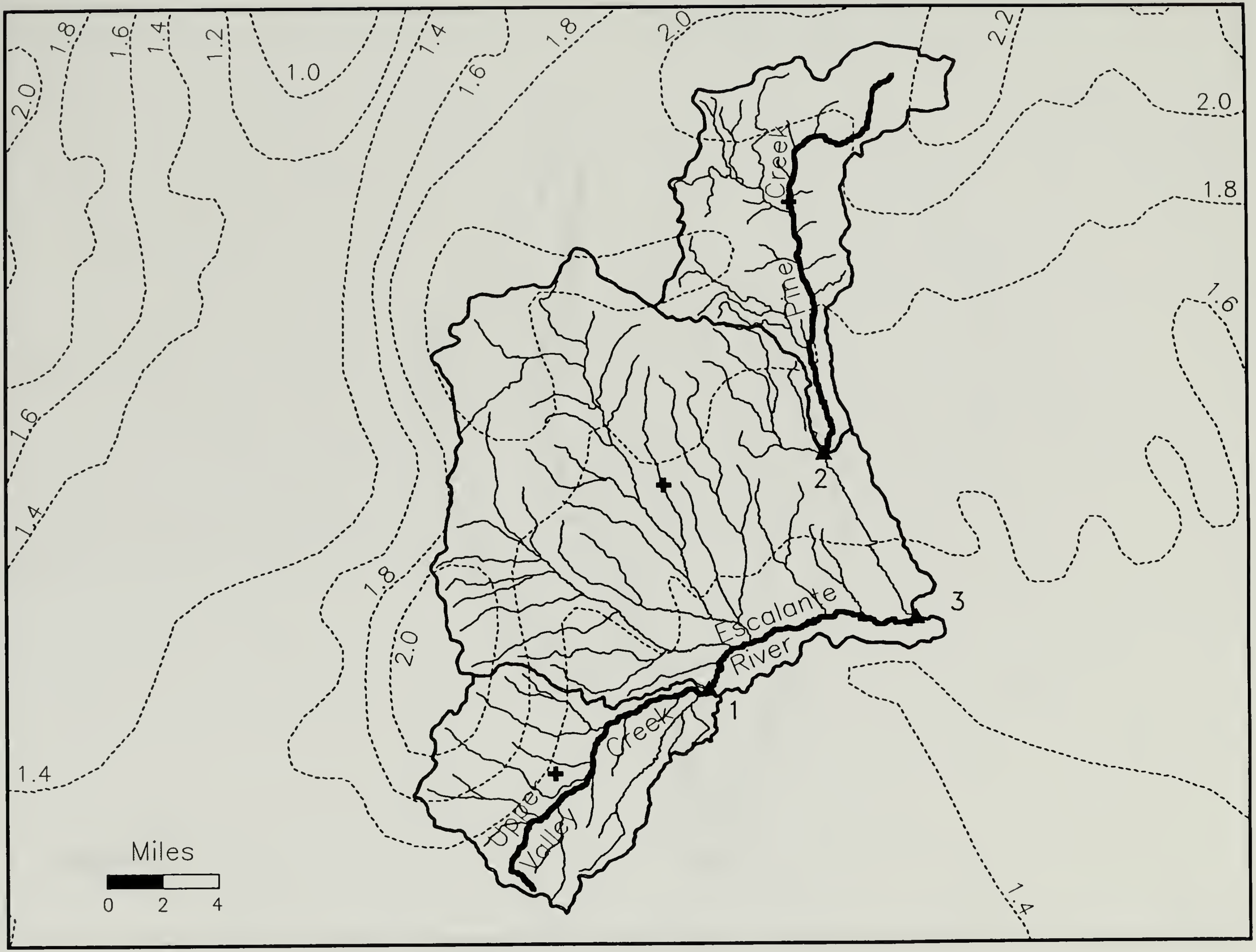
Pine Creek
Escalante River
Upper Valley Creek
1
2
3
Miles
0
2
4
1.0
1.2
1.4
1.6
1.8
2.0
2.2

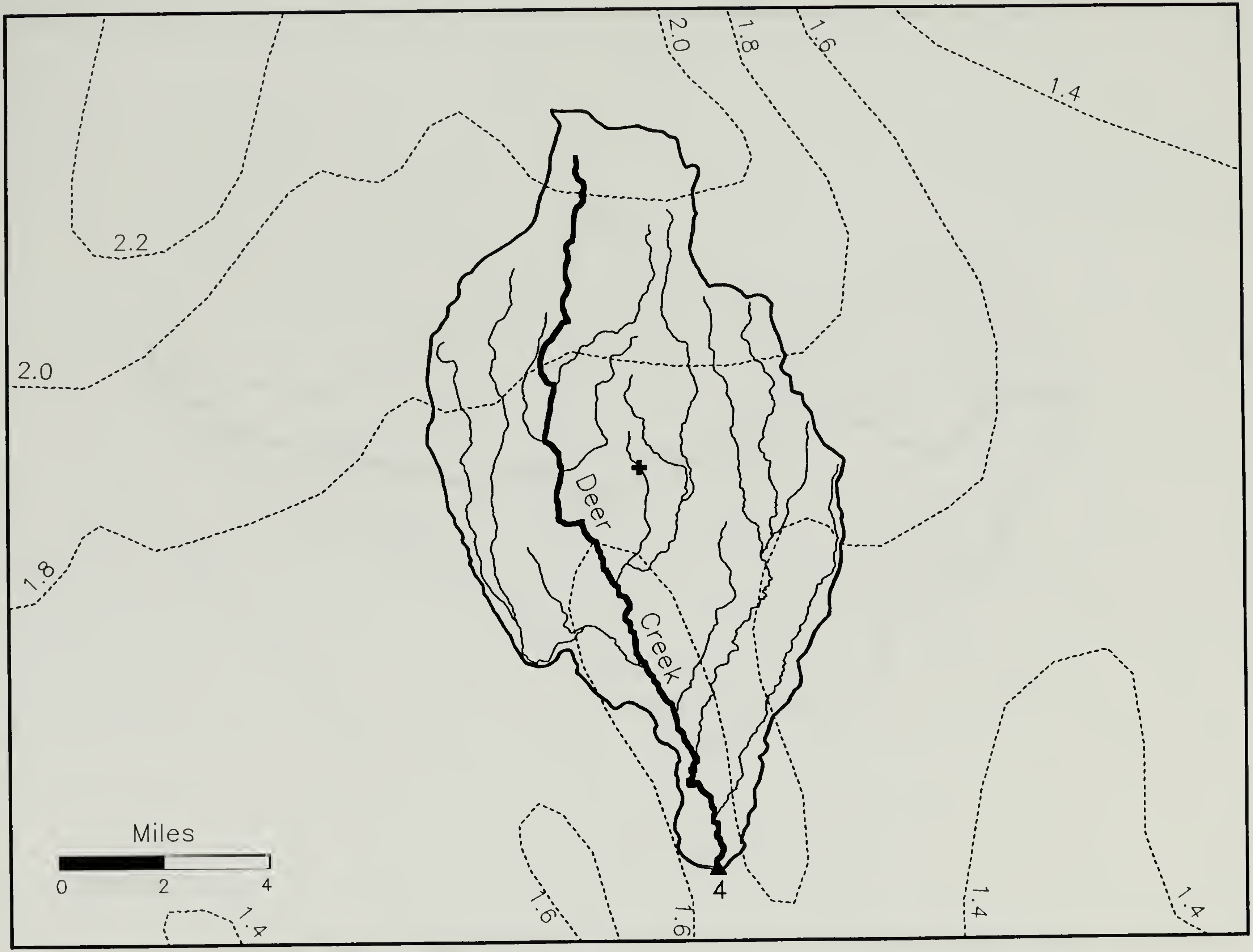

Deer
Creek
4
Miles
0
2
4
2.2
2.0
1.8
1.6
1.4

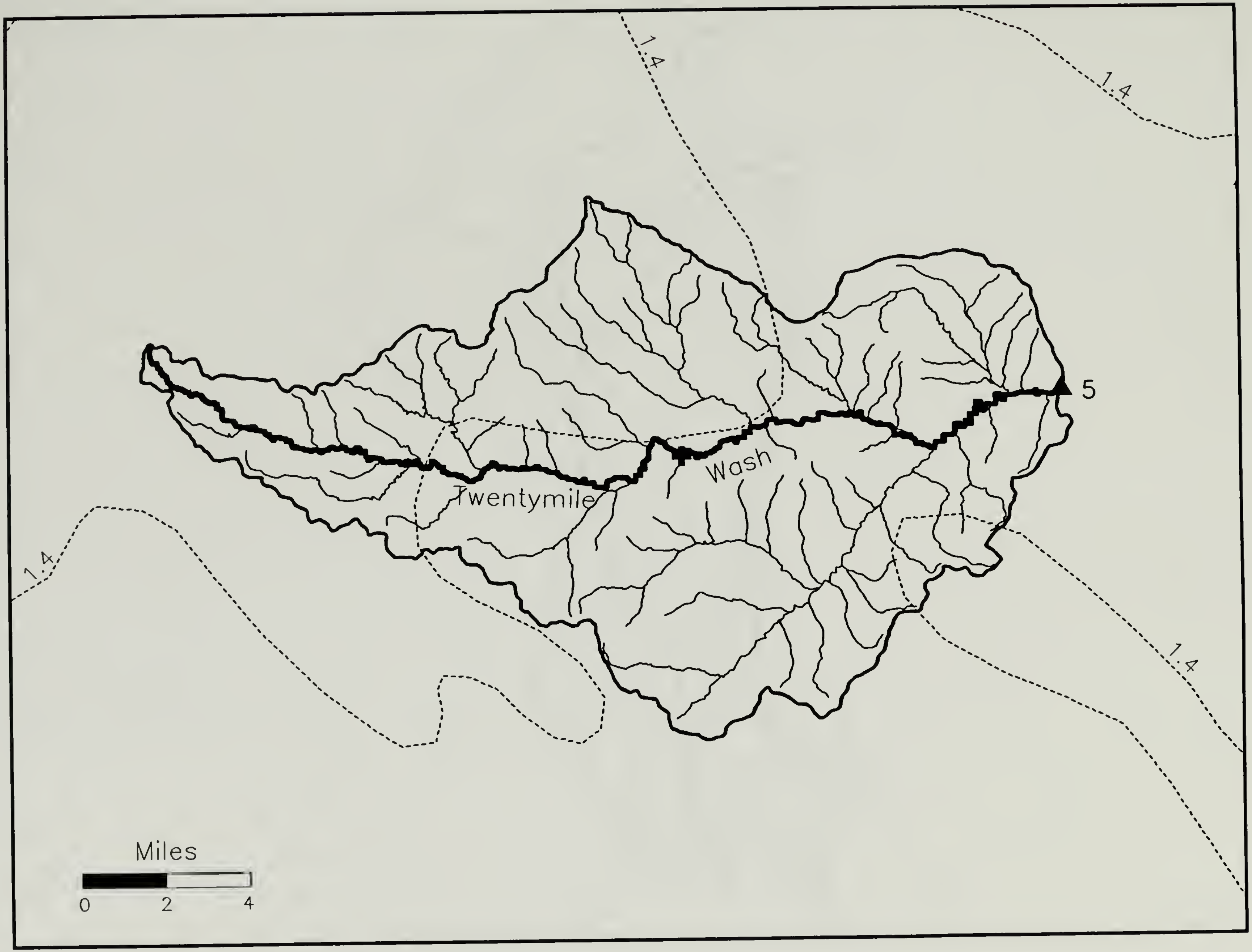
1.4
1.4
1.4
1.4
5
Wash
Twentymile
Miles
0
2
4

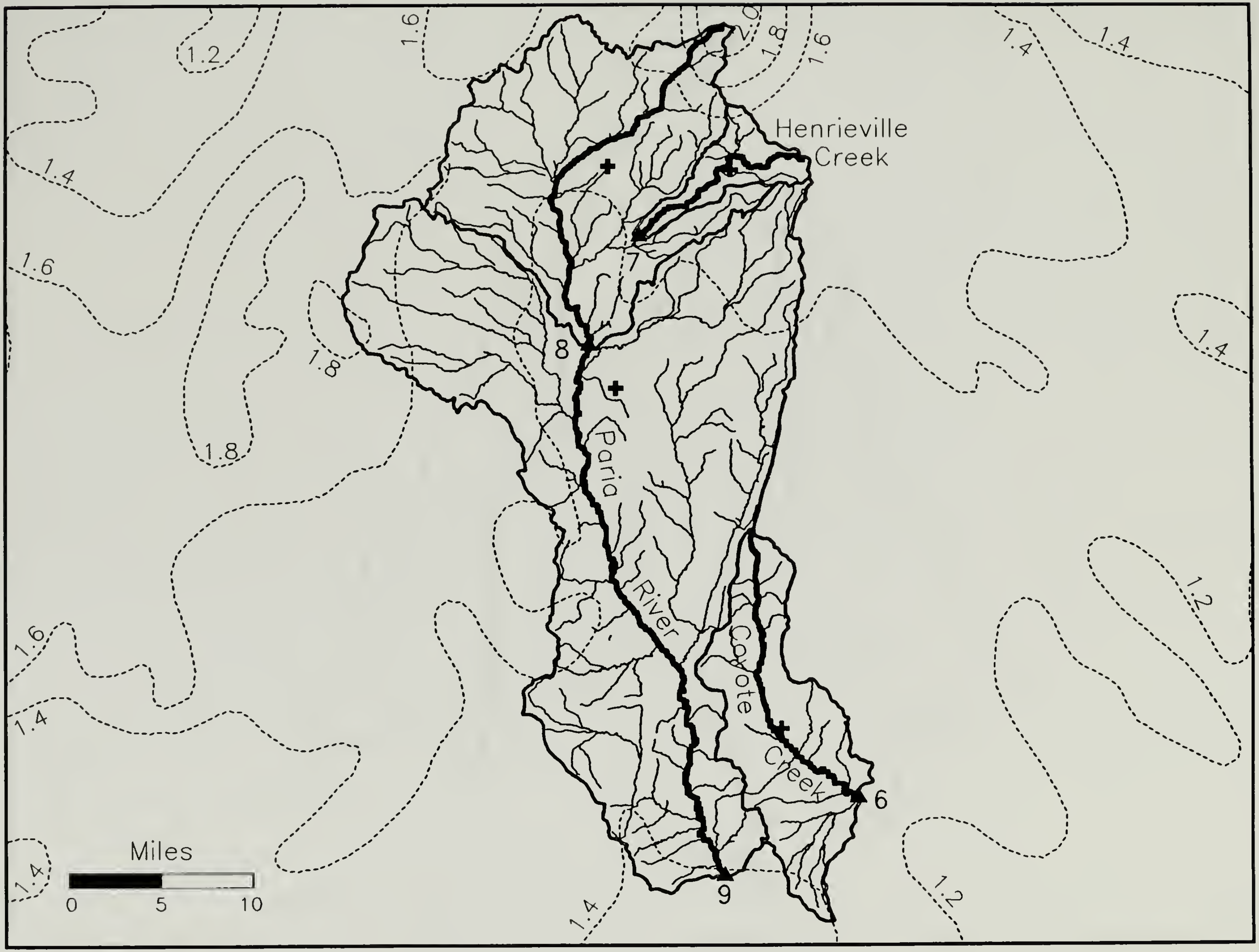
Henrieville Creek
Paria River
Coyote Creek
6
7
8
9
Miles
0
5
10
1.2
1.4
1.6
1.8
2.0

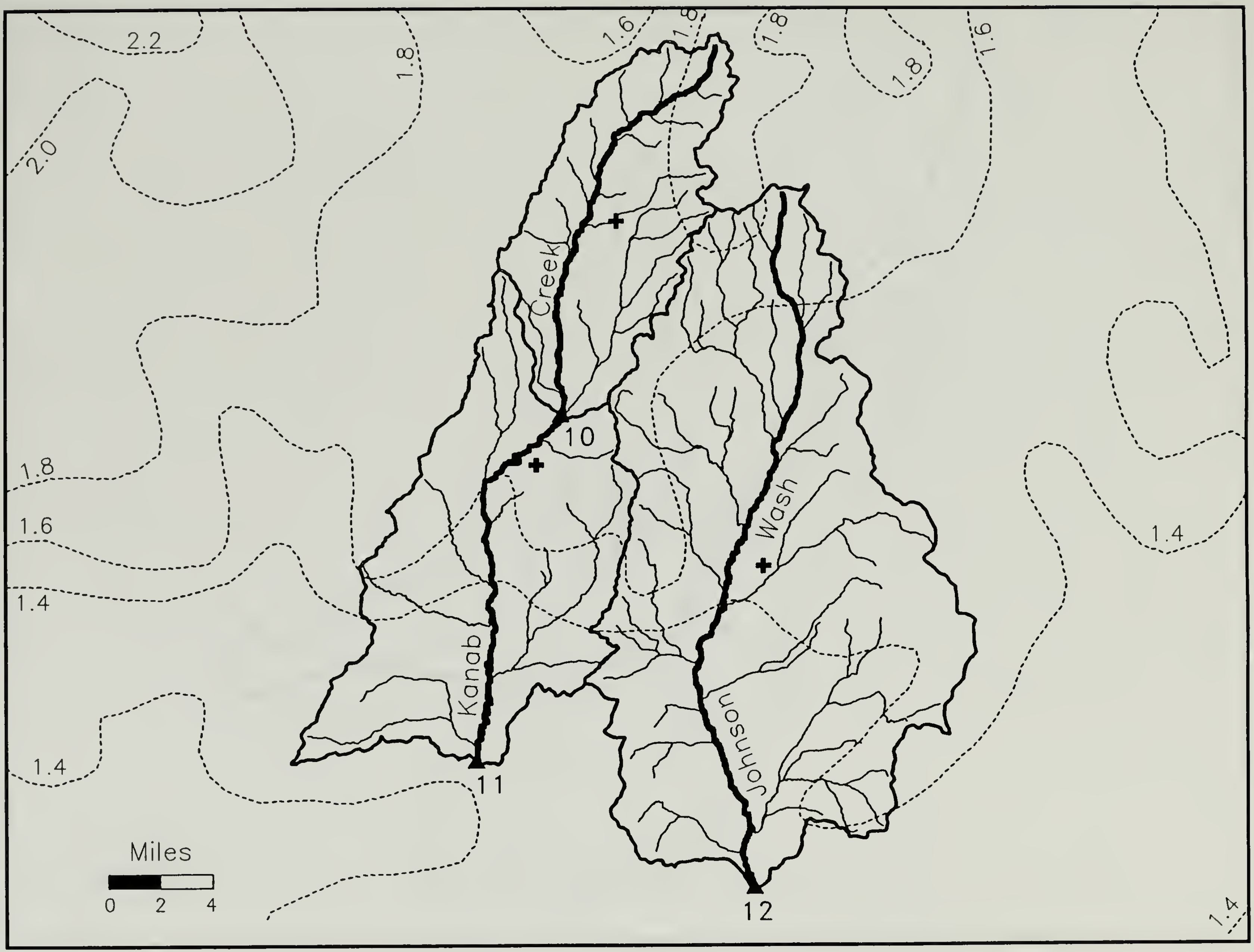

Kanab
Creek
Johnson
Wash
10
11
12
Miles
0
2
4
2.2
2.0
1.8
1.6
1.4

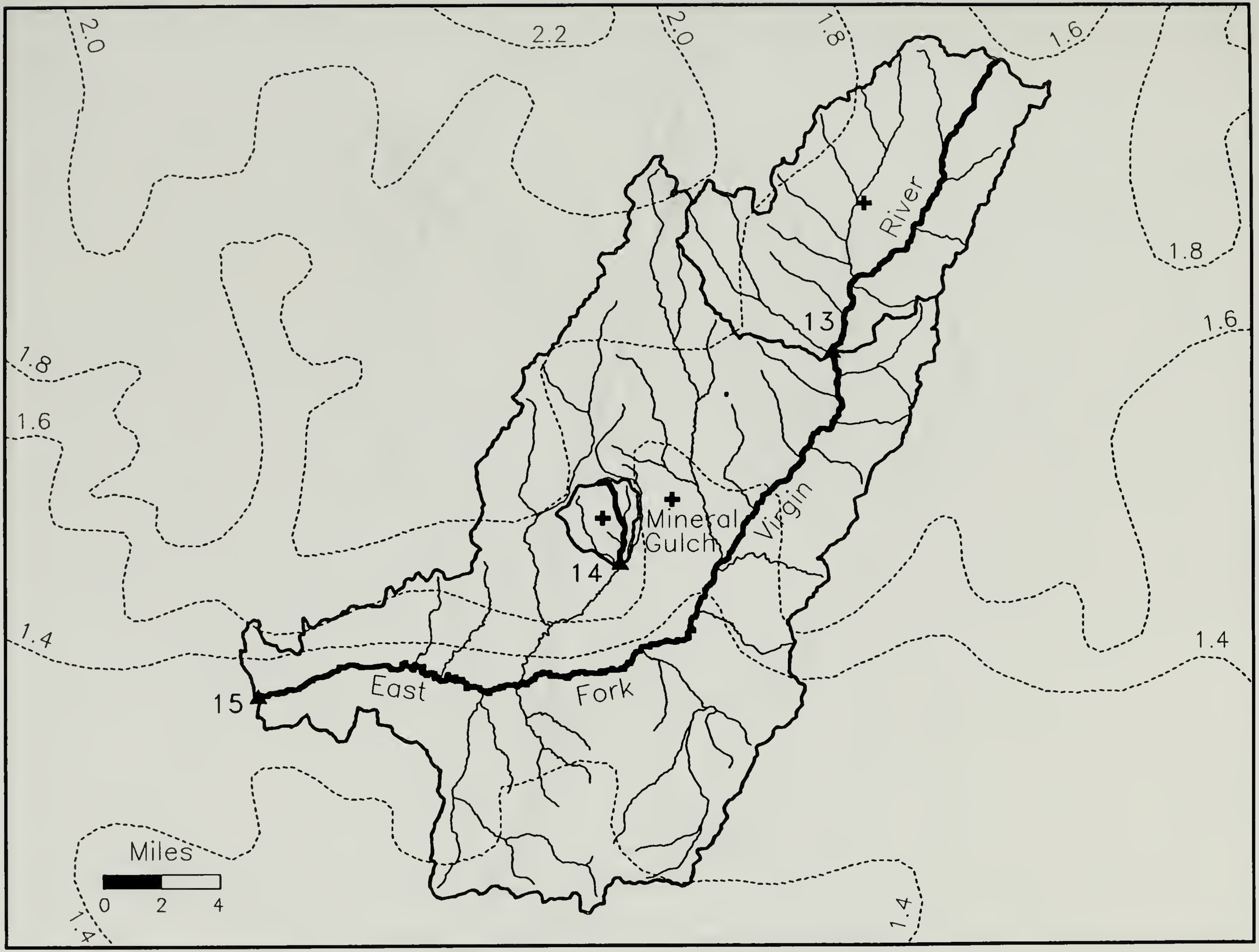

2.0
2.2
2.0
1.8
1.6
1.8
1.6
1.8
1.6
1.4
1.4
1.4
1.4
River
13
Virgin
Mineral
Gulch
14
East
Fork
15
Miles
0
2
4

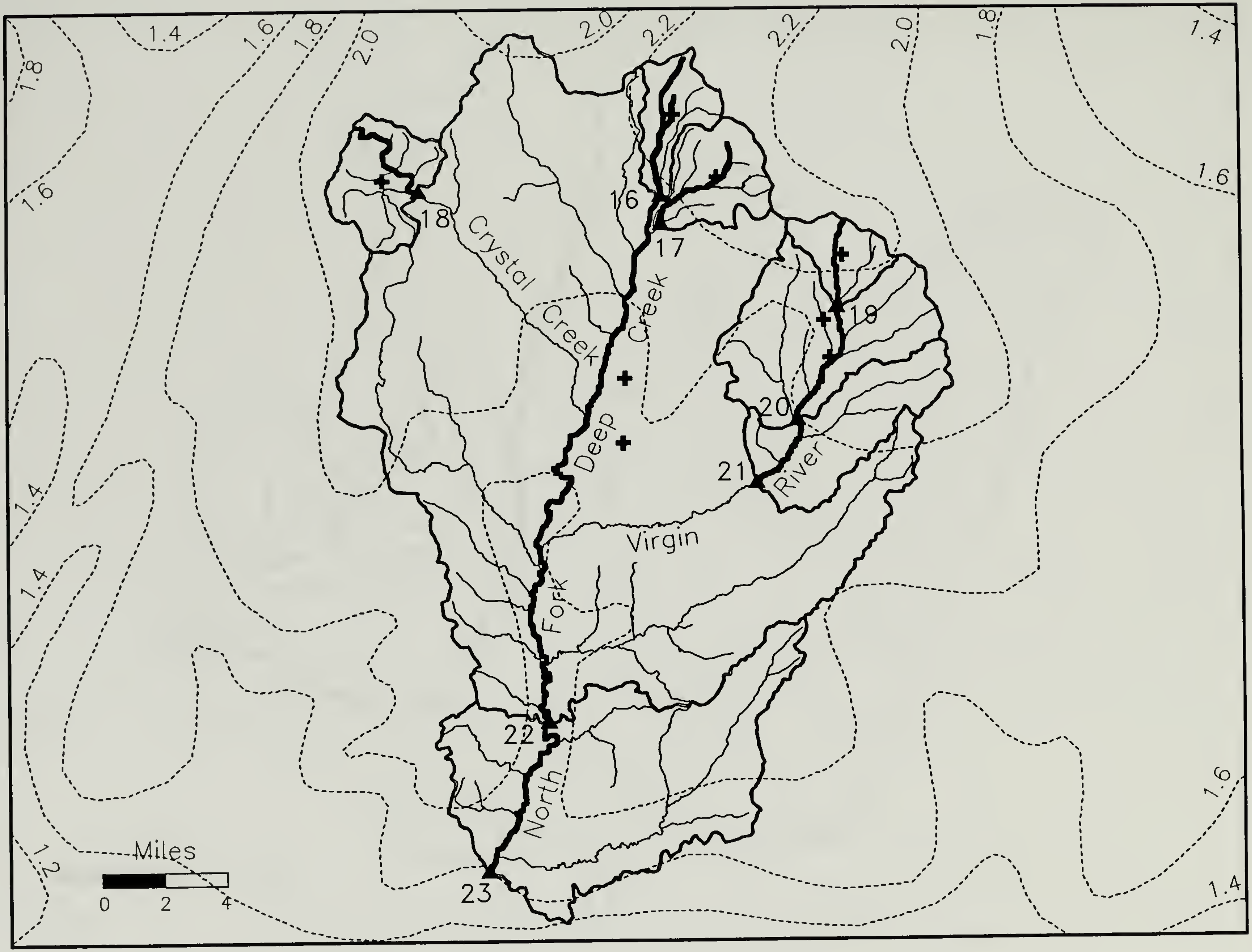
Crystal Creek
Deep Creek
Virgin River
North Fork
16
17
18
19
20
21
22
23
Miles
0
2
4
1.2
1.4
1.6
1.8
2.0
2.2

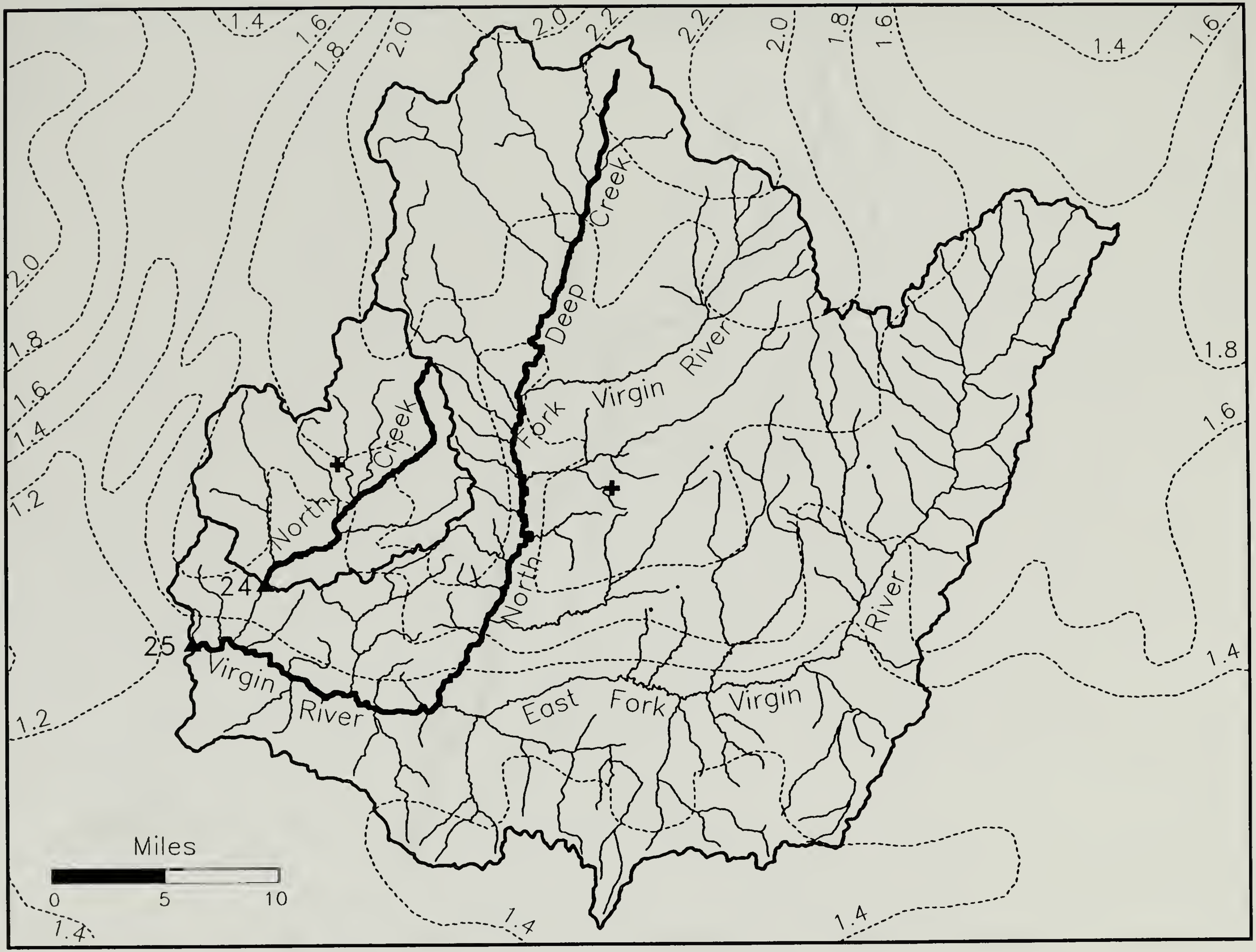

Deep Creek
North Fork Virgin River
North Creek
North Creek
East Fork Virgin River
Virgin River
24
25
Miles
0
5
10

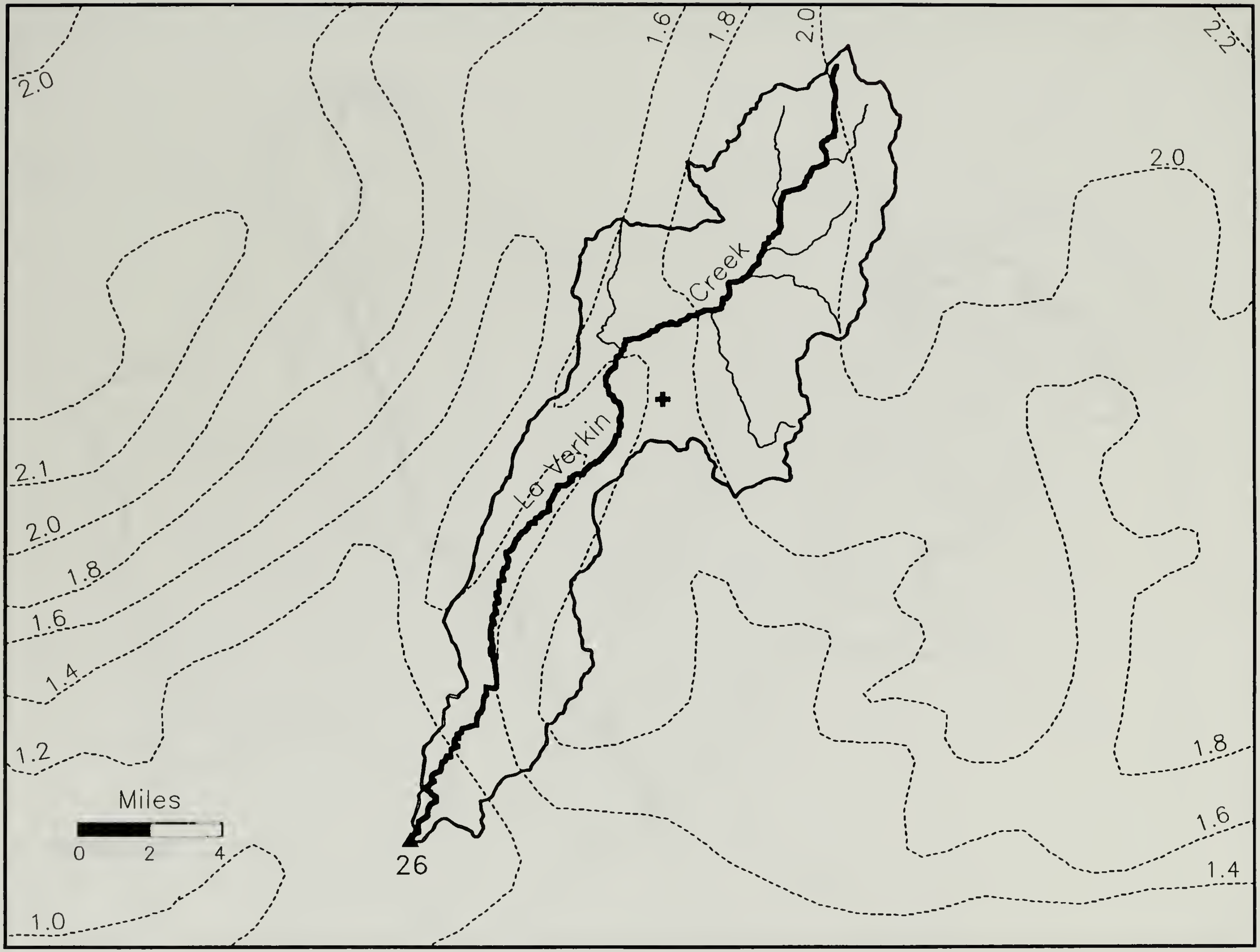

2.0
1.6
1.8
2.0
2.2
2.0
Creek
La Verkin
2.1
2.0
1.8
1.6
1.4
1.2
1.8
1.6
1.4
1.0
Miles
0
2
4
26

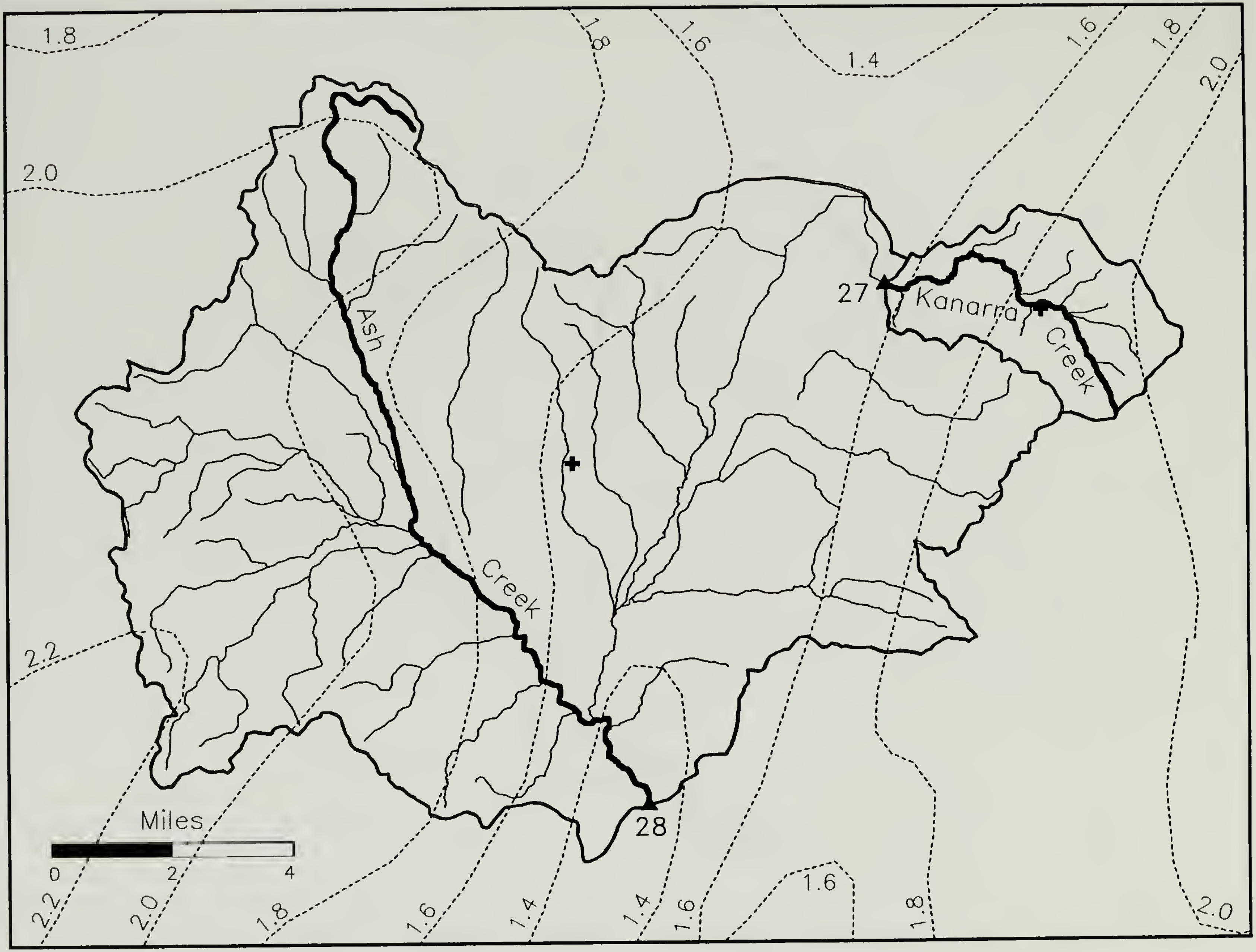
Ash
Creek
Kanarra
Creek
27
28
Miles
0
2
4
1.4
1.6
1.8
2.0
2.2

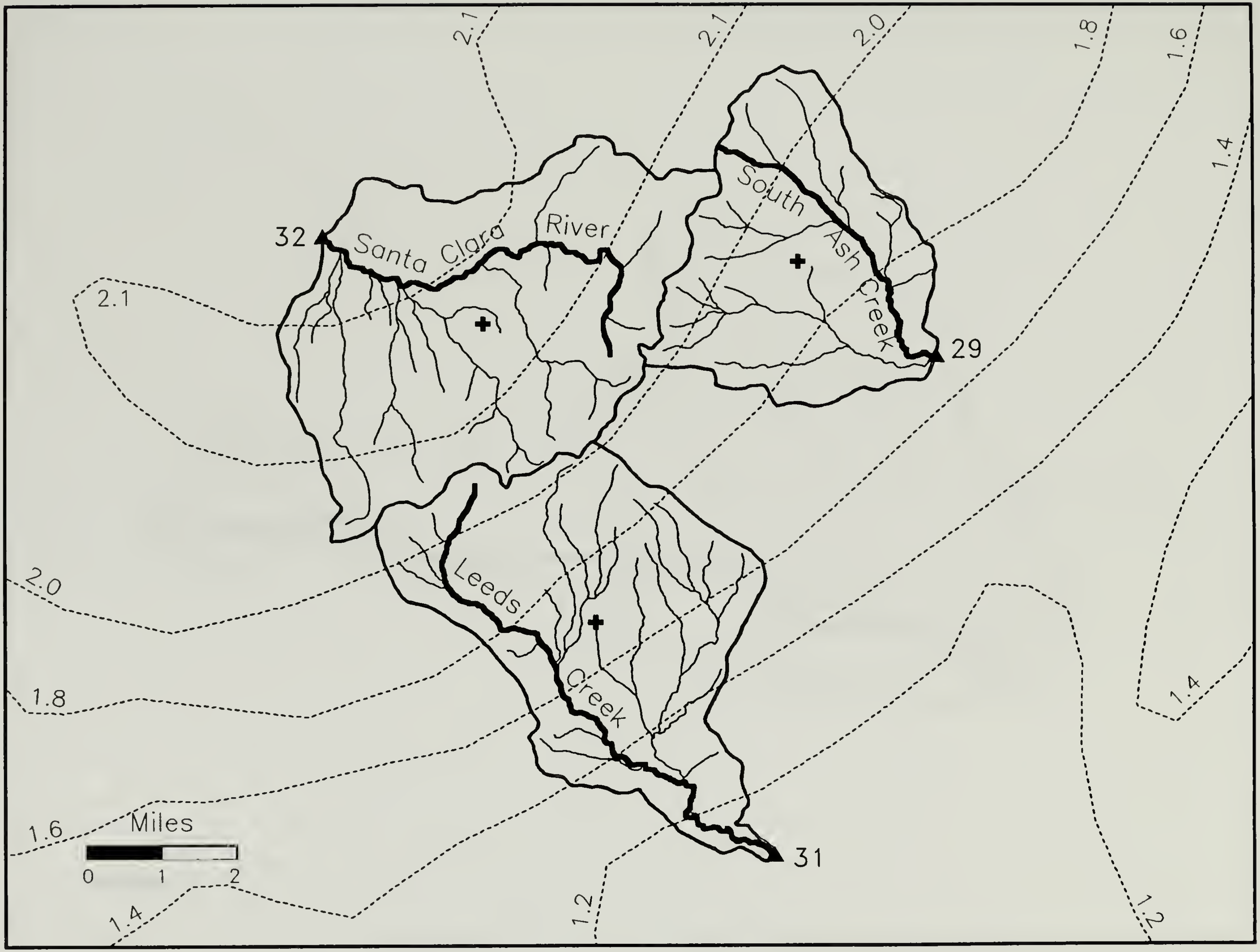

32
Santa Clara River
South Ash Creek
29
Leeds Creek
31
2.1
2.1
2.0
1.8
1.6
1.4
2.1
2.0
1.8
1.6
1.4
1.2
1.2
1.4
Miles
0 1 2

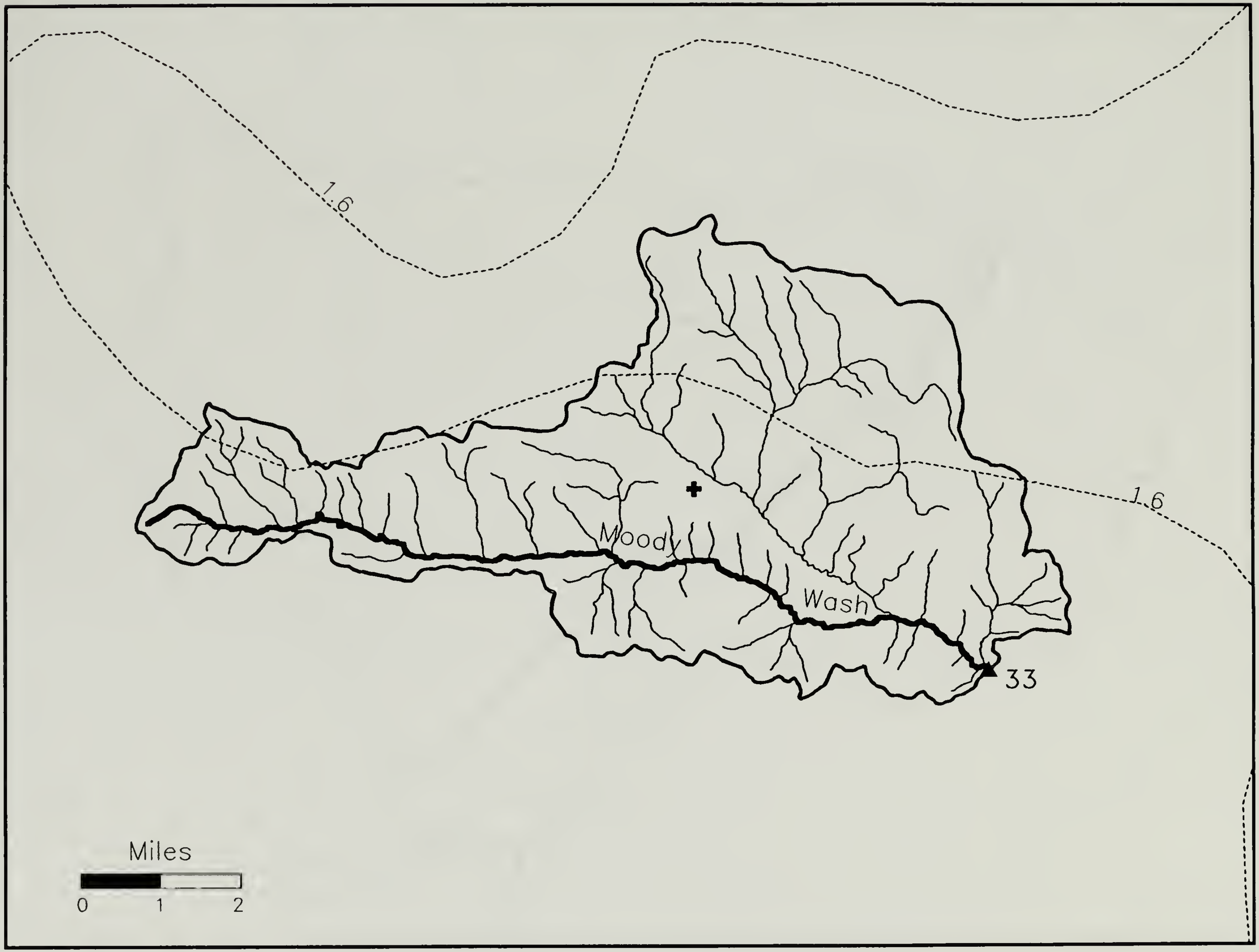
1.6
1.6
Moody Wash
33
Miles
0
1
2

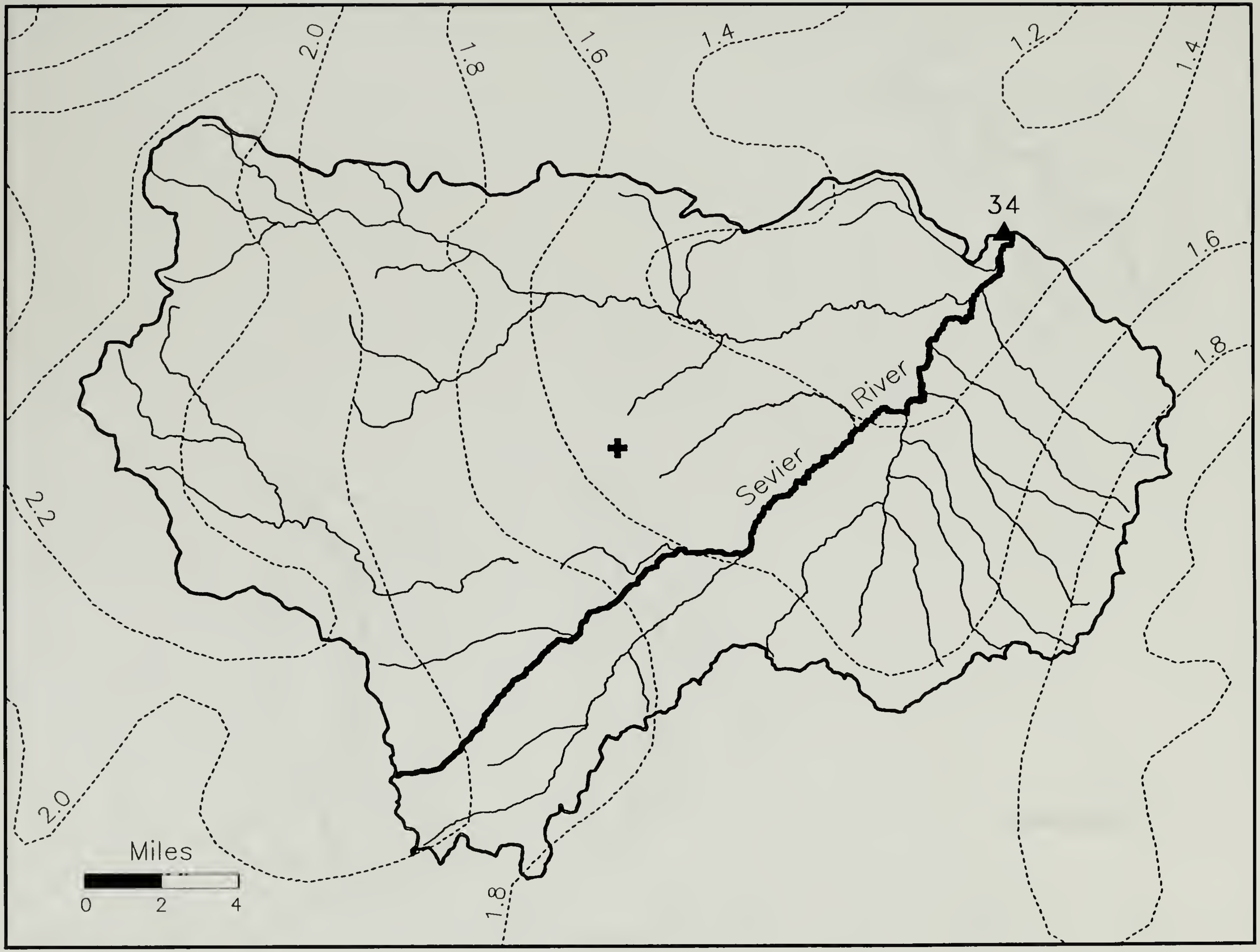

2.0
1.8
1.6
1.4
1.2
1.4
34
1.6
1.8
River
Sevier
2.2
2.0
Miles
0
2
4
1.8

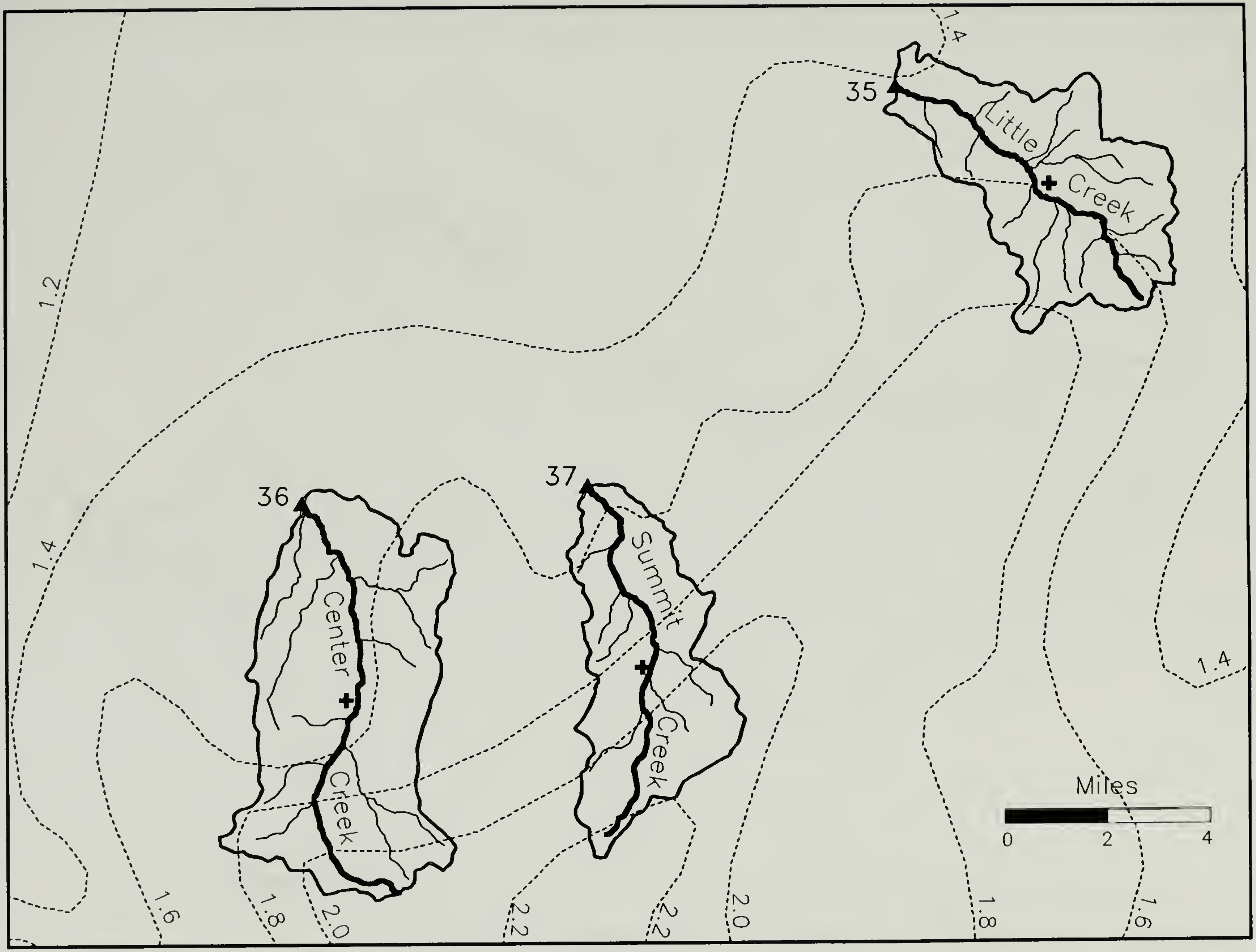
Little Creek
35
Center Creek
36
Summit Creek
37
Miles
0
2
4
1.2
1.4
1.6
1.8
2.0
2.2

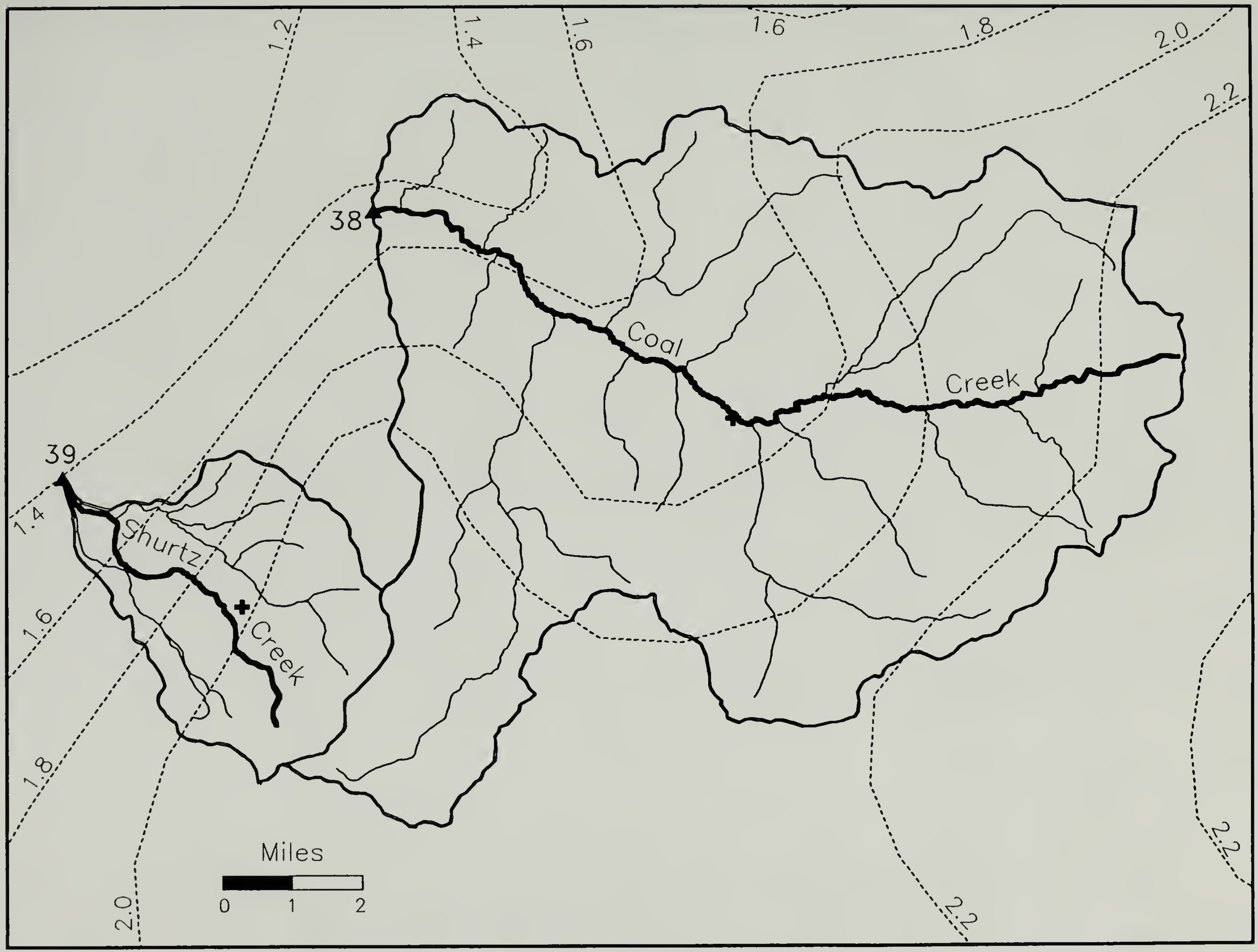

Coal
Creek
Shurtz
Creek
38
39
1.2
1.4
1.6
1.8
2.0
2.2
Miles
0
1
2